2023

Identification of Conditions That Promote Biofilm Formation by Vibrio Fischeri and Elucidation of The Underlying Signal Transduction Pathway

Courtney Noelle Dial

LOYOLA UNIVERSITY CHICAGO

IDENTIFICATION OF CONDITIONS THAT PROMOTE BIOFILM FORMATION BY *VIBRIO FISCHERI* AND ELUCIDATION OF THE UNDERLYING SIGNAL TRANSDUCTION PATHWAY

A DISSERTATION SUBMITTED TO

THE FACULTY OF THE GRADUATE SCHOOL

IN CANDIDACY FOR THE DEGREE OF

DOCTOR OF PHILOSOPHY

PROGRAM IN MICROBIOLOGY AND IMMUNOLOGY

BY

COURTNEY NOELLE DIAL

CHICAGO, ILLINOIS

MAY 2023

ACKNOWLEDGMENTS

First, I would like to thank Dr. Karen Visick for letting me join her lab as a trained Virologist. I also wanted to thank her for letting me be very independent while in her lab. I would also like to thank various members of the Visick lab, past and present, who were a great support system in science and life: Brittany Fung, Natasha Peterson, Jeremy Esin, Steven Eichinger, Ali Razvi, Dave Christensen, and Alice Tischler.

The late Dr. Adam Driks told me that your committee is not only a group of friends but soon–to–be colleagues and a support system outside of your mentor. I took these words to heart and have genuinely leaned on my committee for many things. I would like to broadly thank my committee and address each of them and their contributions to me as a scientist and a person. First, I would like to thank the chair of my committee, Dr. Francis Alonzo, who has been on every committee since I started here at Loyola. He has been the most incredible committee chair, a constant support system, confidant, voice of reason, and like-minded horror enthusiast. Second, Dr. Bryan Mounce, my master's mentor, has continued to be an excellent mentor throughout my Ph.D. His door has always been open for me to come in and scream, cry, vent, and everything in between. Dr. Alan Wolfe has watched me grow as a scientist from day one as I rotated in his lab during the first semester of my first year as a master's student. He has made himself available for genetics questions and to be an outside perspective when I got in my head a bit too much. Dr. Eric Stabb has also made himself available for scientific advice; especially when we first found pABA and needed a *V. fischeri* metabolic expert to try and help us figure

out what pABA is doing. He has also been an excellent second *V. fischeri* mentor. Our monthly meetings with his lab are immeasurably valuable. Last but certainly not least, Dr. Jonathan Allen. He has been a great support system, a place for me to vent, a confidant, and (probably most importantly) gotten me into contact with clinical microbiologists who have helped with my future career. He truly puts students first, and that one little contact he made for me helped me get into a fellowship and will continue to help me throughout my career. I could not be more thankful. Thank you all.

I wanted to thank everyone who has helped me not only figure out my career path but also supported me along the way to obtaining a clinical microbiology fellowship. Drs Evann Hilt and Cecilia Thompson were instrumental in my finding out about this career path. Further, they helped me throughout the application process, and Cecilia has been a great support system while I have been trying to navigate the unknown parts of clinical microbiology. Drs. Samantha Giffen and Ken Gavina supported me throughout the application process, helping me with interviews, giving me tours, and being a place to vent. They have been truly instrumental in my success in finding a fellowship. Lastly, Dr. Amanda Harrington has been the world's best mentor, colleague, and friend. She helped with the application, interview, and decision process. Dr. Harrington allowed me to get my hands "dirty" in the clinical lab. She allowed me to become more involved and immersed in the clinical environment. I could not have asked for a better clinical mentor. Thank you so much!

Lastly, most importantly, thank you to my friends and family. My friends have supported me throughout this process; you have been encouraging and uplifting even when I wanted to give up. I also wanted to give a special shoutout to my partner, Nick Rissler, who has always had my back throughout the good and bad days. To the boys of Last Podcast on the Left, Marcus Parks,

Ben Kissel, and Henry Zebrowski, I honestly do not know how I would have gotten through those long days in the lab without you guys. Thank you for helping me embrace my weirdness, keeping me company in the lab/at the bench, and putting out the highest content for us weirdos. Hail Gein, Hail Yourself, Hail Satan, and Megustalations! My family, specifically my mother and father, have always supported this journey and encouraged me to go down this route. I feel their pride every time they talk about the path I chose for myself. Thank you both for supporting me every step of the way. Most importantly, I want to thank my late grandparents, Jim and Carol Hopkins. My grandfather sparked my interest in science. When I was tiny, he would take my cousins and me to various museums over the summer and instilled my curiosity in science through his own passion. My grandma supported my education every step of the way and nurtured an inquisitive mind. They both passed before they saw me get my master's and now my Ph.D., but I'd like to think they would be proud. I love and miss you both very much. Thank you.

For my grandparents, Jim and Carol Hopkins

TABLE OF CONTENTS

LIST OF FIGURES

LIST OF TABLES

ABSTRACT

Biofilms are communities of microorganisms that have intrinsically antimicrobial properties and are difficult to treat in the clinical setting. The marine bacterium *Vibrio fischeri* efficiently colonizes its symbiotic squid host, *Euprymna scolopes*, by producing a transient biofilm dependent on the symbiosis polysaccharide (SYP), making it the perfect model system to study biofilm dynamics. *In vitro*, however, wild-type (WT) strain ES114 fails to form SYP – dependent biofilms. Instead, genetically engineered strains, such as those lacking the negative regulator BinK, have been developed to study SYP biofilms. Historically, *V. fischeri* has been grown using LBS, a complex medium containing tryptone and yeast extract; supplementation with calcium is required to induce biofilm formation by a *binK* mutant. Here, I discovered that yeast extract inhibits biofilm formation, which allowed us to uncover signals and underlying mechanisms that control *V. fischeri* biofilm formation.

In contrast to its inability to form a biofilm on unsupplemented LBS, a *binK* mutant formed cohesive, SYP – dependent biofilms when grown in tTBS without supplementation. Further, WT formed SYP- dependent biofilms when both calcium and the vitamin para-aminobenzoic acid (pABA) were present; neither molecule alone was sufficient, indicating that this phenotype relies on coordinating two cues. Cells grown in tTBS with pABA/calcium were enriched in transcripts for biofilm-related genes and predicted diguanylate cyclases, which produce the second messenger cyclic – di – GMP (c-di-GMP). They also exhibited elevated levels of c-di-GMP, which were required for biofilm formation as phosphodiesterase overproduction abrogated biofilm formation.

I also determined that these SYP – dependent biofilms were reliant on the positive *syp* regulator RscS, as the loss of this sensor kinase abrogated biofilm formation and *syp* transcription. This result was significant because the loss of RscS exerts little to no effect on biofilm formation under other genetic and media conditions. Deletion or mutations in the sensory domain(s) of RscS also resulted in a loss of biofilm formation, suggesting that RscS might be the primary sensory regulator. Overexpression of *rscS* on a multi-copy plasmid, but not the corresponding vector control, permitted biofilm formation on media supplemented with pABA alone, supporting the hypothesis that RscS may be responsible for recognizing the pABA signal. Another key sensor kinase in the *syp* regulatory network is SypF, which acts as the central regulator funneling phosphoryl groups from RscS to phosphorylate the response regulator; SypG. Expression of an RscS-SypF chimera that contains the N-terminal domains of RscS fused to the C-terminal HPT domain of the required sensor kinase SypF was sufficient to promote biofilm formation on media supplemented with only pABA as long as a full-length copy of *rscS* was also present. Lastly, pABA induced biofilm formation when I introduced *rscS* into a heterologous system that does not respond positively to pABA. These data suggest that RscS might be responsible for recognizing pABA to induce biofilm formation. This work thus provides insight into signals and regulators that promote biofilm formation by *V. fischeri* and a role for RscS in recognizing the environment to induce biofilm formation.

CHAPTER ONE

LITERATURE REVIEW

Introduction

Bacteria recognize and respond to various signals in their environment and adapt accordingly. These signals can include temperature, pH, nutrients, small molecules, and even surfaces. Once sensed, these cues provide bacteria with information concerning their location and can promote adaptation of bacterial behavior necessary for survival in their current environment. One of those adaptations is regulating gene expression that can promote biofilm formation, or a community of microorganisms connected by a protective matrix of secreted polysaccharides, proteins, and/or other molecules. Various signals promote biofilm formation, including glucose sugars, amino acids, polyamines, and calcium (Karatan and Watnick 2009). Sensors sense these signals from the environment, resulting in a signal cascade down to a response regulator that turns on or off gene expression. Signal transduction itself is tightly regulated as the cost of turning on the expression of unnecessary genes at the wrong time could be deadly. This regulation occurs in various organisms, including pathogens, commensals, and symbionts.

The *Vibrio fischeri – Euprymna scolopes* symbiotic relationship is a well-studied, excellent model for host-microbe interactions in the context of biofilm formation (Visick, Stabb, and Ruby 2021; Nyholm and McFall-Ngai 2021). *V. fischeri* colonization is driven both by the bacterium and its squid host; an essential part of initiating this process is the formation of a biofilm on the surface of the squid's light organ. Several signals have been

identified that alter genetically modified *V. fischeri* biofilm formation, such as nitric oxide (NO) and calcium (Thompson et al. 2019; Tischler et al. 2018). However, none of these signals alter wild-type *V. fischeri* biofilm formation. My dissertation focused on identifying a novel biofilm-inducing signal, para–Amino Benzoic Acid (pABA), and the mechanism(s) by which pABA induces wild-type biofilms.

In this first chapter of my dissertation, I will provide a comprehensive literature review necessary to understand and have context for the data I will present here. I will first describe sensor kinases, two-component systems, and the pertinent signals that initiate phosphorylation cascades. I will then describe essential biofilm formation steps and the role that cyclic-di-GMP plays in this formation. Next, I will detail the symbiotic relationship between *V. fischeri* and *E. scolopes*, the model used throughout my dissertation. Lastly, I will review what we know about *V. fischeri* biofilm formation and the controlling signals.

Two – Component Systems, Sensor Kinases and Signals

Introduction. In the broadest sense, bacteria need to be able to sense a change in the environment and react accordingly to promote survival. Bacteria have a wide array of signaling mechanisms that allow environmental sensing and, in turn, the up/down-regulation of genes that will allow them to survive under those conditions. A signal will activate a protein that will, either directly or indirectly through a signaling cascade, promote a response via a transcriptional regulator.

Sensor kinases are often called the “head” of this signaling cascade known as a two-component system. The kinase will sense the environmental cue, which triggers autophosphorylation (Sharan et al. 2017; Liu et al. 2018). From there, the phosphoryl group gets

directly donated to a receiver domain either on the same protein or from the sensor kinase to a response regulator (typically a transcriptional regulator) (Sharan et al. 2017; Liu et al. 2018).

Sensor kinases can sense a wide variety of environmental cues. Some examples of signals include pH, temperature, oxygen, and small molecules. It is likely that more than one of these signals, in conjunction with one another, triggers the signaling cascade and eventual transcriptional change(s). This section will review the current knowledge on two-component signaling, sensor kinases, and the signals that activate them.

Sensor kinase and two–component signaling. Two-component systems (TCS) are the predominant way bacteria sense and respond to their environment (Liu et al. 2018). At their most basic level, these systems consist of two main proteins; the sensor histidine kinase (HK) and a cognate response regulator (RR)(Fig.1a).

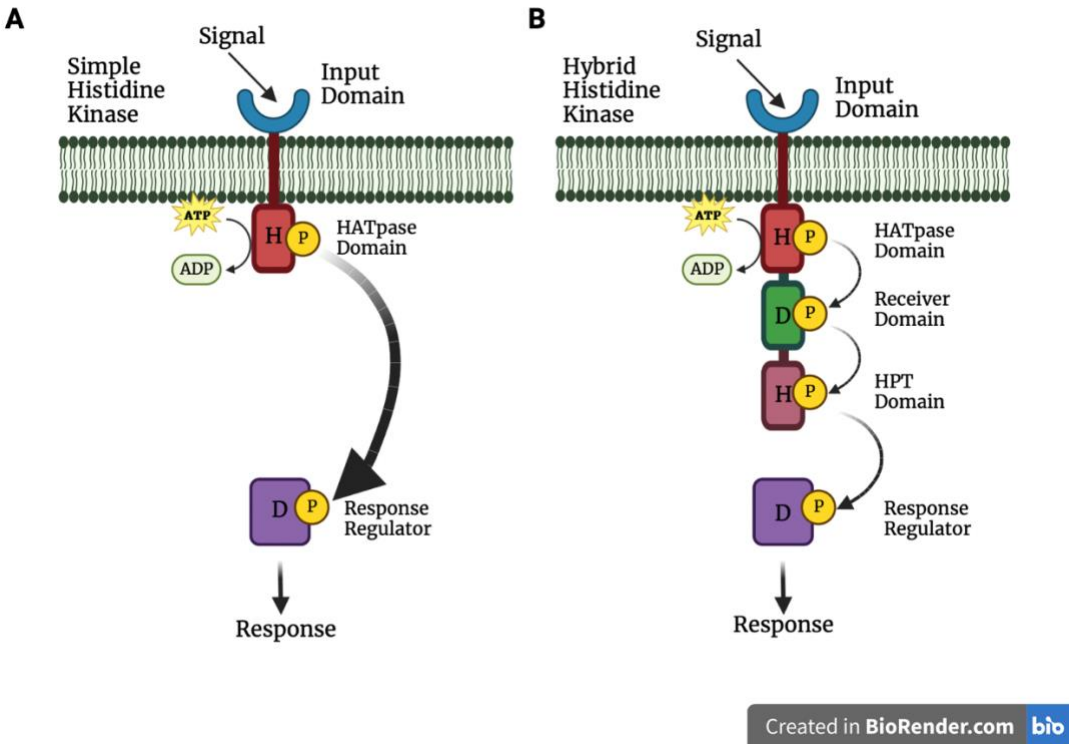

Figure 1. Two-Component Signaling Cascade: Image adapted from Sharan et al. 2017 and made in BioRender. (**A**) a simple signaling cascade, signal input results in autophosphorylation of the HK (HATpase domain). The phosphoryl-group is then donated to a RR, triggering a response to the input. **(B**) a hybrid TCS, signal input results in autophosphorylation of the HK (HATpase domain) which is then donated to the receiver domain on the same protein and then down to the HPT domain. The phosphoryl group on the HPT domain is then donated to the response regulator, triggering a response (Sharan et al. 2017).

Typically, sensor kinases are transmembrane proteins meaning they are localized to three cell compartments: the periplasmic space (in Gram negatives), the membrane, and the cytoplasm (Liu et al. 2018). HK sensing and transmission to the transmitter domain (sometimes referred to as the catalytic core) of the kinase is mediated by the variable domains at the N-terminus of the HK (Liu et al. 2018; Szurmant, White, and Hoch 2007). One of the most common sensory domains is the PAS domain, commonly referred to as the cytoplasmic signaling domain (Szurmant, White, and Hoch 2007). This domain is found in several signaling proteins, not just sensor kinases (Szurmant, White, and Hoch 2007). The corresponding signals bind to the area of the PAS domain that is not hindered in the lipid bilayer (Szurmant, White, and Hoch 2007). From there,

the PAS domain induces a structural change to modulate kinase activity. Presumably, when the PAS domain binds its ligands, it triggers autophosphorylation in the HK, and this phosphoryl group can then be passed down to the next domain in line.

HKs can be divided into three main groups, dependent on the phosphoryl group transfer domains present. First, and most simply, the HK can sense a specific signal and autophosphorylate a histidine reside in its histidine kinase/ATPase (HATPase) domain. From there, the phosphoryl group is donated to an aspartic residue in the receiver domain (REC) of the RR (Zschiedrich, Keidel, and Szurmant 2016; Gao and Stock 2009). The REC domain itself is a kinase and autophosphoylates using the phospho-histidyl residue as a phospho-donor (Wolfe 2010). This two-step phosphor-relay is commonly referred to as the classical version (Liu et al. 2018). The second type of TCS, known as the unorthodox version, has its HATPase domain on the HK followed by an additional REC and H2 domain which then, after transferred down the HK, the phosphoryl group is donated to the REC domain of the RR (Liu et al. 2018). The last version is a hybrid version where the signaling cascade is very similar to the unorthodox version. The only difference between the hybrid and unorthodox version is that the H2 domain is a phosphotransferase module that acts as an individual protein (HPT domain) (Gao and Stock 2009; Zschiedrich, Keidel, and Szurmant 2016) (Fig. 1b).

Once the RR is phosphorylated, it typically undergoes a conformational change, which activates effector domains and changes the signaling output (Liu et al. 2018). One such change would be the up/down-regulation of gene expression, resulting in cellular physiological changes (Liu et al. 2018), culminating in bacterial changes that allow the bacterium to better adapt and survive in its new/changed environment.

Known sensor kinase signals. Although a relatively understudied area, there are known signals, or ligands, that bind to sensor kinases to produce a response. As mentioned above, a typical signaling domain is the PAS domain, which can be separated into different sub-families. Several sub-families of PAS domains have ligands known to bind and signal. I will discuss a couple here, namely: PAS, PAS 4 and PAS 9. In *Azotobacter vinelandii*, cellular redox is tracked by the N-terminus of the PAS domain in NifL, which binds an FAD co-factor. Crystal structure analysis of the PAS domain of NifL found FAD-bound to the active site (Key et al. 2007). Efficient biofilm formation and root colonization capabilities in the rhizobacterium *Bacillus amyloliquefaciens* depend on the ResDE TCS (Zhou et al. 2018). ResDE has been shown to sense the NAD+/NADH pool through its PAS domain, stimulating its kinase activity and subsequent activation of the RR (Zhou et al. 2018). Lastly, 4 – hydroxycinnamic acid acts as a ligand for the PAS domain in *Halorhodospira halophila* and *Rhodospirillum centenum* (Mix et al. 2016).

In bacteria that contain a PAS 4 domain, such as *Pseudomonas putida* and *Pseudomonas mendocina*, differently substituted aromatic hydrocarbons act as ligands, and in *Xanthomonas campestris* pv. *Campestris*, different dodecanoic acids are the ligands for the PAS 4 domain (Busch et al. 2009; Busch et al. 2007; Lacal et al. 2006; Silva-Jimenez et al. 2012; Koh et al. 2016; An et al. 2014). PAS 4 has also been shown to be activated by O_2. In *Staphylococcus carnosus*, the NreB TCS responds to O_2 and controls, through the response regulator NreC, the expression of nitrate/nitrite respiration genes (Mullner et al. 2008; Klein, Kretzschmar, and Unden 2020).

Riboflavin, in *Erythrobacter litoralis*, has been shown to bind and activate PAS 9, resulting in signal transduction (Rivera-Cancel et al. 2014). Other PAS 9 activation signals include Zn (II)

in *Staphylococcus aureus,* which activates the WalKR TCS, the only essential TCS in *S. aureus* (Monk et al. 2019). FAD has also been shown to signal through TCS MmoS in *Methylococcus capsulatus* (Ukaegbu and Rosenzweig 2009).

Aside from the PAS domain, other domains might act as a sensor for ligands. These domains typically consist of loops between membrane-spanning segments, mainly in the periplasm. The ligands for domains of this class are also under investigation, and we know some of these for loop domains (Matilla et al. 2022). Numerous signals have been identified for sensor histidine kinases with two or more transmembrane (TM) regions where signals are sensed by the periplasmic segment connecting the TM regions. In *Enterococci spp.*, the $VanR_AS_A$ TCS is responsible for antibiotic resistance and is regulated by vancomycin and teicoplanin, which were found to bind $VanS_A$ at different affinities (Hughes et al. 2017). Vancomycin has also been shown to bind the TCS VanS from *Streptomyces coelicolor* (Lockey et al. 2020). Extra cytoplasmic ferric iron activates the PmrA/PmrB TCS in *Salmonella spp.,* which results in the transcription of PmrA – activated genes and resistance to the antibiotic polymyxin B (Wosten et al. 2000). ColRS is a TCS that, in many bacterial species, has been shown to contribute to membrane functionality and stress tolerance, as well as virulence and plant pathogenesis in *Pseudomonas putida*, *P. aeruginosa,* and pathogenic *Xanthomonas spp.*, respectively. ColRS is activated by excess iron, zinc, manganese, or cadmium, which results in modified gene expression of ColR – regulated genes (Ainsaar et al. 2014). Further, *Xanthomonas campestris* pv. *campestris* encodes a TM SK with an N-terminal segment in the periplasm with sensor function; this SK has been shown to bind to a diffusible signal factor (namely a medium–chain fatty acid) (Cai et al. 2017).

Calcium as a TCS signal. Several TCSs have also been identified to sense calcium and regulate gene expression, both positively and negatively. CvsSR is a TCS found in *Pseudomonas syringae* that positively regulates gene expression in response to calcium. CvsSR is required for pathogenicity and, after calcium stimulation, enhances transcription of the genes for the type 3 secretion system and sRNAs, which concurrently repress alginate and flagella biosynthesis (Fishman, Giglio, et al. 2018).

The most well-known TCS that senses calcium, among other signals, is PhoPQ. In numerous Gram-negatives including *E. coli*, *Pseudomonas aeruginosa*, *Yersinia pestis*, *Shigella flexneri*, and *Salmonella enterica*, calcium acts to negatively regulate gene expression (Garcia Vescovi, Soncini, and Groisman 1996; Vescovi et al. 1997; Lesley and Waldburger 2001; Chamnongpol, Cromie, and Groisman 2003; King et al. 2020). In *Vibrio cholerae*, the TCS CarRS is negatively regulated by calcium (Bilecen and Yildiz 2009). CarRS responds to calcium via downregulation of VpsR transcription. VpsR is the primary transcriptional regulator of the *Vibrio* polysaccharide (*vps*) locus, which synthesizes VPS, the main biofilm polysaccharide in *V. cholerae* (Bilecen and Yildiz 2009; Casper-Lindley and Yildiz 2004; Conner et al. 2017).

Coordinate signaling. Often, genes regulated by a network of TCS have multiple signal inputs that come together to elicit a response. Some of these networks concurrently rely on two separate signal inputs to upregulate gene expression. In *P. aeruginosa*, for example, the sensor kinases LadS and GacS recognize signals and then relay them through GacA, which eventually promotes biofilm formation and chronic infection (Ventre et al. 2006; Goodman et al. 2004). Further, LadS and GacS are antagonists of another sensor kinase, RetS. The RetS and LadS/GacS pathways all converge and control the transcription of the small regulatory RNA, RsmZ (Ventre et al. 2006; Goodman et al. 2004). This interplay and reliance on more than one

sensor kinase to elicit an effect is how *P. aeruginosa* tightly controls whether it produces a chronic or acute infection within a human host.

Another example, in *Vibrio* species, is the signaling mechanism through which luminescence is induced. Two autoinducers signal through two separate sensor kinases to upregulate luminescence transcription (Henke and Bassler 2004; Lupp and Ruby 2004). The two synthases, LuxS and AinS, both function to control luminescence in *V. fischeri* and will be discussed in greater detail in a later section (Lupp and Ruby 2004). Luminescence is a costly phenotype/mechanism and must be turned on properly during colonization. Therefore, luminescence regulation is not controlled by one regulator/signal alone but rather by multiple to ensure proper activation at the right time and place.

Summary. There are an abundance of ways bacteria can control the expression of specific genes. One of the most common ways is through two-component systems. Regulation is likely an entire network of two-component systems that control energetically taxing genes. These systems/networks can then be turned on by signals that ensure proper expression. For example, when a bacterium is at a specific location, a specific signal, which might only present within a host, will elicit a response from the bacterium to turn on gene expression at the appropriate moment. Calcium is one molecule known to regulate expression of genes via TCSs, and although regulators like PhoPQ are well-researched, most TCSs have yet to have their signal identified. The lack of known signals highlights a significant and vital area of investigation in the TCS research field. TCSs work to control numerous systems among broad genera of bacteria, all responding to different stimuli, making TCSs excellent tools in bacterial toolboxes to control gene expression with precision. Lastly, due to the nature of these tightly regulated genes being at

some fitness advantage, there are cases where these genes will be regulated by multiple signals to ensure proper expression.

Biofilms and Cyclic – di - GMP

Introduction – biofilms. Biofilms are the most common bacterial community in the environment (Flemming and Wuertz 2019; O'Toole, Kaplan, and Kolter 2000). A biofilm is a complex community of microorganisms surrounded by an extracellular matrix that allows them to adhere to surfaces and each other. Bacteria within the biofilm are embedded within this secreted and protective extracellular matrix composed of polysaccharides, extracellular DNA, and proteins (Flemming and Wingender 2010; Flemming et al. 2016). This matrix serves not only to help bacteria adhere to surfaces but also to protect them from a variety of environmental stresses such as antibiotics, desiccation, predation, and the host immune system (Sutherland 2001; Flemming, Neu, and Wozniak 2007; Matz et al. 2005; Chang et al. 2007). Due to these advantageous properties that biofilms confer to bacteria, biofilms have become a major scourge in the medical, industrial as well as environmental fields (Cunliffe, Upstill-Goddard, and Murrell 2011; Dobretsov, Abed, and Teplitski 2013; Beloin et al. 2014), which I will further elaborate on in the next section. I will then introduce the stages of biofilm development: initiation/attachment, maturation, and dispersal (Fig. 2). Lastly, I will introduce the second messenger c-di-GMP and explain the connection between c-di-GMP and biofilm formation.

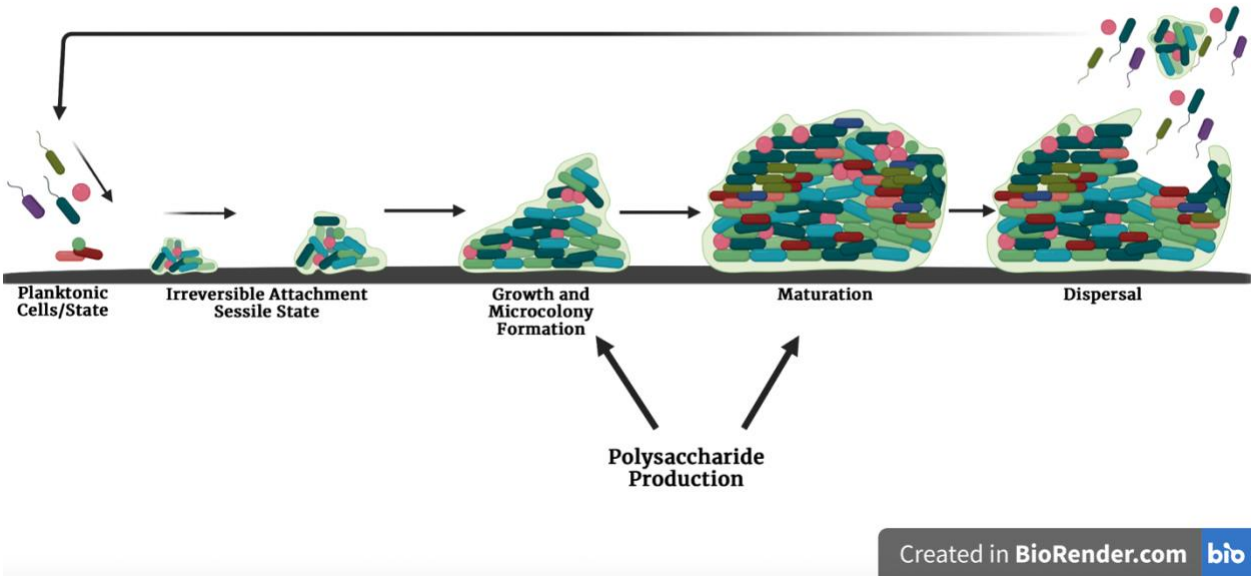

Figure 2. Diagram of Biofilm Formation: Image adapted from Magana et al. 2018 and made in BioRender. Planktonic cells reversibly attach to an ideal surface, such as a nutrient rich environment. The bacteria then attach, irreversibly and grow into a multicellular community in a sessile state of life. The community grows and as it matures begins to produce polysaccharides. Once nutrients become depleted or a signal is received a portion of the biofilm bacteria will transition to a planktonic state of life and begin the cycle again (Magana et al. 2018).

Biofilm significance. In the medical field, pathogenic bacteria encased in a biofilm are associated with numerous diseases and chronic infections (Donlan 2002). For example, the biofilms that can and do form on various prosthetic devices and catheters cause persistent and chronic infections that clinicians have an increasingly difficult time treating. Bacteria within these biofilms have a lower susceptibility to antimicrobials than their planktonic cell counterparts, making treatment of biofilms in the human body a challenge (Bryers 2008). Further, industrial fields that revolve around the ocean also have challenges due to biofilms, as biofilms readily form on wet aquatic surfaces. These biofilms can lead to ship drag and metal corrosion, which culminates in an increase in fuel consumption resulting in industrial waste

(Chambers et al. 2006). Lastly, biofilms that form on the nets and cages in fish farms affect both fish health and yield (Braithwaite and McEvoy 2005).

There are also numerous benefits that biofilms offer the environment as a whole. Natural biofilms that form in rivers and streams offer food for the bottom-chain organisms. Biofilms also form around plant roots, helping them gather nutrients from the environment/soil and providing nitrogen fixation for plants (Wang et al. 2017). Lastly, biofilms that form in the human gut might provide protection from pathogens entering the environment as well as helping the host uptake important bacterial metabolites, but the work in this field is ongoing and is sure to expand our knowledge of gut microbiome biofilms (Motta et al. 2021).

Initiation/attachment. Biofilms form when planktonic bacteria respond to an environmental cue that facilitates bacterial attachment to a surface (Stanley 1983) (Fig. 2). The subsequent stages of biofilm formation are, then, typically related to a foreign surface after the initial sensing and interaction (Kostakioti, Hadjifrangiskou, and Hultgren 2013; Rumbaugh and Sauer 2020). This initial attachment is reversible if the bacteria sense that the conditions on the surface are not favorable (Donlan 2002; Kostakioti, Hadjifrangiskou, and Hultgren 2013). This initial attachment is mediated by surface molecules that promote attachment via the bacteria, such as flagella, pili, and LPS (O'Toole and Kolter 1998; Pratt and Kolter 1998; Watnick and Kolter 1999). Many species of bacteria express attachment molecules that have surface-sensing functions (Cairns et al. 2013). To then remain on the surface and attach irreversibly, attachment organelles such as the pili, curli, and adhesins of the bacteria must maintain their grip on the surface and spread to cover more area (Pratt and Kolter 1998; Shrout et al. 2006; Donlan 2002; Kostakioti, Hadjifrangiskou, and Hultgren 2013). After irreversible attachment, the biofilm can grow and mature before eventually dispersing.

Maturation. As described above, attachment to a surface or other bacteria triggers a change in gene expression that moves the bacteria from a planktonic to a sessile state (Fig. 2). This stage of development is called maturation and is also where polysaccharide production begins. Bacteria produce and secrete the matrix components of the biofilm, which accounts for nearly 90% of its dry mass (Flemming and Wingender 2010). The extracellular matrix, produced via the bacteria, protects against a multitude of things, including UV, predation, shifts in pH, desiccation, and the host immune system (Elasri and Miller 1999; Matz et al. 2005; Davey and O'Toole G 2000; Chang et al. 2007; Donlan and Costerton 2002). The matrix also encases the cells and gives the biofilm its shape, which varies from mushroom-shaped forms to dense, diverse microbial mats, micro-clusters, and monolayers (Flemming et al. 2016; Persat et al. 2015; Kostakioti, Hadjifrangiskou, and Hultgren 2013).

The organization of the cells and the matrix itself will also limit the diffusion of resources to the lower layer of the cells. The resource gradient, and lack of resources in certain positions within the biofilm, will facilitate the formation of channels and pores throughout the biofilm, allowing for an exchange of nutrients. These channels and pores also aid in communication between species; however, nutrient, oxygen, pH, and quorum-sensing molecule gradients arise, leading to a very heterogenous cell population. The heterogeneous bacterial cells perform different functions in the biofilm depending on their niche (Vlamakis et al. 2008; Lopez, Vlamakis, and Kolter 2009). This bacterial heterogeneity correlates to the biofilm's ability to withstand all environmental stressors (Boles et al. 2004). Lastly, during maturation, there is an increased rate of genetic exchange and secondary metabolite production, which can facilitate a more diverse population and an upregulation of specific genes (O'Toole, Kaplan, and Kolter 2000).

Dispersal. The last stage in biofilm development is dispersal (Fig. 2). Dispersal is thought to occur due to overcrowding or a lack of nutrients in an old/aged biofilm and is defined as an active event where sessile bacteria convert to a more planktonic-like condition that can be induced by a variety of factors (Rumbaugh and Sauer 2020). The inducing signals of dispersal include autoinducers, small molecules such as nitric oxide (NO), oxygen, iron, fatty acid signaling, and nutrient availability (Barraud et al. 2006; Cutruzzola and Frankenberg-Dinkel 2016; Rumbaugh and Sauer 2020; Kostakioti, Hadjifrangiskou, and Hultgren 2013). After this signal is received, a subpopulation of cells within the biofilm will recognize the signal, which induces genetic and metabolic changes that eventually lead to the breakdown of the biofilm matrix (Purevdorj-Gage et al. 2005). The breakdown of the matrix occurs via degradative enzymes such as endonucleases and glycoside hydrolases (Gjermansen et al. 2005; Mann et al. 2009; Rumbaugh and Sauer 2020) and allows motile cells to leave the matrix. The cells that leave the biofilm, however, have not fully returned to their planktonic way of life and instead are somewhere between sessile and motile as they express flagella and motile elements while still retaining their virulency and adhesion abilities (Rumbaugh and Sauer 2020). This middle-ground phenotype is short-lived as bacterial cells quickly readjust to being fully planktonic (Rumbaugh and Sauer 2020).

Introduction – c-di-GMP. Bis (3’ – 5’) cyclic dimeric guanosine monophosphate (c-di-GMP) is a small ubiquitous second messenger that numerous bacteria use to modulate behavior, including biofilms formation, motility, and virulence (Romling, Galperin, and Gomelsky 2013; Valentini and Filloux 2016). As shown in Figure 3, c-di-GMP is synthesized from 2 GTP molecules via a diguanylate cyclase (DGC) in a two-step reaction that results in a 5’ – pppGpG intermediate and two pyrophosphate bioproducts (Ross et al. 1987). DGC proteins contain a

conserved GGDEF domain. After activation, DGCs form catalytically active homodimers whose active site is at the dimer interface (Tal et al. 1998; Paul et al. 2007; Romling, Galperin, and Gomelsky 2013) these homodimers then synthesize c-di-GMP. C-di-GMP is then broken down into a 5-pGpG intermediate via a phosphodiesterase (PDE), which contains a characteristic EAL or HD-GYP domain; this intermediate is then broken down further into GMP (Ross et al. 1987; Tal et al. 1998; Galperin et al. 1999).

The number of DGCs and PDEs within a bacterial genome can vary greatly, depending on the species; however, many organisms contain numerous c-di-GMP-related genes, which points to the importance of c-di-GMP as a signaling molecule (Romling, Galperin, and Gomelsky 2013). The activation signals for DGCs and PDEs is as diverse as the amount within a given species. The signal for DGC/PDE activation is often linked to environmental cues and signal transduction pathways as sensor domains are common domains found within DGCs and PDEs (Romling, Galperin, and Gomelsky 2013). In the last bit of this section, I will examine the known relationship between c-di-GMP and biofilm formation.

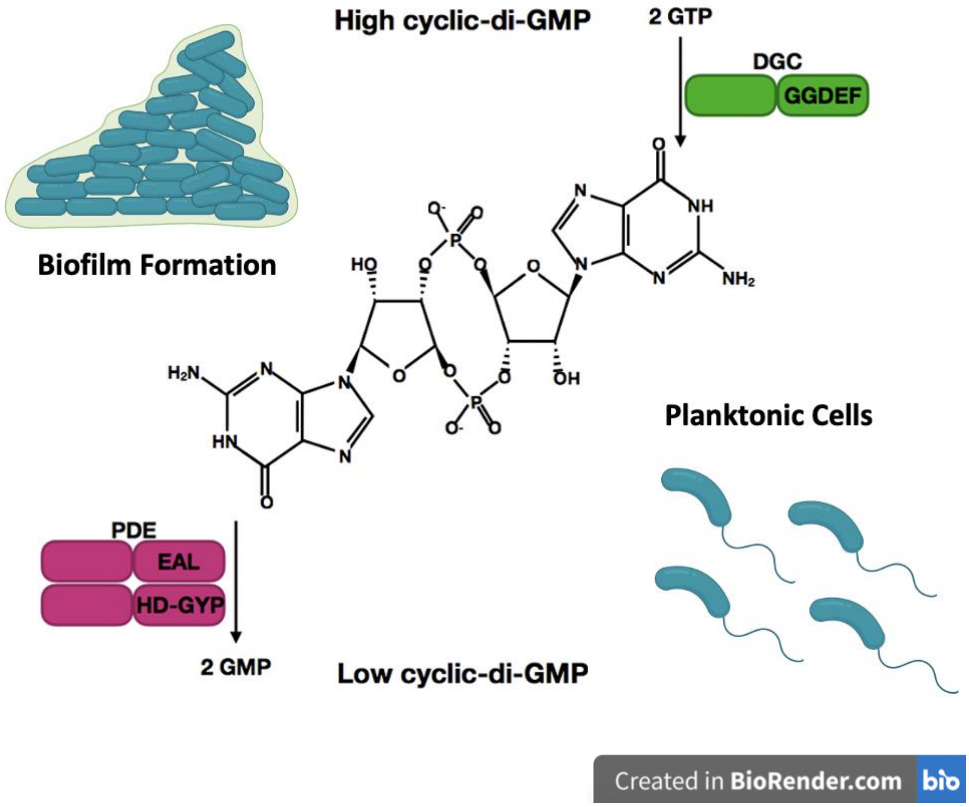

Figure 3. C-di-GMP Production and Biofilm Formation: Image adapted from a figure developed by Dr. Alice Tischler using BioRender. C-di-GMP is synthesized from 2 GTP via a diguanylate cyclase (DGC) with a characteristic GGDEF domain. C-di-GMP (the molecule in the middle) is broken down into 2 GMPs via a phosphodiesterase (PDE) with a characteristic EAL or HD-GYP domain. High levels of c-di-GMP are associated with sessile or a biofilm state of living bacteria. Low levels of c-di-GMP are associated with planktonic/free-living bacteria.

C-di-GMP and biofilm formation. The link between c-di-GMP and biofilm formation has been theorized to be the following: high levels of c-di-GMP lead to sessile bacteria, and low levels of c-di-GMP lead to planktonic bacteria (Fig. 3) (Romling, Galperin, and Gomelsky 2013). This theory has been shown to be true across a wide variety of biofilms and species; however, the mechanisms behind how c-di-GMP regulates biofilms behaviors vary greatly and can be species-specific (Romling and Galperin 2015; Romling, Galperin, and Gomelsky 2013). The first link between c-di-GMP and biofilm formation was between c-di-GMP and cellulose production such that c-di-GMP is a critical co-factor without which the cellulose synthase

enzyme was non-functional and this link has only been strengthened over time (Ross et al. 1987). Outside of cellulose production, a role for c-di-GMP was not established until 2004 and has since been implicated in the production of numerous polysaccharides across a variety of species at multiple levels of control (Paul et al. 2007; Tischler and Camilli 2004).

There are many examples in which increased levels of c-di-GMP lead to an increase in transcription of genes for polysaccharide synthesis, such as in *P. aeruginosa* and *V. cholerae.* In *P. aeruginosa,* c-di-GMP binds to the transcriptional regulator FleQ and promotes the transcription of both the *pel* and *psl* genes, which ultimately results in the upregulation of the PEL and PSL polysaccharides leading to biofilm formation (Hickman and Harwood 2008; Baraquet et al. 2012; Lee et al. 2007). A similar mechanism can be found in *V. cholerae*, where c-di-GMP directly binds to the transcriptional regulators VpsR and VpsT to active the expression of the *vps* gene locus, which produces Vibrio polysaccharide, upregulating biofilm formation (Zamorano-Sanchez et al. 2015).

There are also several biofilm-associated regulators that c-di-GMP controls post-transcriptionally. In *Escherichia coli, Komagataeibacter xylinus,* and *Rhodobacter sphaeroides*, c-di-GMP binds to and activates the cellulose synthase complex of BcsA – BcsB in order to produce and translocate cellulose, inducing biofilm formation (Morgan, McNamara, and Zimmer 2014). C-di-GMP also controls curli production in both *E. coli* and *Salmonella enterica* through the upregulation of *csgD* both transcriptionally and post-transcriptionally. After upregulation, CsgD activates the *csgBAC* operon, encoding the subunits of culi, which increases biofilm formation (Tagliabue et al. 2010; Sommerfeldt et al. 2009). Overall, there are multiple mechanisms and organisms in which c-di-GMP plays a role in biofilm formation to some extent, showing its utilitarianism throughout the bacterial domain of life.

Summary. Biofilms are a crucial component of life, both positive and negative, that have implications in our everyday. Biofilms are found throughout the environment, whether in a human patient or the outside environment. There are multiple stages in biofilm formation, which involve vital steps to create this stable microenvironment that can help many bacterial species grow and survive. Biofilms are also intimately linked with the levels of the second messenger, c-di-GMP, and although c-di-GMP is not the whole story, it is a central part of how bacteria form these protective forms of life. Given the importance of biofilm formation and the implications that biofilms have across all domains of life, it is imperative to develop models to study biofilm formation in all aspects and fully understand this complex way of living.

The *Vibrio fischeri* – *Euprymna scolopes* Symbiosis

Introduction. One of the most well-characterized models for bacterial-host interactions is the symbiotic relationship between the marine bacterium *Vibrio fischeri* and its Hawaiian bobtail squid host, *Euprymna scolopes.* This host-microbe symbiosis has provided remarkable scientific insights into both bacterial and host processes due, in part, to the ability to assess both partners separately and together. This wealth of knowledge is also readily obtainable due to the easy manipulation that can be done to both partners. *V. fischeri* is a highly genetically tractable organism that can be readily grown and manipulated in the laboratory (Visick et al. 2018; McFall-Ngai 2014; Visick, Stabb, and Ruby 2021; McFall-Ngai and Bosch 2021) and *E. scolopes* can be well maintained in an artificial marine system and can be readily bred for colonization experiments.

Many host-relevant phenotypes have been well-defined for *V. fischeri,* including biofilm formation, motility, chemotaxis, and luminescence, which makes phenotypic characterization of mutants easy. Inoculation of an aposymbiotic juvenile squid can occur quickly, sometimes in as

little as 15 minutes (Bongrand et al. 2016) and can be monitored through various techniques such as bacterial enumeration, luminescence, microscopy, and RNAseq. As *V. fischeri* is the exclusive colonizer of the squid's symbiotic (light) organ, this model allows us to test specific hypotheses and assess specific colonization requirements for both partners. In this section, I will describe the steps in colonization and the factors that impact symbiosis.

Initiation. Newly hatched juvenile *E. scolopes* hatch aposymbiotic, lacking *V. fischeri,* and therefore must acquire the marine bacterium from the environment. *V. fischeri* is at a very low abundance in the ocean and only represents a small fraction of all the bacteria in that environment (Lee and Ruby 1995; Lee and Ruby 1992). Nevertheless, colonization of the squid is highly specific, as *V. fischeri* is the sole colonizer of a specialized symbiotic organ known as the light organ (McFall-Ngai and Ruby 1991). In order for this colonization to occur, the squid ventilates seawater through the mantle cavity and across the symbiotic organ, but the amount of seawater ventilated is minuscule (~1uL) (McFall-Ngai and Montgomery 1990; Ruby and Lee 1998) (Fig 4). Therefore, both the squid host and the bacteria have developed specialized mechanisms to increase colonization chances. Newly hatched/hatching *E. scolopes* have a partially developed light organ complete with a ciliated epithelial field located on the surface (McFall-Ngai and Montgomery 1990). The light organ is a bilobed structure that takes up most of the mantle cavity; the cilia on the organ help to circulate seawater containing *V. fischeri,* increasing the odds of colonization (Fig. 4).

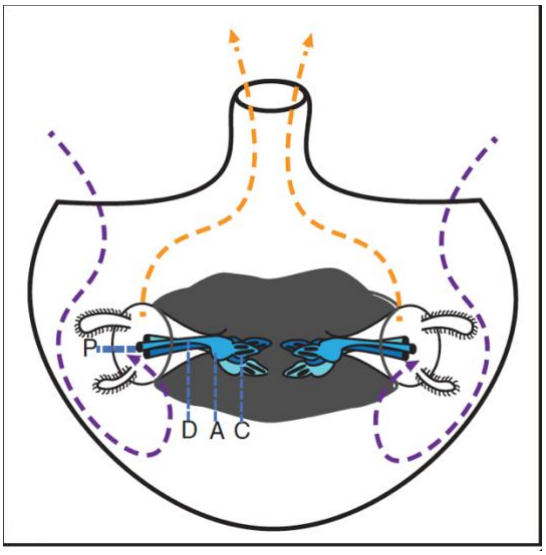

Figure 4. Path of Seawater Ventilation in *E. scolopes.* Image adapted from Alice Tischler 2019 (Tischler, Hodge-Hanson, and Visick 2019). The flow of water across the symbiotic organ of *E. scolopes.* Seawater containing *V. fischeri* is ventilated across the symbiotic organ (purple lines) through the six pores (P) which each lead to separate ducts (D). After the ducts *V. fischeri* travels into the antechambers (A) and into the deep crypt spaces (C). Ventilation then occurs by route of the orange lines, after the night cycle.

The light organ is divided into two sections, each of which contains three pores leading to the organ's interior. The pore leads to ciliated ducts, eventually opens to the antechamber, which then leads into the crypt space (McFall-Ngai and Montgomery 1990; Montgomery and McFall-Ngai 1998; Sycuro, Ruby, and McFall-Ngai 2006). Bacteria travel through these spaces and replicate within the crypt space, and once *V. fischeri* reaches a high enough cell density, the cells begin to bioluminesce, an essential step for persistence of the symbiosis (Visick et al. 2000; Koch et al. 2014) (Fig. 5). The light produced by *V. fischeri* protects the squid from predation in a process called counterillumination (Jones 2004), where the squid diffuses the light to mask its silhouette on the ocean floor. As the squid is nocturnal, masking is crucial to protect them during their food hunt (Ruby 1996). While the squid needs the light *V. fischeri* provides for survival, the bacterium has a nutrient-rich environment within the light organ to thrive in; however, it must

avoid or withstand the innate immune cells and antimicrobials present within the organ in order to survive (McAnulty and Nyholm 2016).

Recruitment and restriction of bacteria via the host. As mentioned, this symbiotic relationship is highly specific to *V. fischeri;* therefore, the squid has various mechanisms to prevent colonization by non-symbiotic bacteria in the environment. There are two types of cilia on the surface of the light organ, long (~25μM) and short (~10μM), which are on the appendages and work together to create a flow that draws in organisms of <4μM to a sheltered zone near the entry of the pores and move larger particles >4μM away from the light organ (Nawroth et al. 2017). This sorting scheme allows the squid to select for small bacterial species, such as *V. fischeri*, to the sheltered zone. The sheltered zone contains signaling, specificity, and effector molecules sensed by both the host and symbiont to promote colonization (Nawroth et al. 2017). The ciliated epithelial cells on the surface of the light organ begin to secrete mucus a process triggered by the presence of peptidoglycan and other microbe-associated molecular patterns (MAMPs), which suggests that this response is to bacteria in general and not a specific strategy to identify *V. fischeri* (Nyholm et al. 2002; Nyholm et al. 2000; Nyholm and McFall-Ngai 2004).

Nitric oxide (NO) is a small, diffusible molecule involved in eukaryotic cell signaling and innate immunity found in the squid's mucus (Wang and Ruby 2011). During *V. fischeri* colonization, NO acts as an antimicrobial agent restricting the aggregation of both symbiotic and non-symbiotic organisms within the host mucus (Davidson et al. 2004). *V. fischeri* can respond to NO signals through HnoX and NsrR (NO-sensing proteins), which leads to an alteration of iron metabolism and detoxification pathways to prepare for later stages of colonization (Davidson et al. 2004; Wang and Ruby 2011). Once colonization is complete, *V. fischeri* releases tracheal cytotoxin (TCT) and lipopolysaccharide (LPS), which trigger *E. scolopes* to reduce NO

production (Altura et al. 2011). The complex interplay between squid and bacteria highlights the importance of NO as a signaling molecule during colonization.

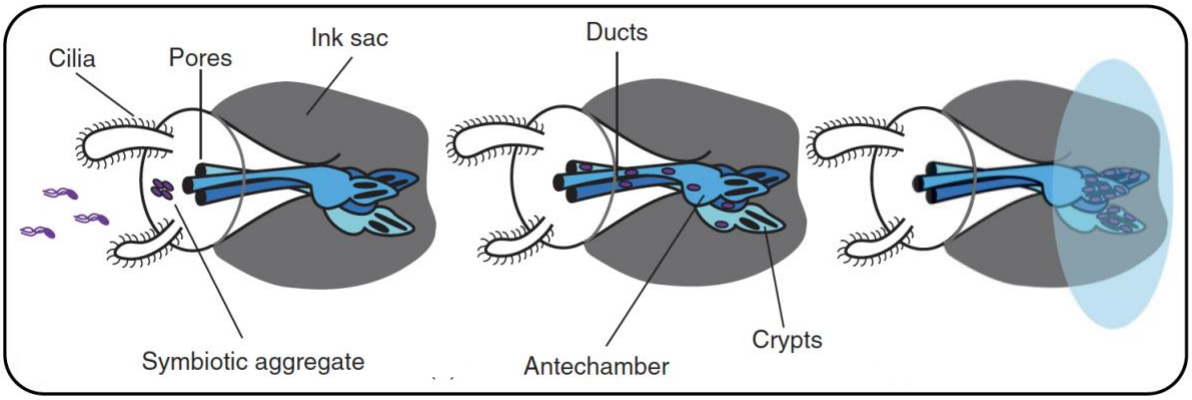

Figure 5. Colonization of *E. scolopes* by *V. fischeri*. Image from Tischler et al., 2019 (Tischler, Hodge-Hanson, and Visick 2019). Planktonic *V. fischeri* (purple) are brought in towards the light organ via circulating seawater and the ciliated appendages. *V. fischeri* then forms a symbiotic aggregate (biofilm) on the surface of the light organ before dispersing and entering one of the six pores. The bacterium then travel from the ducts, through the antechamber, before eventually reaching the deep crypt spaces. Once inside the crypts *V. fischeri* will reach a high enough cell density to start producing light (blue circle).

Biofilm formation. As mentioned above, *V. fischeri* has developed mechanisms to colonize *E. scolopes* despite the inhospitable nature of the squid's mucus. First, *V. fischeri* binds to the cilia and forms an aggregate of cells in the mucus on the surface of the light organ (Altura et al. 2013; Nyholm et al. 2000). Further, this aggregate of cells represents the first biofilm *V. fischeri* forms during colonization (Nyholm et al. 2000; Flemming and Wingender 2010; Yip et al. 2006).

Biofilm formation by *V. fischeri* is primarily controlled by the symbiosis polysaccharide (Syp) pathway, an extensive two-component signaling network (Hussa, Darnell, and Visick 2008; Yip et al. 2006; Yip et al. 2005). The Syp pathway regulates the production of the Syp polysaccharide (SYP), the major component of the biofilm matrix, along with other polysaccharides, such as cellulose. SYP permits surface aggregation and bacterial cell-cell interactions. *V. fischeri* uses SYP production/ surface aggregation to initiate symbiosis and

colonize the squid. *V. fischeri* strains that are unable to make SYP cannot form aggregates of cells or efficiently colonize *E. scolopes* (Yip et al. 2006). Conversely, cells that are hyper-aggregators/exhibit enhanced biofilm formation display a colonization advantage over their wild-type counterparts (Bongrand and Ruby 2019; Yip et al. 2006; Nyholm et al. 2000; Morris and Visick 2013a). The Syp pathway and its two-component regulators will be described in greater detail in later sections.

Dispersal. In order to enter the light organ, the bacteria must disperse from the biofilm and enter a planktonic lifecycle to travel through one of the six pores (Fig. 5). The mechanism of bacterial dispersal from the aggregate on the light organ is still unknown, and an active area of research; however, it is known that flagella-based motility and chemotaxis direct movement towards the pores (Nyholm et al. 2000; Mandel et al. 2012). Only bacteria able to disperse and become motile can reach the crypt spaces and colonize the squid, as non-motile strains exhibit colonization defects (Graf, Dunlap, and Ruby 1994; Millikan and Ruby 2002, 2004; Wolfe et al. 2004). Hyper-flagellated mutants also fail to colonize, demonstrating that proper flagellation/propulsion is crucial for squid colonization (Millikan and Ruby 2002). Motility in *V. fischeri* is mediated via the 1 – 5 sheathed flagella located at the pole of the cell (Millikan and Ruby 2002). *V. fischeri* cells perform chemotaxis, a mechanism that allows motile bacteria to move towards an attractant through chemotaxis gradients that lead into the light organ. *V. fischeri* encodes conserved proteins shown to be involved in chemotaxis, indicating it has evolved for squid colonization (DeLoney-Marino, Wolfe, and Visick 2003; Deloney-Marino and Visick 2012; Hussa et al. 2007; Brennan, DeLoney-Marino, and Mandel 2013). *V. fischeri* performs chemotaxis to a variety of substrates, including N-acetylneuraminic acid (NANA), N – acetylglucosamine (GlcNAc), and the disaccharide $(GlcNAc)_2$, the latter two being chitin

derivatives (Wier et al. 2010; Mandel et al. 2012; Nyholm et al. 2000; DeLoney-Marino, Wolfe, and Visick 2003). The apical surface of the ciliated epithelium contains chitin synthases that are concentrated around the pores (Kremer et al. 2013) and the chitin derivatives, further inside the pores (like those mentioned above), are likely generated via host degradation of chitin (Kremer et al. 2013). Due to *V. fischeri* performing chemotaxis to chitin subunits, it is clear that *V. fischeri* has developed chemotactic mechanisms to sense squid-derived products to enter the light organ and eventually colonize the deep crypt spaces (Mandel et al. 2012).

Colonization. For *V. fischeri* to successfully colonize *E. scolopes,* the cells must survive the antechamber and passage through a bottleneck to reach the deep crypt spaces (Nyholm et al. 2002). Once in the crypt space, the environment allows for metabolite exchange and signals for luminescence. Multiple strains of *V. fischeri* can colonize a single light organ since each of the six pores leads to a distinct crypt space (Bongrand and Ruby 2019; Visick, Stabb, and Ruby 2021). The anatomy of the squid and metabolites within contribute to the dynamic relationship between *E. scolopes* and its symbiotic partner.

Bioluminescence. The viability of *E. scolopes* does not depend on colonization by *V. fischeri* (Claes and Dunlap 2000), suggesting that the major contribution that *V. fischeri* brings to the symbiotic relationship is its ability to bioluminesce (Fig. 5). Bioluminescence can begin 12 hours after initial colonization and allows the squid to camouflage via counterillumination (as described above) (Stabb 2009; Jones 2004). *E. scolopes* can direct and change the intensity of the light emitted through a muscle-controlled ink sac, a lens, and reflective proteins in the tissues surrounding the light organ (Mandel and Dunn 2016; Montgomery and McFall-Ngai 1992). The squid's ability to modulate light is crucial in adapting to the day/night cycle.

In *V. fischeri*, light production is mediated through the *lux* operon. The *lux* operon encodes the luciferase enzyme as well as the substrates, byproducts, and metabolites for the light reaction (Reviewed in (Stabb 2008) and (Visick, Stabb, and Ruby 2021)). The *lux* operon is controlled via quorum sensing, a mechanism that allows populations of bacteria to coordinate gene expression/behavior using signaling molecules, or autoinducers, inducing gene expression dependent on population density (Stabb 2008). The *lux* pathway is tightly controlled as LuxI produces the autoinducer *N* – 3 – oxohexanoyl-homoserine lactone (3 – oxo-C6); 3-oxo-C6 diffuses across the cell membrane to equilibrate autoinducer levels inside and outside of the cell. As the density of *V. fischeri* increases, so do the levels of 3-oxo-C6. Further, as the concentration of 3-oxo-C6 increases so does the probability that binding will occur. When the probability is high enough and there are sufficient amounts of the 3-oxo-C6-LuxR complex, this stable complex will activate transcription the *lux* genes, inducing bioluminescence. Two other quorum sensing systems are involved in light production/that regulate this pathway: AinS/AinR and LuxS/LuxP/LuxQ (Stabb 2008; Miyashiro and Ruby 2012).

In order to promote successful and long-term colonization of *E. scolopes, V. fischeri* must bioluminesce as mutants defective for luminescence do initially colonize but do not persist or induce normal development of the host light organ (Visick et al., 2000). Further, squid colonized with *lux* mutants can be recolonized, indicating that *lux* mutants cannot relay to the host that colonization has already occurred (Koch et al. 2014). *E. scolopes* produces phototransduction proteins (Chun et al. 2008; Mandel and Dunn 2016), which possibly allow the squid to sense colonization, highlighting the importance of light production in this symbiotic relationship.

Light organ interactions. Until recently, colonization and symbiosis were almost exclusively studied with a single bacterial strain isolated from the *E. scolopes* light organ, *V.*

fischeri ES114. However, exploring additional isolates, including those collected from *E. scolopes* in two distinct Hawaiian bays, has increased insights into *V. fischeri* colonization mechanics (Bongrand et al. 2016).

The exploration of these diverse isolates showed that strains of *V. fischeri* compete with one another for space in the light organ. Studies comparing strains have grouped them, dependent on their ability to share (S) or dominate (D) a single deep crypt space (Bongrand et al. 2016). Due to the anatomy of the squid, namely the six separate crypt spaces, a signal squid can be colonized with multiple S/D strains at any given time. However, the ability for both S and D strains to colonize efficiently is perplexing as, presumably, there must be an evolutionary advantage to having both in the environment; otherwise, why are S strains still able to colonize at all? Comparisons between S and D strains showed that D strains have roughly 200 open reading frames exclusive to group D, which are likely responsible for the dominant phenotypes (Bongrand et al. 2016). These phenotypes include greater aggregate sizes, increased aggregate formation, a faster entrance to the light organ, increased luminescence, and increased levels of c-di-GMP (Koehler et al. 2018; Bongrand and Ruby 2019; Dial, Eichinger, et al. 2021). However, the increase in aggregate size and formation does not correlate with successful colonization, indicating that this phenotype is likely exclusive to these strains' ability to dominate over other strains rather than being essential for colonization (Bongrand and Ruby 2019). The dominance of one strain over another is likely a multi-factorial mechanism that allows some strains to be the sole colonizers of a deep crypt space.

Persistence. Once *V. fischeri* successfully colonizes *E. scolopes,* this association is sustained over the lifetime of the squid. A healthy symbiotic relationship is a dynamic one maintained by both host and bacterial factors to ensure that *V. fischeri* remains the exclusive

organism in the crypts. This dynamic relationship results in many changes for the bacteria and the squid, including morphological changes, a decrease in antimicrobial production, and the downregulation of immune responses.

Bacterial changes. As mentioned above, both *V. fischeri* and *E. scolopes* change during symbiosis. Within the first 24hrs, *V. fischeri* cells within the light organ undergo two distinct morphological changes. First is a reduction in cell size, presumably due to the specific environmental growth conditions (Ruby and Asato 1993). The second morphological change is the loss of the polar flagella (Ruby and Asato 1993); seemingly, the flagella are rendered unnecessary in the crypt spaces once they have achieved a high cell density. However, once released from the squid, *V. fischeri* can rapidly regrow their flagella (Ruby and Asato 1993). The exact signal (s) that control these events are largely unknown.

Host – responses. The squid's responses to symbiotic colonization are diverse since it has to protect itself from harmful bacterial colonization while also protecting its symbiotic partner. Mucus production within the crypt spaces increases after colonization while mucus secretion around the ciliated appendages decreases, and this decrease can be reversed if *V. fischeri* is removed via antibiotic treatment (Nyholm et al. 2002). The ciliated appendages regress and undergo apoptosis triggered by TCT and LPS, bacterial toxins (Koropatnick et al. 2014). This regression and apoptotic episodes are thought to protect both squid and symbionts from further bacterial invasion/infection. Lastly, morphologically, the microvilli become dense, and the cells swell, further supporting the interaction between host and colonizer (Lamarcq and McFall-Ngai 1998).

E. scolopes, similar to other invertebrates, does not have an adaptive immune system but instead relies on its innate immune system, with hemocytes being the predominant cell type

(Castillo, Goodson, and McFall-Ngai 2009). Hemocytes are phagocytic cells associated with pathogen control but, in this context, also play a crucial role in the symbiotic relationship between squid and beneficial microbe. *V. fischeri* colonization induces changes in hemocyte transcription and protein expression, presumably due to bacterial–host communication during symbiosis (Collins et al. 2012; Schleicher et al. 2014). In terms of symbiosis, hemocytes play critical roles. The first is chitin production, which supports bacterial growth (Schwartzman et al. 2015). Second, bacterial–produced signals/molecules recruit hemocyte trafficking, which provides information to induce light organ maturation (Koropatnick, Kimbell, and McFall-Ngai 2007; Altura et al. 2013). Lastly, hemocytes cannot readily engulf *V. fischeri* as they bind poorly to the bacteria, whereas other species are readily engulfed (Nyholm et al. 2009). This contributes to the exclusivity of light organ colonization and depends on *V. fischeri* exposure, as hemocytes from aposymbiotic hosts can effectively engulf *V. fischeri* (Nyholm et al. 2009). This is likely due to the production of outer membrane porin OmpU in *V. fischeri,* as loss of this production increases hemocyte phagocytosis/ binding ability (Nyholm et al. 2009).

E. scolopes also produce antimicrobials as a line of defense against antagonistic bacteria. Evidence suggests that the squid produces a peroxidase whose reactive oxygen species (ROS) could harm the bacteria (Tomarev et al. 1993; Small and McFall-Ngai 1999; Schleicher and Nyholm 2011). *V. fischeri* overcomes ROS production through the inhibition of the respiratory burst within the cell. Two proteins, HvnA and HvnB, are thought to mediate the inhibition of the respiratory bursts; however, the roles of these proteins during the other stages of symbiosis remain unclear (Stabb, Reich, and Ruby 2001). *V. fischeri* might also compete for hydrogen peroxide as a substrate, effectively out-competing host peroxidase activity (Visick and Ruby 1998).

These morphological and systemic changes are facilitated via the colonization of *V. fischeri* as the sole symbiont in the light organ. This highlights the importance of host-microbe interactions in virtually every part of animal biology.

Daily rhythm. As mentioned above, the symbiotic relationship between *E. scolopes* and *V. fischeri* is dynamic, and these changes occur daily on a light/dark cycle rhythm (Nyholm and McFall-Ngai 1998; Boettcher 1996). Each day, when dawn breaks, ~90% of the symbionts are expelled from the light organ by muscle contraction, and the remaining bacterial cells grow to re-populate the organ (Nyholm and McFall-Ngai 1998). During this process, the interiors of the deep crypt spaces are effaced, and the expulsion consists of bacteria and host cells along with acellular matrix material (Nyholm and McFall-Ngai 1998; Wier et al. 2010; Graf and Ruby 1998). This expulsion occurs each day, triggered by light, throughout the life of *E. scolopes.*

After expulsion, the bacteria use the available resources in the light organ to quickly repopulate with a generation time of approximately 30min (Ruby and Asato 1993; Graf and Ruby 1998). The primary resources used are thought to be amino acids and glycerophospholipids as the symbiotic bacteria have modified expression of genes utilized in glycerol metabolism and altered lipid profiles, compared to a lab-grown strain, which suggests the incorporation of glycerophospholipids (Ruby and Asato 1993; Graf and Ruby 1998; Wier et al. 2010). Once night falls and the bacterial population reaches a high enough cell density, chitin utilization appears to become critical, as chitin catabolism genes are most highly expressed before dawn (Schwartzman et al. 2015; Wier et al. 2010). Concurrently, lysed hemocytes, a key source of chitin (as mentioned above), are most abundant in the light organ at night, and the transcription of chitin-degrading enzyme chitotriosidase is elevated in *E. scolopes* (Schwartzman et al. 2015). The elevated use of chitin acidifies the surrounding tissues, releasing oxygen from hemocyanin

carriers (Schwartzman et al. 2015). In luminescence, needed by the squid during the night, oxygen is the limiting reagent to generate luciferase activity; therefore, bioluminescence peaks immediately after expulsion into the seawater (Boettcher 1996; Miyashiro and Ruby 2012). The levels of bacterial – luminescence fluctuate throughout the day, which imitates the nutrient availability from the host and the bacterial metabolism because of nutrient composition (Boettcher 1996).

Summary. The symbiosis between *V. fischeri* and *E. scolopes* is a simple yet dynamic relationship that requires coordination and morphological/genetic changes from both the bacteria and the squid. The specificity of the association, genetic tractability of the bacteria, and ease of squid colonization visibility led to an ideal model to study complex bacterial behaviors in the host. The factors and mechanisms that influence the interaction between the bacteria and squid are still active areas of research due to the maintainability and ease of this symbiotic relationship. In the next and final section, I will describe biofilm formation in *V. fischeri,* including the Syp regulatory network, the signals that control it, and how the squid could be a potential influence.

Biofilm Formation by *V. fischeri*

Introduction. The symbiosis between *V. fischeri* and *E. scolopes* is a natural model used to study biofilm formation in a host (Visick and Skoufos 2001; Visick and Ruby 2006; Visick, Stabb, and Ruby 2021). *V. fischeri* colonizes its host by first forming a bacterial aggregate on the surface of the light organ and then dispersing from this aggregate to enter and colonize the deep crypt spaces of the organ (Nyholm et al. 2000). This biofilm formation/aggregation is directly related to colonization, as bacterial strains defective for biofilms have a colonization defect, whereas hyper- aggregator strains outcompete WT for colonization (Yip et al. 2006; Yip et al.

2005; Bongrand et al. 2016; Bongrand and Ruby 2019; Koehler et al. 2018; Morris and Visick 2013a, 2013b; Thompson et al. 2019; Shibata et al. 2012).

V. fischeri is known to produce two separate polysaccharides SYP and cellulose (Bassis and Visick 2010; Yip et al. 2006). Whereas the SYP – dependent biofilm is well characterized, the role of the cellulose–dependent biofilm is still relatively unknown. Currently, seven regulators are known to control SYP – dependent biofilm formation. Six of these regulators are TCSs and mutants defective for these TCSs exhibit defective or accelerated biofilm formation in culture and, correspondingly, colonization disadvantages or advantages (Norsworthy and Visick 2015; Yip et al. 2006; Yip et al. 2005).

In vitro biofilm formation can be monitored via the formation of cohesive wrinkled colonies or cell clumping and rings in liquid culture under shaking conditions (Darnell, Hussa, and Visick 2008; Tischler et al. 2018; Yip et al. 2006). Squid–isolated strains, including our WT strain, ES114, can readily form a biofilm in the context of the squid; in *vitro,* however, biofilms have only been observed via genetic manipulation (overexpression of a positive biofilm regulator and/or disruption of a negative regulator).

In the next section, I will discuss what is known about biofilm formation in *V. fischeri,* starting with the SYP – dependent biofilm formation and the multiple TCSs that regulate its production. Lastly, I will describe the lesser-known cellulose component of biofilm formation and move into the signals we know help produce biofilm formation and how it relates to the host.

SYP-dependent biofilm formation. SYP is the main polysaccharide that contributes to biofilm formation by *V. fischeri,* and there is an extensive amount of control over this production, presumably to ensure that its production occurs at the right time and place (Visick, Stabb, and Ruby 2021). Control of SYP production occurs at multiple levels, including

transcription of the 18-gene *syp* locus (Fig. 6), which encodes proteins predicted to produce, export, and control SYP, as well as post-transcriptional control that has yet to be uncovered (Morris, Darnell, and Visick 2011; Shibata et al. 2012; Visick and Ruby 2006; Yip et al. 2006). One other component of SYP – dependent biofilms is the production of Bmp proteins (Ray, Driks, and Visick 2015). A combination of SYP and Bmp are responsible for the wrinkles on biofilm-forming colonies, as strains that lack Bmp still form cohesive biofilms, but they do not have the characteristic wrinkles (Ray, Driks, and Visick 2015).

Two-component signaling and regulation in *V. fischeri*. As mentioned above, TCS positively and negatively regulate the formation of SYP, the significant component of the *V. fischeri* biofilm. Historically, to investigate SYP biofilm formation and the regulators that control it, positive regulators had to be overexpressed, and/or negative regulators had to be deleted. In this section, I will detail the network of TCSs that control *syp* transcription and eventual SYP production/ biofilm formation (Fig. 6).

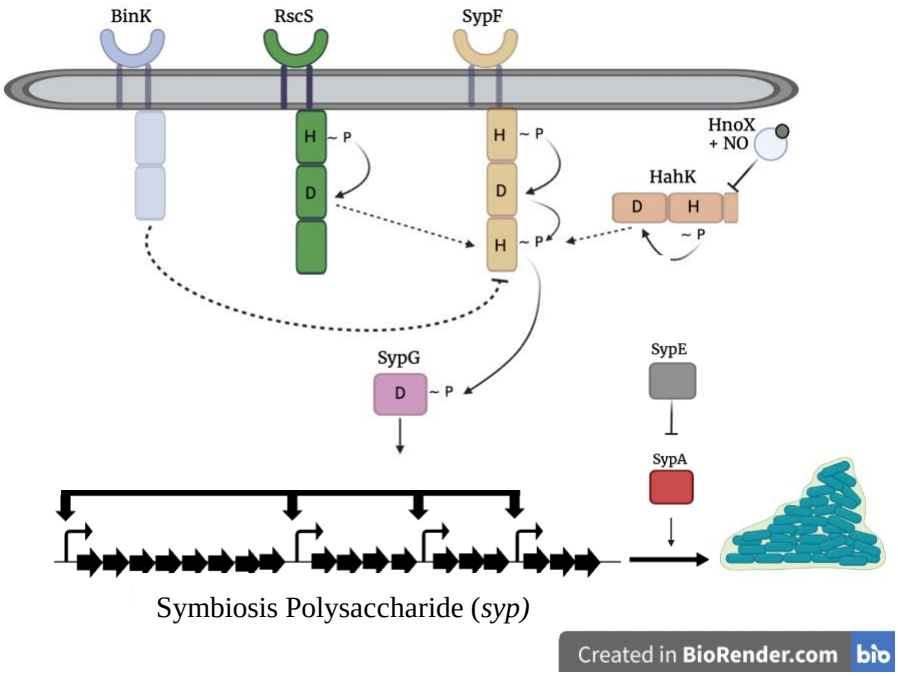

Figure 6. Regulatory Network of the *syp* Locus: Image created in BioRender. The *syp* regulatory network is composed of several two-component regulators, both positive and negative. The central regulator is SypF which, after receiving a signal and autophosphorylating, donates a phosphoryl group to the RR SypG. SypG then upregulates *syp* transcription. The hybrid sensor kinase RscS donates a phosphoryl group (after autophosphorylation) to SypF to elicit *syp* transcription. HahK, another histidine kinase, also donates a phosphoryl group to SypF's HPT domain. HahK is paired with its inhibitory partner HnoX, which is activated by NO. BinK is a potent negative regulator, and it is thought to inhibit SypF/biofilm formation by shuttling phosphates off of the HPT domain. Lastly, SypE inhibits SypA, which acts post-transcriptionally to regulate SYP biofilm formation.

The regulator of symbiotic colonization – sensor (RscS), a hybrid sensor kinase identified through a screen looking for mutants unable to colonize squid (Visick and Skoufos 2001). RscS is very similar to other HKs as it contains conserved residues predicted to be involved in phosphorelay, as well as a PAS domain and periplasmic loop, which are predicted to recognize signals from the environment (Geszvain and Visick 2008; Visick and Skoufos 2001; Yip et al. 2006). An *rscS* mutant was defective for colonization but not growth (Visick and Skoufos 2001); rather the Δ*rscS* mutant was unable to form an aggregate on the surface of the light organ, pointing towards its positive role in biofilm formation (Yip et al. 2006). Interestingly, RscS is

also specific for *E. scolopes* colonization, as when it was introduced into a non-squid colonizing strain (MJ11) on a multi-copy plasmid, MJ11 was then competent to colonize the squid (Mandel et al. 2009).

Further work with RscS showed that RscS functioned to regulate the *syp* locus, as overexpression of an increased activity (presumably through an increase in translation) allele (*rscS1)* from a multicopy plasmid induced *syp* transcription and biofilm formation, whereas the vector control strain failed to form biofilms (Yip et al. 2006). The ability of RscS1 to produce biofilm phenotypes occurred in a *syp*-dependent manner, as loss of the *sypN* structural gene abrogated biofilm phenotypes (Yip et al. 2006). Further, cells overexpressing *rscS1* outcompeted WT for squid colonization, cementing RscS as a positive regulator of SYP-dependent biofilm formation and squid colonization (Yip et al. 2006).

RscS is known as an orphan HK because it is unlinked to an RR. However, the characterization of RscS as a regulator of *syp* led to the identification and characterization of two RRs encoded within the *syp* locus: SypG and SypE. The *syp* locus also encodes a SK: SypF, and subsequent studies revealed that SypF is also crucial for biofilm formation and squid colonization. In RscS overexpression assays, SypF is critical for *syp* transcription and wrinkled colony formation (Norsworthy and Visick 2015). However, even though SypF contains an HATpase, D1 and phosphotransfer domains, only the HPT domain of SypF was required for biofilm formation under RscS-induced conditions (Norsworthy and Visick 2015). RscS does contain its own HPT domain, but it was dispensable for biofilm formation (Geszvain and Visick 2008), indicating that RscS and SypF, specifically the HPT domain of SypF, work together to promote *syp* transcription and eventual biofilm formation. The partnership between RscS and SypF culminates in a model where, after receiving a signal, RscS initiates a phosphorelay and,

through SypF's HPT domain, activates SypG increasing *syp* transcription and SYP- dependent biofilms (Fig. 6).

SypG is the RR responsible for the transcriptional activation of the *syp* locus (Ray et al. 2013). SypG contains three predicted domains: an N-terminal REC domain, a σ^{54} interaction domain, and a C-terminal DNA binding domain. SypG activates *syp* transcription by binding to specific sites on the DNA (Ray et al. 2013). The *syp* locus contains four promoters with σ^{54} binding regions: upstream of *sypA, sypI, sypM,* and *sypP* (Yip et al. 2005). Notably, while SypG is required for *rscS1*-induced biofilms, overexpression of SypG alone does not induce SYP-dependent biofilm formation. However, SypG does induce an increase in crystal violet-stainable material, which is presumably cellulose (Hussa, Darnell, and Visick 2008; Morris and Visick 2013a; Yip et al. 2005). Biofilm formation under overexpression of SypG conditions only occurs if the negative regulator, *sypE*, is also deleted (Hussa, Darnell, and Visick 2008; Thompson et al. 2018).

Two negative regulators also contribute to the regulation of *syp* transcription and eventual biofilm formation: BinK and SypE (Brooks and Mandel 2016; Pankey et al. 2017; Tischler et al. 2018; Hussa, Darnell, and Visick 2008) (Fig. 6). Strains that lack BinK form larger aggregates *in vivo*; however a Δ*binK* mutant did not exhibit a phenotype in the laboratory unless *rscS* was overexpressed (Brooks and Mandel 2016). RscS is crucial for squid colonization, but recently it was shown that a *binK rscS* double mutant is competent to colonize squid (Ludvik, Bultman, and Mandel 2021). Although the double *binK rscS* mutant strain was able to colonize, a competition experiment revealed that the single *binK* mutant significantly outcompeted the double mutant suggesting that RscS plays a role during later stages of colonization (Ludvik, Bultman, and Mandel 2021). Until recently, the Δ*binK* mutant phenotype relied on *rscS* overexpression;

however, when calcium is added to the media, a *binK* mutant can form a biofilm without needing *rscS* overexpression (Tischler et al. 2018). This allows us to unravel this complex phosphorelay network without the need for overexpression.

The other negative regulator mentioned is SypE, which primarily functions as a negative regulator but can function positively, depending on its phosphorylation state (Morris, Darnell, and Visick 2011; Morris and Visick 2013a, 2013b). SypE also contains three domains: a serine kinase, a REC domain, and a serine phosphatase domain. A single copy of SypE is sufficient to prevent biofilm formation even when the other response regulator, SypG, is overexpressed, whereas when SypE is absent under these conditions, SypG-overexpression induces winkled colony formation (Morris, Darnell, and Visick 2011; Morris and Visick 2013a; Hussa, Darnell, and Visick 2008). SypE is predicted to be phosphorylated on a specific residue within the REC domain that controls serine kinase/phosphatase activity. When SypE is phosphorylated, it acts as a phosphatase and a non-phosphorylated SypE has kinase activity (Morris, Darnell, and Visick 2011). Currently, the model proposes that RscS senses a signal, autophosphorylates, donates its phosphoryl groups to the HPT domain of SypF which, then, phosphorylates both SypG and SypE (Fig. 6). SypE, in turn, modulates biofilm formation post-transcriptionally by managing the phosphorylation state of the first protein encoded in the *syp* locus, SypA, whose function(s) remain unknown.

Lastly, as mentioned above, HahK was discovered in an experiment that used a Δ*binK* mutant grown on media supplemented with calcium (Fig. 6) (Tischler et al. 2018). HahK also appears to function upstream of the HPT domain of SypF to promote biofilm formation (Tischler et al. 2018). HahK is predicted to be a hybrid sensor kinase containing HisKA, HATPase, and REC domains but not an HPT domain of its own. HahK is encoded in an operon with the gene

for HnoX, a nitric oxide (NO) sensing protein. HahK is negatively regulated by HnoX when HnoX is bound by NO, inhibiting biofilm formation and *syp* transcription (Thompson et al. 2019; Wang et al. 2010). Thus, the regulatory network includes four positive two-component regulators, two negative two-component regulators, a negative partner regulator, and a protein of yet unknown function. However, changing media conditions might further flush out all of the key players and their respective signals and functions in the future.

Cellulose–dependent biofilm formation. In 2007, data showed that a *vpsR* mutant strain could outcompete WT for colonization (Hussa et al. 2007); however, the link to cellulose was not made until a year later. The cellulose link was made when it was discovered that a SypF variant induced both cellulose and SYP – dependent biofilm formation dependent on their respective regulators VpsR and SypG (Darnell, Hussa, and Visick 2008; Tischler et al. 2021). Similarly, while looking at cellulose–dependent phenotypes, it was found that the PDE BinA exhibited increased cellulose biofilms (Bassis and Visick 2010), connecting cellulose production, in *V. fischeri,* to c-di-GMP levels, as BinA functions to change c-di-GMP levels within the cell (Bassis and Visick 2010). More recently, it was discovered that another c-di-GMP – related gene, *casA,* is activated by calcium, which then, in turn, activates cellulose production dependent on VpsR (Tischler et al. 2021). These data have identified three protein regulators responsible for cellulose-dependent phenotypes and linked cellulose to biofilm formation by *V. fischeri*.

Signals for *V. fischeri*. Under standard laboratory conditions, WT *V. fischeri* does not form biofilms without genetic manipulation. The current hypothesis is that RscS, the sensor at the top of the regulatory network, receives a signal and induces biofilm formation through signal transduction. The exact signal that relays this information through RscS is, at this point, unknown; however, it is an active area of investigation. Recently, work looking at the impact of

salt and nutrient content implicated calcium as a signal for biofilm formation, as highlighted by low calcium concentrations inducing wrinkled colony formation (Marsden et al. 2017). As detailed earlier, calcium has been shown to drive biofilm formation in various species.

Cellulose biofilm formation has also been linked to calcium induction, as described in the last section; another cellulose-promoting signal is arabinose. Specifically, *V. fischeri* grown in 0.2% arabinose exhibited pellicle formation at the air-liquid interface that was not due to enhanced growth but rather cellulose production, as deletion of *bcs* disrupted this formation (Visick, Quirke, and McEwen 2013). The exact mechanisms for arabinose induction remain unknown but point to multiple signals having a role in the production of one polysaccharide.

Calcium as a general signal for biofilm formation. Several examples highlight the importance of calcium as a signal in various pathways at both transcriptional and posttranscriptional levels. These examples span several different bacterial species pointing to the conservation of calcium signaling throughout genera. In *Pseudomonas aeruginosa* and *P. syringae,* calcium activates transcription of genes for surface adhesins and exopolysaccharide (EPS) production (Sarkisova et al. 2005; Fishman, Zhang, et al. 2018). Calcium has also been shown to work through other molecules. For example, in *Vibrio vulnificus,* calcium increases the second messenger c-di-GMP. This calcium-mediated increase of c-di-GMP triggers the production of the Brp polysaccharide by upregulating the *brp* locus at the level of transcription (Chodur et al. 2018). Post-transcriptionally, calcium directly interacts with proteins, such as the pilus-biogenesis factor PilY1 in *P. aeruginosa*; this enables pilus protraction and retraction (Eto et al. 2008). Similarly, calcium interacts with the type I pili to promote *E. coli* to initiate entry into host cells (Khan et al. 2007).

para Aminobenzoic Acid (pABA) as a signal. pABA as a signaling molecule in bacteria is a novel finding; therefore, more research must be done to flush out its role thoroughly. The work being done is limited; there are, however, two examples of pABA being used as a signal. The first example is work done in *Escherichia coli*, this work found that pABA is a potent inhibitor of DNA repair pathways induced by nitric oxide (NO) (Vasilieva et al. 2016). The same paper showed that pABA, in *E. coli,* can inhibit biofilm formation and regulate NO generation, in general (Vasilieva et al. 2016).

The research on pABA and oral biofilm formation is most relevant to my dissertation. pABA's role in inducing biofilm formation has been previously shown in multispecies biofilms formed by oral pathogens *Streptococcus gordonii* and *Porphyromonas gingivalis* (Kuboniwa et al. 2017). *S. gordonii* produces and secretes pABA into the environment, which, in turn, *P. gingivalis* metabolizes, leading to increased expression and production of the fimbrial adhesins necessary for colonization (Kuboniwa et al. 2017). Additionally, pABA treatment of *P. gingivalis* resulted in increased colonization during a mouse model of infection (Kuboniwa et al. 2017).

Although, as of right now, the research being done into pABA as a signaling source is limited, the field is beginning to expand its research into metabolites, such as pABA, inducing biofilm and other phenotypes

Host calcium and essential vitamins. In eukaryotic hosts, such as *E. scolopes*, calcium is a tightly regulated molecule. Colonization by a bacterial friend or foe can trigger dramatic changes in calcium levels that affect both the host and colonizer. This is a rapidly growing area of study, and common trends have emerged among the pathogenic species, which typically colonize

human hosts. A couple of examples of how host calcium is used to the advantage of the bacterium are detailed below.

In *Neisseria meningitidis*, the agent of bacterial meningitis, pili are major virulence factors, as the pilus protein, PilC1, is crucial for adherence and internalization of host cells (Asmat et al. 2014). PilC1 adherence is directly related to the amount of cytosolic calcium levels in the bacterium, as calcium levels increase through a PilC1-mediated phospholipase C activation. Without an increase in calcium induced via bacterial machinery, PilC1-dependent adherence is significantly reduced (Asmat et al. 2014). Multiple other bacterial species use similar mechanisms to control host calcium levels for proper adherence/internalization, including *Borrelia burgdorferi*, *Campylobacter jejuni*, and *P. aeruginosa* (Johnson et al. 2011; Hu, Raybourne, and Kopecko 2005; Grab et al. 2009).

Calcium is not the only host–derived molecule that can be used to a bacterium's benefit. Most eukaryotic hosts need to obtain vitamins and minerals from the environment, which bacteria can also use for their benefit. Examples of essential vitamins and minerals used by both the host and colonizer are detailed below.

According to the National Health Service (NHS), magnesium (Mg) and Iron (Fe) are essential minerals that most eukaryotic organisms need to survive and keep the body healthy (Services 2020). These are also nutrients that bacteria use to their benefit. Mg, for example, activates one of the most well-known TCS: PhoP-PhoQ in *Salmonella*, as well as in *Edwardsiella tarda* (Chakraborty et al. 2010; Bourret et al. 2017). In *E. tarda*, Mg (2+) and temperature regulate type II and VI secretion systems by activating EsrB through PhoPQ (Chakraborty et al. 2010). This is an example of Mg, an essential host nutrient, controlling gene expression and two essential and ever-present signals (Mg and temperature) working

coordinately to activate a common RR (Chakraborty et al. 2010). Lastly, in *Serratia marcescens*, the TCS RssA-RssB (RssAB) directly senses environmental ferric iron (Fe^{3+}) in order to modulate the biosynthesis of flagella at the level of transcription (Lin et al. 2016).

Summary. *V. fischeri* is a highly tractable genetic organism that exhibits distinct phenotypes, such as motility, biofilm formation, and bioluminescence. These properties make *V. fischeri* an ideal organism to study, especially when biofilm formation is of particular interest. The ability of *V. fischeri* to colonize its host, *E. scolopes,* relies on its ability to form an aggregate of cells, or biofilm, making it the perfect natural model to study biofilms.

V. fischeri biofilm formation is a complicated yet largely controlled process that requires numerous TCSs/regulators. Many of these regulators have been identified, yet the signals that positively and negatively regulate them and biofilm formation, in general, are largely unknown. Therefore, the identification of signals, and their cognate receptors, are of great interest and will further our understanding of the dynamic process that is biofilm formation in not just *V. fischeri* but other organisms as well.

CHAPTER TWO

MATERIAL AND METHODS

Strains and Media.

V. fischeri strains used in this study are shown in Table 1. Plasmids used in the study are shown in Table 2. Wild-type ES114 as well as wild-type KB2B1 were the parent strains used in this study. *E. coli* strains were grown in LB (1% tryptone, 0.5% yeast extract and 1% sodium chloride)(Christensen and Visick 2020). *V. fischeri* strains were cultured in either LBS medium (1% tryptone, 0.5% yeast extract, 2% sodium chloride and 50 mM Tris, pH 7.5) or tTBS (1% tryptone, 2% sodium chloride and 50 mM Tris, pH 7.5) where noted(Christensen and Visick 2020). All assays on solid media were performed using Gibco (Difco) tryptone and all assays in liquid media were performed using Fisher tryptone. To test the possible role of vitamins in inhibiting biofilm formation, tTBS medium was supplemented individually with the following vitamins at various concentrations: nicotinic acid, choline, inositol, para-aminobenzioic acid, pyridoxine, folic acid and thiamine. The concentration of pABA used here (9.7 mM) was determined empirically as the amount sufficient to promote biofilm formation while not substantially impairing bacterial growth. pABA was added either before autoclaving as a powder or after autoclaving as a filter sterilized liquid; both methods were used equally. Autoclaving pABA does not alter the ability of WT to produce a biofilm on pABA/calcium media. To test the specificity of pABA, the other benzoic acids tested were 4-acetamidobenzoic acid, 4-aminosalicylic acid, 4-aminobenzamide, and anthranilic acid all were added at a concentration of 9.7mM. For motility experiments, cells were grown in TBS broth (1% tryptone, 2% sodium

chloride and buffered with 50 mM Tris, pH 7.5 when pABA was added)(O'Shea et al. 2005; Dial, Speare, et al. 2021) and inoculated onto TBS soft agar plates that were solidified with 0.25% agar and supplemented with 35 mM $MgSO_4$ and either 10 mM $CaCl_2$ and/or 9.7 mM pABA where noted (Christensen and Visick 2020).

For growth in minimal medium, Tris-Minimal Medium (TMM) was used (Christensen and Visick 2020). Antibiotics were included as appropriate at the following final concentration. For *V. fischeri*: Tetracycline (Tet), 2.5 μg/ml; Kanamycin (Kan), 100 μg/mL; Chloramphenicol (Cm), 5 μg/mL; Gentamycin (Gent) 10 μg/mL. For *E. coli*: Cm, 12.5 μg/mL; Kan, 50 μg/mL; and Gent 10 μg/mL. For growth of *E. coli* thymidine auxotroph strain π3813 (Le Roux et al. 2007), the conjugal plasmid pEVS104 (Stabb and Ruby 2002) was transformed into π3813 and used to facilitate conjugations, thymidine (Thy) was added to a final concentration of 0.3 mM.

Plasmid Conjugation.

Bacterial conjugation was used to transfer the plasmids of interest into the strains noted as described previously (Christensen, Tepavčević, and Visick 2020). Briefly, the recipient *V. fischeri* strains were inoculated into 5 mL of LBS and grown overnight at 28°C. Donor *E. coli* strains (carrying the plasmid of interest) were inoculated into LB with the appropriate supplements (antibiotics) and the helper *E. coli* strain was inoculated into LB with the appropriate supplements (Thy and Kan) and grown overnight at 37°C. The strains were then subcultured, in the same growth conditions, and grown to early exponential phase. Then, 1 mL of the *V. fischeri* recipient, and 250 μL of each of the *E. coli* strains were added to 1.5 mL microcentrifuge tubes and concentrated using a microcentrifuge for 2 min at 13,300 rpm at room temperature (Christensen, Tepavčević, and Visick 2020). Separately, as a negative control, each *V. fischeri* recipient culture was also concentrated alone by centrifugation as described above.

Supernatants were decanted and the remaining liquid was used to resuspend the pellets at the bottom of the tube. An aliquot (~15 μl) was then spotted onto LBS without antibiotics and placed into the 28°C incubator for a minimum of 3 hrs or overnight. The colonies were then streaked onto media with the appropriate antibiotics and grown overnight at 28°C. The resultant colonies were then re-streaked onto the appropriate media and the individual colonies were grown in liquid cultures and saved.

Molecular Techniques and Strain Construction.

Mutations in ES114 were generated through TfoX- mediated transformation (Christensen, Tepavčević, and Visick 2020; Pollack-Berti, Wollenberg, and Ruby 2010). Briefly, ~500bp segments upstream and downstream of genes of interest were PCR amplified using high-fidelity KOD polymerase (Novagen, EMD Millipore), and PCR splicing by overlap extention (SOE; (Horton et al. 1989)) was used to fuse segments to an antibiotic cassette as previously described (Visick et al. 2018). The fused product was amplified and transformed into the recipient *V. fischeri* strain (ES114) carrying a TfoX-overproducing plasmid (plostfoX-Kan (Brooks et al. 2014) or pJJC4 (Cohen et al. 2021) and recombinant cells were selected for using media containing the appropriate antibiotic. Allelic replacement was confirmed via PCR with outside primers using Promega *Taq* polymerase. Following generation of the initial deletion, genomic DNA (gDNA) was isolated from a given recombinant strain using the Quick-DNA Miniprep plus kit (Zymo Research) and was used to introduce the mutation into other desired strain backgrounds. Insertions were introduced at the intergenic (IG) region between *yeiR* and *glmS* as described previously (Visick et al. 2018). These insertions were made using the PCR amplification and SOE method described above. Genes of interest were fused to an upstream Erm cassette for selection, driven by the native promoter or a constitutive P*ndrR* promoter. In

cases where Erm^R, or another antibiotic cassette, needed to be removed, Flp recombinase was used, which acts on the Flp recombination target (FRT) sequences to delete the intervening sequences as previously shown (Cherepanov and Wackernagel 1995).

Wrinkled Colony Assays.

One day prior to experimentation, either LBS (+/- Ca) or tTBS plates (+Ca, + pABA, and +Ca + pABA) were made by pipetting 25 ml of the appropriate medium into petri dishes and left to dry overnight. Cultures were inoculated from frozen and grown overnight in 5 mL of tTBS with shaking at 28°C. The strains were then subcultured (100 μL into 5 mL tTBS) and grown with shaking at 28°C for 1-2 hrs. Next, the cultures were normalized to an OD_{600} of 0.2 in tTBS. The normalized cultures were then spotted onto the tTBS plates with or without additives at 10 μL per spot and left to dry completely before inverting and incubating at 24°C or 28°C where noted. After 24, 48, 72 and/or 96 hrs, the spots were assessed under a dissecting microscope, and photographed before and after being disrupted with a toothpick; this "toothpick" assay permits an assessment of the relative stickiness of the colony biofilm (Ray, Driks, and Visick 2015). Measurements of KB2B1 size, for figure 36, were done using the non-cropped pictures and a centimeter ruler.

Liquid/Shaking Biofilm Assay.

The denoted strain was inoculated in 5 mL of either LBS or tTBS from a frozen stock and grown with shaking at 28°C overnight (~16 h). The next day, 2 mL of the appropriate medium (*e.g.*, tTBS, tTBS + 10mM Calcium, tTBS + 9.7mM pABA and tTBS + Calcium and pABA) were inoculated with 2 μL of the overnight culture. The tubes were then incubated with shaking at 24°C for 4-20 hrs. After the designated incubation period, the tubes were gently removed from the shaker (so as not to disrupt biofilm formation) and pictures were taken using an iPhone

camera. For quantifying the biofilm, a volume of 100 μL to 1 mL of the culture was added to a cuvette and tTBS was added as needed for a final volume of 1 mL. The OD_{600} was measured using a spectrophotometer in triplicate and the OD_{600} was adjusted for the appropriate dilution factor (1:10).

Growth Curves.

Cells were grown overnight at 24°C in tTBS medium. In the morning, the strains were subcultured to a starting OD_{600} of 0.05 in tTBS and grown with shaking at 24°C, in 250 mL baffled flasks. Aliquots of cultures (1 mL) were taken at 30 min to 1 hr intervals and the OD_{600} was measured using a spectrophotometer. Cultures were diluted for more accurate measurements when the OD_{600} was above 1.

β-galactosidase Assays.

Reporter strains were streaked onto tTBS plates and grown at 28°C overnight (~16 h). A single colony was then picked and used to inoculate 5 mL tTBS in 18 x 150 mm tubes. Three different colonies were used for three different replicates, and these tubes were grown at 24°C with shaking overnight. In the morning, all three replicates of the reporter strain were subcultured in 125 mL baffled flasks with 20 mL of the 4 different media types (tTBS, tTBS + Calcium, tTBS + pABA and tTBS + Calcium + pABA). For the P*sypA-lacZ* reporter, strains were grown for 22 hrs, while the P*bcs-lacZ* reporter strains were subcultured for 3 hrs. The final concentrations of calcium and pABA were 10 mM and 9.7 mM, respectively. After the indicated growth period, an aliquot (5 mL) of each culture was concentrated by centrifugation and a β-galactosidase assay (Miller assay(Miller 1972)) was performed as previously described (Tischler et al. 2018)**.** The OD_{420} and OD_{550} were then measured using a 96-well plate reader and Miller units were calculated as previously described (Tischler et al. 2018)**.**

Motility Assays.

Bacteria were grown overnight at 28°C in TBS and then subcultured in the same media and allowed to grow to an OD_{600} of between 0.2 and 0.4. The cultures were then normalized to an OD of 0.2 and 10 μL aliquots were spotted onto soft-agar motility plates (TBS-Mg) with or without 10 mM calcium and/or 9.7 mM pABA. The plates were then incubated at 28°C for 6-8 hrs. Spot diameter measurements were taken at the times indicated and pictures were taken with plates illuminated from below using a iPhone camera.

Visualization of c-di-GMP-induced RFP Production.

From frozen stock, ES114 containing pFY4535 (Zamorano-Sanchez et al. 2019) was inoculated into 5 mL of tTBS and grown overnight in the 28°C incubator. pFY4535 contains a constitutively active AmCyan followed by a c-di-GMP riboswitch which controls the production of RFP. The next day, the cultures were subcultured for 2 hrs, normalized to an OD_{600} of 0.2 and spotted on tTBS media containing either 10 mM calcium, 9.7 mM pABA or both. The plates were then placed in the 24°C incubator for 24 hrs. After the incubation period, the colonies were transferred to paper and photographed.

Flow Cytometry.

Strains carrying pFY4535 (Zamorano-Sanchez et al. 2019) were grown in Gentamycin-containing tTBS medium with shaking overnight at 24°C, and then subcultured for 16-24 hrs under the same conditions. An aliquot (1 μL) of each sample was added to 1 mL of phosphate-buffered saline (PBS) and these diluted samples were then evaluated for production of RFP and GFP using the LSR Fortessa flow cytometer (BD Biosciences, San Jose, CA). using the AmCyan and PE-TexasRed channels. The data were then analyzed using FloJo software (Ashland, OR). The resulting data were first gated on live cells using forward scatter (FSC) and side scatter

(SSC), then for AmCyan + RFP double positive cells. The geometric mean fluorescence intensities of the PE-TexasRed were quantified, analyzed and graphed, where the y-axes was normalized to mode to account for differences in event counts of the samples.

Statistics.

All error bars shown represent standard deviations. Prism 9 (GraphPad, San Diego, CA, United States) was used to generate graphs and perform statistical analyses. One-way or two-way ANOVAs and unpaired T-tests were used to analyze data for each graph as noted. For ANOVAs analyses, either Tukey's multiple comparisons test or Šídák's multiple comparisons test was used, where the independent variable was on the x-axis and the dependent variable was on the y-axis.

Table 1: Strains Used in this Study

Strain	Genotype	Construction	Reference
ES114	Wild type	N/A	**(Boettcher and Ruby 1990)**
KV5195	Δ*sypR*	N/A	**(Shibata et al. 2012)**
KV8078	Δ*sypQ*::Cm attTn*7*::P*bcsQ-lacZ*	N/A	**(Tischler et al. 2018)**
KV8616	Δ*bcsA*::FRT-Trim	N/A	**(Christensen et al. 2020)**
KV9380	Δ*bcsA*::FRT Δ*sypQ*::FRT	N/A	**(Christensen et al. 2020)**
KV1787	Δ*sypG*	N/A	**(Hussa et al. 2007)**
KV6475	Δ*sypG* attTn*7*::*sypG* – FLAG	N/A	**(Ray, Driks, and Visick 2015)**
KV5367	Δ*sypF*	N/A	**(Norsworthy and Visick 2015)**
KV6659	Δ*sypF* attTn*7*::*sypF* – FLAG	N/A	**(Norsworthy and Visick 2015)**

KV7226	Δ*sypF* attTn*7*::*sypF*-HPT- FLAG	N/A	**(Norsworthy and Visick 2015)**
KV8079	Δ*sypQ*::FRT-Cm IG (*yeiR-glmS*)::P*sypA lacZ* attTn*7*::Erm	N/A	**(Tischler et al. 2018)**
KV9191	Δ*sypG*::FRT - Spec	N/A	**Visick lab collection**
KV10186	Δ*sypF*::FRT - Spec	TT ES114 transformed with PCR SOE product generated with primer sets 1194 & 1160 (ES114), 2089 & 2090 (pKV521), and 2297 & 271 (ES114) (amp with primers 1194 and 27)	**This study**
KV10307	Δ*sypG* Δ*sypQ*::FRT-Cm IG (*yeiR-glmS)*::P*sypA lacZ* attTn*7*::Erm	TT KV8079 with PCR amplified DNA from KV9191 (amp with primers 1223 and 427)	**This study**
KV10317	Δ*sypF* Δ*sypQ*::FRT-Cm IG (*yeiR-glmS*)::P*sypA lacZ* attTn*7*::Erm	TT KV8079 with PCR amplified DNA from KV10186 (amp with 1194 and 271)	**This study**
KV7964	Δ*hahK*::FRT - Cm	N/A	**(Tischler et al. 2018)**
KV8025	Δ*hnoX*::FRT - Erm	N/A	**(Thompson et al. 2019)**
KV8484	Δ*hnoX – hahK*::FRT - Erm	N/A	**(Thompson et al. 2019)**
KV9968	Δ*hahK*::FRT Δ*sypF* attTn*7*::*sypF*-HPT-flag	N/A	**Visick lab collection**
KV10185	Δ*hnoX* ::FRT - Spec	TT ES114 transformed with PCR SOE product generated with primer sets 2155 & 2156 (ES114), 2089 & 2090 (pKV521), and 2157 & 2158 (ES114) (amp with 2155 and 2158)	**This study**
KV10226	Δ*hnoX*::FRT Δ*sypF* attTn*7*::*sypF*-HPT-flag	Derived from KV7226 using KV10185	**This study**
KV9501	Δ*rscS*::FRT - Spec	N/A	**Visick lab collection**
KV10130	Δ*rscS*::FRT	N/A	**Visick lab collection**

KV10154	IG (*yeiR*-FRT-Erm/*glmS*)::*rscS*-3' end-flag	N/A	**Visick lab collection**
KV10004	IG (*yeiR*-FRT-Erm/*glmS*)::P*nrdR-sypA*-HA	N/A	**Visick lab collection**
KV9571	Δ*rscS*-PP::FRT-Erm	N/A	**Visick lab collection**
KV10083	IG (*yeiR*-FRT-Erm/*glmS*)::*rscS*-3' end-HA	N/A	**Visick lab collection**
KV9624	IG (*glpR-rscS*)::FRT-Erm	N/A	**Visick lab collection**
KV10101	IG (*yeiR*-FRT-Erm/*glmS*)::P*rscS rscS*-HA	N/A	**Visick lab collection**
KV10162	IG (*yeiR-FRT*-Erm*/glmS*)::P*rscS-rscS*-flag	N/A	**Visick lab collection**
KV10166	Δ*rscS*::FRT IG (*yeiR*-FRT-Erm*/glmS*)::P*rscS-rscS*-flag	N/A	**Visick lab collection**
KV9953	Δ*rscS*::FRT Δ*sypF* attTn*7::sypF*-HPT-flag	N/A	**Visick lab collection**
KV9653	Δ*rscS* Δ*sypQ::*FRT-Cm IG *(yeiR-glmS)::*P*sypA lacZ* attTn*7::*Erm	TT KV8079 with gKV9501	**This study**
KV10304	Δ*hahK* Δ*sypQ::*FRT-Cm IG *(yeiR-glmS)::*P*sypA lacZ* attTn*7::*Erm	TT KV8079 with gK7964	**This study**
KV8232	IG (*yeiR-glmS*)::ErmR-trunc TrimR	N/A	**(Visick et al. 2018)**
KV10299	IG (*yeiR*-FRT-Erm*/glmS*)::P*rscS-rscS*-Periplasmic Loop	TT KV8232 with SOE products 2290 & 4111 (KV10165) and 4112 & 1487 (KV10165), (amp with 2291 and 2289)	**This study**
KV10303	Δ*rscS*::FRT IG (*yeiR*-FRT-Erm*/glmS*)::P*rscS-rscS*-periplasmic Loop	TT KV10130 with gKV10299	**This study**
KV10019	IG (*yeiR*-FRT-Erm/*glmS*)::P*nrdR-sypF*-HA	N/A	**Visick lab collection**

KV10255	IG (*yeiR*-FRT-Erm/*glmS*)::P*nrdR-sypF*-Flag	N/A	**Visick lab collection**
KV10298	IG (*yeiR*-FRT-Erm/*glmS*)::P*rscS-rscS*/*sypF* Chimera	TT KV8232 with SOE products from 2290 & 3350 (KV10162) and 3351 & 1487 (KV10255), (amp with 2291 and 2289)	**This study**
KV10305	Δ*sypF*::FRT-Spec Δ*rscS*::FRT	TT10130 with gKV10186	**This study**
KV10312	Δ*sypF*::FRT-Spec Δ*rscS*::FRT IG (*yeiR*-FRT-Erm/*glmS*)::P*rscS-rscS*/*sypF* Chimera	TT 10305 with gKV10298	**This study**
KV10351	Δ*sypF*::FRT Δ*rscS*::FRT IG (*yeiR*-FRT/*glmS*)::P*rscS-rscS/sypF* Chimera	Derived from 10312	**This study**
KV10301	Δ*sypF*::FRT IG (*yeiR*-FRT-Erm/*glmS*)::P*rscS-rscS*/*sypF* Chimera	TT KV5367 with gKV10298	**This study**
KV10355	Δ*sypF*::FRT IG (*yeiR*-FRT/*glmS*)::P*rscS-rscS/sypF* Chimera	Derived from KV10301	**This study**
KV10302	Δ*rscS*::FRT IG (*yeiR*-FRT/*glmS*)::P*rscS-rscS/sypF* Chimera	TT 10130 with KV10298	**This study**
KB2B1	Wild Type	N/A	**(Wollenberg and Ruby 2009; Dial, Eichinger, et al. 2021)**
CD84	KB2B1 IG (*yeiR*-FRT-Erm/*glmS*)::P*rscS-rscS*-flag (ES114)	TT KB2B1 with gKV10162	**This study**
KV10255	IG (*yeiR*-FRT-Erm/*glmS*)::P*nrdR-sypF*-Flag	N/A	**Visick lab collection**
KV10389	KB2B1 IG (*yeiR*-FRT-Erm/*glmS*)::P*nrdR-sypF*-Flag (ES114)	TT KB2B1with gKV10255	**This study**
KV9782	*rscS*-FLAG-FRT-Erm	TT ES114 with SOE product amplified with primers 40 & 3138 (ES114), 2354 & 2090	**This study**

		(pKV494) and 3139 & 2921 (ES114)	
KV10390	P*rscS-rscS*/*sypF* Chimera IG (*rscS-glpK*)::FRT-Erm (*rscS* native site)	TT ES114 with SOE product amplified with primers of 40 & 3141 (gKV10302) and 2354 & 2921 (gKV9782) (amp with 40 & 2921)	**This study**
KV10397	Δ*sypF*::FRT Δ*rscS*::FRT IG (*yeiR*-FRT/*glmS*)::P*rscS-rscS/sypF* Chimera P*rscS-rscs*/*sypF* Chimera IG (*rscS-glpK*)::FRT-Erm	TT KV10351 with gKV10390	**This study**
KV10388	KB2B1 Δ*rscS*::FRT-Spec IG (*yeiR*-FRT-Erm/*glmS*)::P*rscS-rscS*-flag (ES114)	TT CD84 with gKV9501	**This study**
KV9341	Δ*vpsR*::FRT-Spec	N/A	**(Tischler et al. 2021)**
KV8920	Δ*casA*::FRT-Spec	N/A	**(Tischler et al. 2021)**
KV10020	Δ*sypE*::FRT-Erm	N/A	**Visick lab collection**
KV10163	Δ*sypE*::FRT	Derived from KV10020	**This study**
KV10181	Δ*rscS*::FRT Δ*sypE*::FRT-Erm	TT KV10130 with gKV10020	**This study**
KV9189	Δ*sypA*::FRT-Erm	N/A	**Visick lab collection**
KV10183	Δ*rscS*::FRT Δ*sypA*::FRT-Erm	TT KV10130 with gKV9189	**This study**
KV9222	Δ*sypG*::FRT-Erm	N/A	**Visick lab collection**
KV10182	Δ*rscS*::FRT Δ*sypG*::FRT-Erm	TT KV10130 with gKV9222	**This study**

Abbreviation(s): HA, HA epitope tagged; flag, FLAG epitope tagged; IG, intergenic between *yeiR* and *glmS* (adjacent to the Tn*7* site) unless otherwise noted; FRT, the antibiotic cassette was resolved using Flp recombinase, leaving a single FRT sequence. TT, TfoX-mediated transformation of a TfoX-overexpressing version of the indicated strain with the indicated genomic DNA (g) or with a PCR-SOE product generated using the indicated primers and templates.

Table 2: Plasmids Used in this Study

Name	Description	Reference
pEVS104	Conjugal helper plasmid (Kan^r)	**(Stabb and Ruby 2002)**
pKV69	Vector Control	**(Visick and Skoufos 2001)**
pLMS33	Wild Type *rscS* on pKV69	**(Visick and Skoufos 2001)**
pJJC4	*tfoX*$^+$ + Cm^r	**(Cohen et al. 2021)**
pJFB9	*pLosTfox* + Kan^r	**(Brooks et al. 2014)**
pCLD54	Wild Type *sypF* on pKV69	**(Darnell, Hussa, and Visick 2008)**
pKV496	*flp*$^+$ + Kan^r	**(Visick et al. 2018)**
pKV521	pJET + FRT-$Spec^r$	**(Visick et al. 2018)**
pKV506	pJET + *yeiR*-FRT-Erm^r-*PnrdR*	**(Visick et al. 2018)**
pKV494	pJET + FRT-Erm^r	**(Visick et al. 2018)**
pKV502	pJET + *yeiR*-FRT-Erm^r	**(Visick et al. 2018)**
pKV503	pJET + *glmS*	**(Visick et al. 2018)**
pFY4535	c-di-GMP biosensor plasmid that encodes RFP under the control of a c-di-GMP dependent riboswitch and AmCyan under control of a constitutive promoter	**(Zamorano-Sanchez et al. 2019)**
pKV302	pKV69 + *VF_0087*	**(Dial, Eichinger, et al. 2021)**
pSS22	pVSV105 containing *sypR*	**(Shibata et al. 2012)**
pVSV105	Stable expression vector (Cm^r)	**(Dunn et al. 2006)**

Table 3: Primers Used in this Study

Primer Number	Sequence
1223	GAATGTCTTGCTAAGTACCTG
2089	CCATACTTAGTGCGGCCGCCTA
2090	CCATGGCCTTCTAGGCCTATCC
427	TAATACCGTTGTTTTGCT TGG
1194	TTATGTGCGAGGCCTAATGC
1160	taggcggccgcacttagtatgGATGCACTGAATAATTGAGATACC
2297	ggataggcctagaaggccatggAAACAAGGTTTCTCAAAATAAAAG
271	CTCGGCGCATACTTCTTTAC
27	AGGTGATGAAGCCGCTCGA
2155	ATCTCTTGAGCACTTGTTTGAG
2156	taggcggccgcactaagtatggAATAATCCCTTTCATAAACACTCC
2157	ggataggcctagaaggccatggAAATCATAAACGATTAAGGCGGG

2158	TCGCGCCACATTGTATTTGG
2921	GTACGATTGTAGGCTTAACTCG
2290	AAGAAACCGATACCGTTTACG
4111	gagtttttatcgtttcagattgggtATATTGTTTTACAGGATGGTTCCTCG
4112	cgaggaaccatcctgtaaaacaatatACCCAATCTGAAACGATAAAAACTC
1487	GGTCGTGGGGAGTTTTATCC
2291	CAGGTAAAGGGCATTTAACG
2289	AATTGCTGTTGAAGCATCTCTG
3138	ttatttatcatcatcatctttataatcTTGTGTTTCATACTTCTCTAATAATC
2354	gattataaagatgatgatgataaataaCCATACTTAGTGCGGCCGCCTA
3350	aataatagctcattatccatTGCATCATCTGAAAGTTTATATTTAG
3351	taaactttcagatgatgcaATGGATAATGAGCTATTATTAGTAG
40	GTCAACGACTAGGACATAAG
3139	ggataggcctagaaggccatggACTTCGTCATAAAAAAAGGAGCAC
3141	taggcggccgcactaagtatgga

Lowercase letters denote nonnative or tail sequences.

CHAPTER THREE

EXPERIMENTAL RESULTS

pABA, Calcium, and c-di-GMP Induce Cohesive, SYP-dependent Biofilm Formation in ES114.

Introduction.

My dissertation research started by looking at transposon mutants that Dr. Alice Tischler had constructed. My specific interest was in a transposon inserted within the *aga* operon. The *aga* operon facilitates the acquisition of N-acetyl-galactosamine, which is a prominent component of the cell wall. This transposon was inserted within the gene *agaR* and displayed interesting biofilm phenotypes on LBS with or without calcium (Appendix A; Fig. 44). I wanted to determine why this sugar uptake gene was having effects on biofilm structure and therefore decided to look at different media types/ media content (Marsden et al. 2017).

The typical strains used to measure biofilm formation are WT ES114 and a Δ*binK* mutant, which are negative and positive controls, respectively. These two strains are used because the canonical WT strain of *V. fischeri*, ES114, forms a productive biofilm *in vivo* but not in laboratory conditions (LBS). In contrast, on LBS supplemented with calcium, the Δ*binK* mutant forms a cohesive SYP – dependent biofilm (Tischler et al. 2018). The juxtaposition between these two strains makes them perfect controls for determining the level of biofilm formation via other strains. Through the use of varying media types, I discovered several interesting phenotypes I will discuss in this section.

First, I discovered that new media conditions induced biofilm formation via Δ*binK* without adding calcium. Further, arguably more importantly, I found conditions that induced biofilm formation in ES114. I also determined the optimal conditions under which ES114 can form biofilms, this induction of biofilm formation occurs at the level of *syp* transcription, and these conditions globally change the transcriptome of ES114. Lastly, I have established a potential crosstalk between SYP and cellulose polysaccharide production and SYP and c-di-GMP levels.

Biofilm Formation via ES114.

I started my efforts to find other factors contributing to biofilm formation using a 1% tryptone media type, which lacks yeast extract (tTBS). Previously, we saw that altered media content resulted in altered biofilm phenotypes (Marsden et al. 2017). Due to the colony morphology I saw from the *agaR* mutants (Appendix A; Fig. 44), I decided to look at tTBS conditions in order to try and understand the impact of the *agaR* mutation. Along with the *agaR* mutants, I also looked at WT, and the hyper-biofilm former, Δ*binK*, on this media as controls where WT does not form biofilms on any media and the Δ*binK* mutant will form biofilms with the addition of calcium (Tischler et al. 2018).

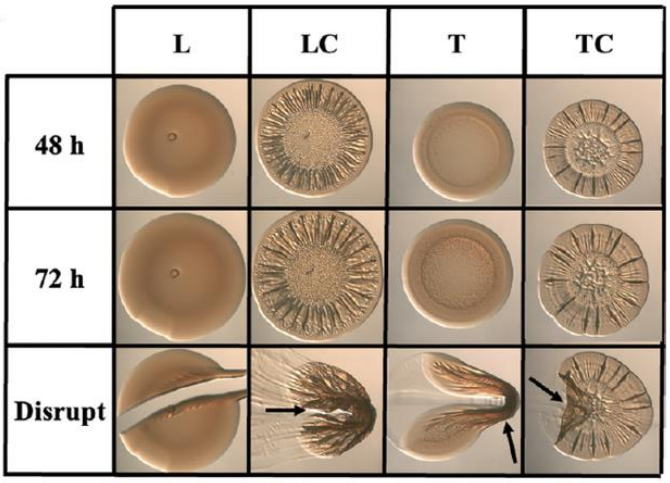

Figure 7. Yeast Extract Inhibits Δ*binK* Mutant Biofilm Formation. Colony biofilm formation by the Δ*binK* mutant (KV7860) was evaluated following growth on LBS (L), LBS + 10 mM calcium (LC), tTBS (T), and tTBS + 10 mM calcium (TC). Pictures were taken using a dissecting light microscope at 48 and 72 hrs. Each colony was disrupted using a toothpick after 72 hrs. Pictures are representative of 3 separate experiments. Arrows indicate where "pulling," indicating cohesion, was observed (Dial, Speare, et al. 2021).

Surprisingly, I found that the Δ*binK* mutant displayed some colony architecture on tTBS conditions, although it differed from the fully wrinkled phenotype, and the colony was completely cohesive (Fig. 7). This phenotype occurred on a medium without calcium supplementation, which is needed for Δ*binK* to form robust biofilms on LBS (Fig. 7). The data in Figure 7 indicate that a specific component in yeast extract inhibits biofilm formation by a Δ*binK* mutant. Therefore, I looked at the different components that are at a higher concentration in yeast extract compared to tryptone. The most considerable differences were seen in the vitamin concentration(s).

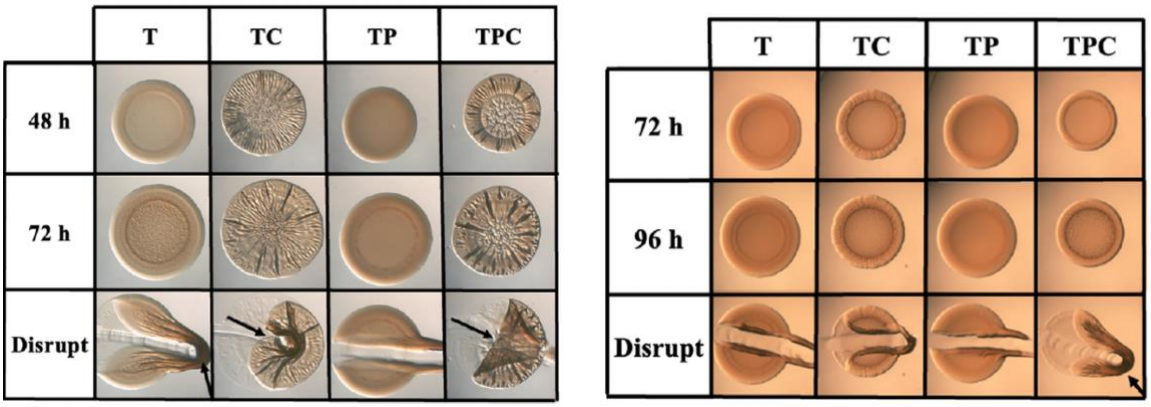

Figure 8. pABA Inhibits Δ*binK* Biofilm Formation while, with the Addition of Calcium, Induces Biofilm in WT. Colony biofilm formation by the Δ*binK* mutant (KV7860; left) and wild-type strain ES114 (right) was assessed following growth on tTBS (T), tTBS + 10 mM calcium (TC), tTBS + 9.7 mM pABA (TP), and tTBS + pABA/calcium (TPC). Pictures were taken using a dissecting light microscope at 72 and 96 hrs. The colony was disrupted using a toothpick after 96 hrs (Dial, Speare, et al. 2021).

I screened a multitude of vitamins, including nicotinic acid, choline chloride, inositol pyridoxine, thiamine, folic acid, and para-aminobenzoic acid (pABA). I found that pABA inhibited the biofilm formation of the Δ*binK* mutant (Fig. 8, left), which led us to believe we found the inhibitory component in yeast extract. Surprisingly, however, when I looked at our ES114 strain, I found that pABA, in conjunction with calcium, induced biofilm formation (Fig. 8, right). This biofilm induction was exciting, as we now have a condition that promotes biofilm formation in our wild-type (WT) strain and will allow us to investigate biofilm formation without excessive genetic manipulation. Further, these conditions might better mimic the squid environment.

Optimal Conditions for Biofilm Formation, SYP – dependent Biofilm Formation, and *syp* Transcription.

Due to the robustness of pABA/calcium to induce biofilm formation in the wrinkled colony assay, I wanted to explore if pABA/calcium could induce biofilms under other biofilm

assay conditions. Moreover, I wanted to determine the optimal conditions under which pABA induces biofilm formation, if these biofilms were, in fact, SYP – dependent and if the upregulation of biofilm formation occurs at the level of transcription. Multiple ways have been developed to look at biofilm formation via *V. fischeri* (Christensen and Visick 2020). The most common way to look at biofilm formation is solid media-induced wrinkled colony formation, but another frequently used method is shaking culture conditions. In shaking cultures, tubes are inoculated with the desired strain and conditions and observed over 16 hrs; after this time, if a strain was poised to form biofilms, we will see characteristic structures related to different biofilm components. Rings at the top of the tube are related to cellulose biofilm formation, clumps at the bottom indicate SYP formation, and trees spanning the tube are attributed to both cellulose and SYP (Tischler et al. 2018; Darnell, Hussa, and Visick 2008). Lastly, to quantify these biofilms, we can monitor the OD_{600} of the culture, being careful to just extract the planktonic bacteria without disturbing the biofilms; the higher the OD, the less biofilm that has been formed.

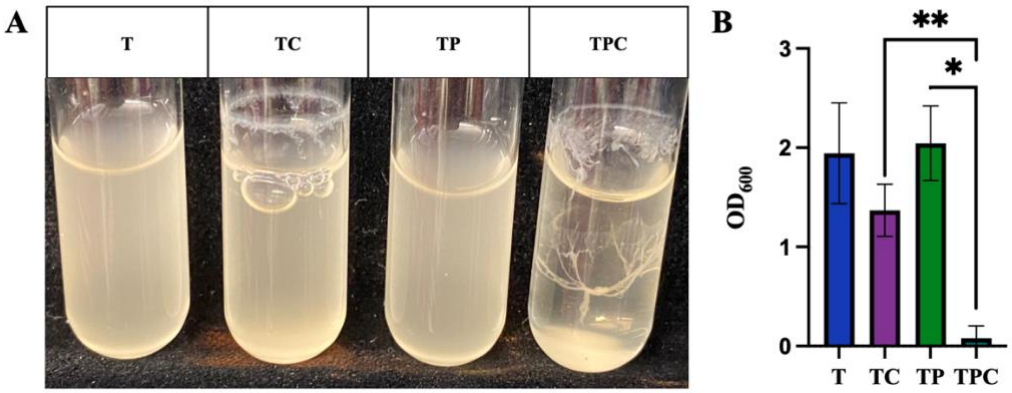

Figure 9: pABA/calcium Induces Shaking Biofilm Formation. The ability of ES114 to produce biofilms during growth in liquid with shaking was evaluated following growth of the strain in tTBS (T), tTBS + calcium (TC), tTBS + pABA (TP), and tTBS + pABA/calcium (TPC). Pictures (A) and OD_{600} readings (B) were taken after 16 hrs. All pictures are representatives of 3 separate experiments. All experiments were done at 24°C. Statistics for B were performed via a one-way ANOVA using Tukey's multiple comparisons test, where OD_{600} was the dependent variable (Dial, Speare, et al. 2021). **P= 0.0098 and *P = 0.0360

Shaking biofilm conditions revealed that the addition of calcium alone decreased the $OD_{600,}$ which is consistent with the readily observable cellulose ring above the liquid surface of the tube (Fig. 9A). The addition of pABA/calcium to these media conditions caused a further decrease in OD_{600}, which is consistent with the observed clump, ring and tree that formed under these conditions (Fig. 9A and B). These data indicate that pABA/calcium can induce biofilm formation under both solid media conditions and the more dynamic shaking culture conditions.

Most *V. fischeri* biofilm experiments, both those described thus far and in previously published literature, have been performed at 24°C or room temperature, and some temperature – dependence has been noted, particularly for *rscS* overexpression (Yip et al. 2006; Brooks and Mandel 2016; Tischler et al. 2018; Hussa, Darnell, and Visick 2008). Due to the newness of pABA/calcium conditions and some temperature dependence described previously, I wanted to explore if temperature would impact pABA/calcium-induced biofilm formation by ES114 and establish the optimal conditions that pABA/calcium can induce biofilms.

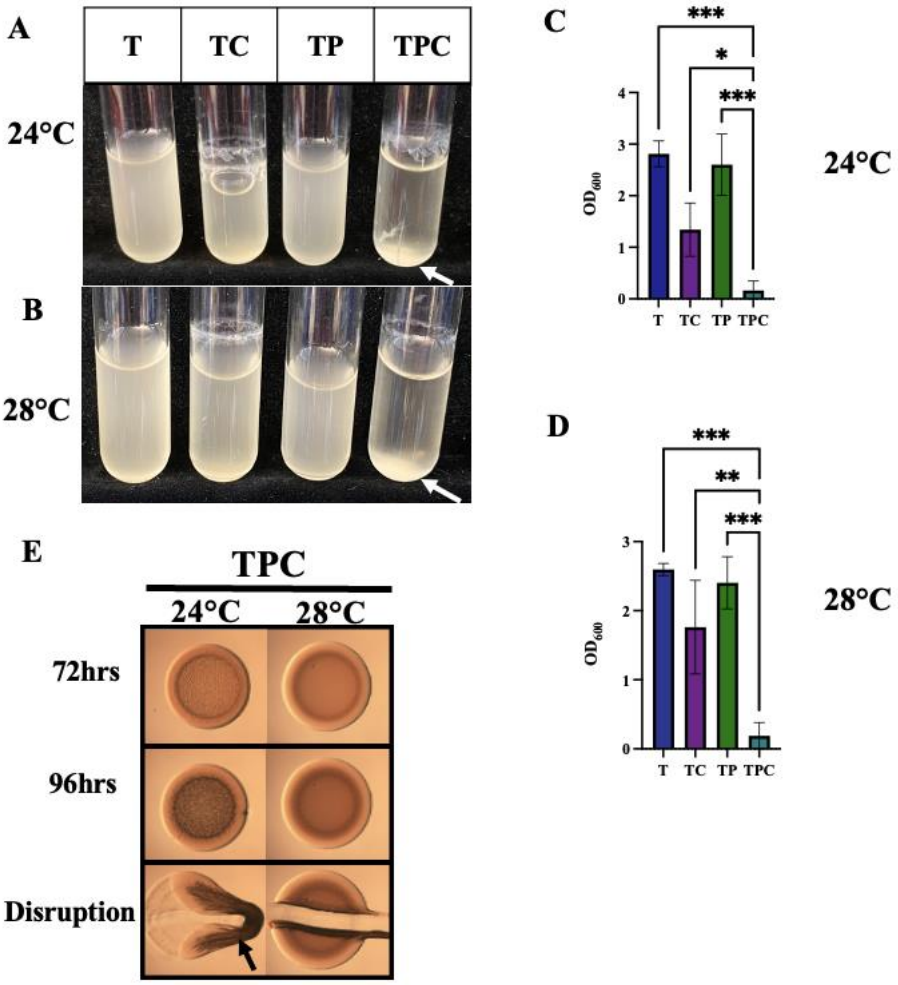

Figure 10. Impact of Temperature on pABA/calcium-Induced Biofilms. (A-D) The ability of ES114 to form biofilms during growth in liquid with shaking biofilms was assessed following growth tTBS, tTBS + calcium, tTBS + pABA, and tTBS + pABA/calcium. Pictures (A & B) and OD_{600} readings (C & D) were taken after 16 hrs for cultures incubated at 24°C (A & C) or 28°C (B and D). All pictures are representatives of 3 separate experiments. Statistics for C and D were performed using one-way ANOVA using Tukey's multiple comparisons test, where OD_{600} was the dependent variable. *P < 0.05 **P = 0.006 and ***P < 0.0007 (E) Colony biofilm formation by ES114 was assessed following growth on tTBS, tTBS + 10 mM calcium, tTBS + 9.7 mM pABA and tTBS + pABA/calcium. Spotted colonies were incubated at both 24 and 28°C. Pictures were taken using a dissecting light microscope at 72 and 96 hrs. Each colony was disrupted using a toothpick after 96 hrs. Arrows indicate where "pulling" and clumps, indicating cohesion, were observed (Dial, Speare, et al. 2021).

I found that, in shaking biofilm cultures, pABA/calcium could induce biofilm formation at 28°C to roughly the same amount as occurs at 24°C, although no tree formation occurred at

28°C as did at 24°C (Fig. 10A to D). In contrast, pABA/calcium was not able to induce biofilm formation on plates at 28°C (Fig. 10E). Thus, temperature seems to be a controlling factor on plates rather than in liquid; however, overall, 24°C resulted in more substantial biofilm formation, indicating that 24°C is the optimal condition for pABA/calcium-induced biofilms.

I also wanted to determine the optimal concentration of pABA needed to induce biofilm formation and the timing for measuring shaking biofilm formation. The concentration of 9.7mM was chosen based on solubility data and, therefore, somewhat randomly. I wanted to determine if 9.7mM was optimal or if another concentration might work better. Additionally, this is the first time we have seen the WT strain forming shaking biofilms, so I wanted to ensure that the time at which I was taking data points was the optimal time for ring, tree, and clump formation. I also wanted to determine these time points for the transcriptomic experiment I will discuss later in my results section.

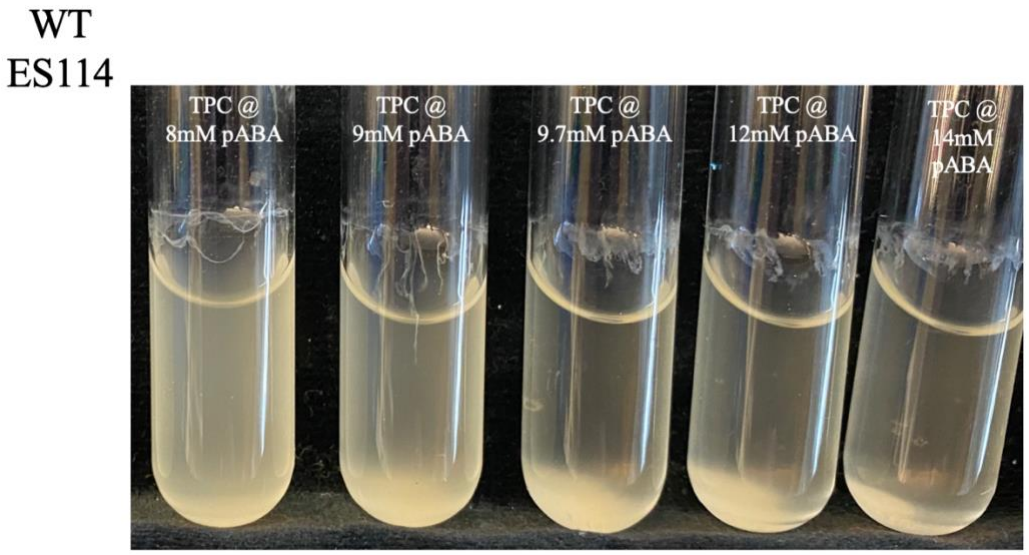

Figure 11. 9.7mM of pABA is the Optimal Concentration for Shaking Biofilm Formation. The ability of ES114 to produce biofilms during growth in liquid with shaking was evaluated following growth of the strain in tTBS + pABA/calcium (TPC) with varying concentrations of pABA (8, 9, 9.7, 12, and 14 mM). Pictures were taken after 16 hrs. All experiments were done at 24°C.

I found that the optimal concentration for shaking biofilm formation was, in fact, 9.7mM pABA (Fig. 11). Although in figure 11, it looks as if 12mM is the ideal concentration, after using that concentration in plates, I saw a severe growth defect (data not shown/data not gathered) and decided that 9.7mM was the concentration that allowed us to get robust biofilm formation while not causing a severe growth defect. Therefore, 9.7mM pABA was the concentration utilized in all future experiments. I also wanted to determine the optimal time point that I should take for shaking biofilm experiments. Typically, the timepoint is between 14 – 18hrs, and, occasionally, 24hr time points have been taken. Due to the overall newness of the condition, I wanted to determine which time point I should use for shaking biofilm conditions. We were also working with a collaborator to determine the transcriptomics under pABA conditions, and I wanted to determine when, under pABA/calcium conditions, we see the characteristic cellulose rings and SYP clumps begin to form (Tischler et al. 2018).

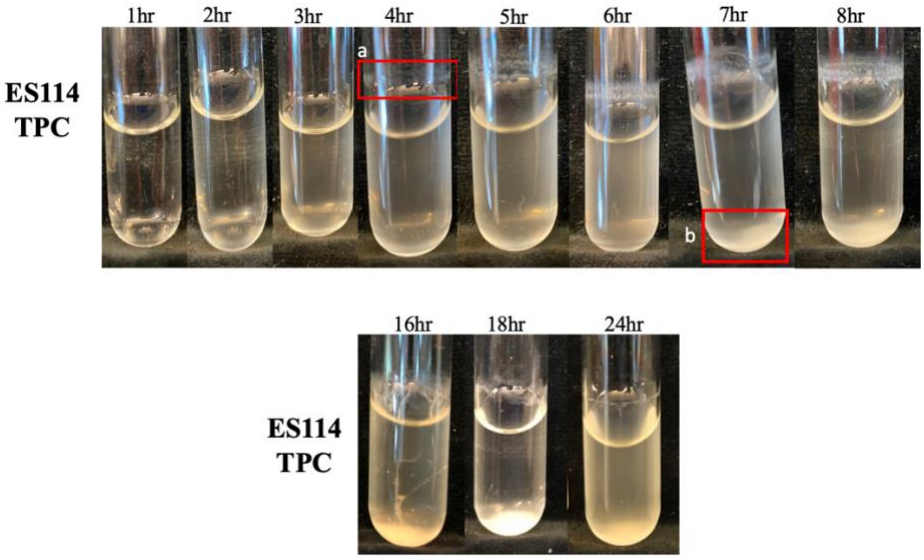

Figure 12. The Optimal Time Point of TPC-Induced Shaking Biofilms in 16hrs. The ability of ES114 to produce biofilms during growth in liquid with shaking was evaluated following growth of the strain in tTBS + pABA/calcium (TPC). Pictures were taken at various time points 1 – 8hrs, 16, 18, and 24hrs. The box in red labeled (a) is, presumably, indicative of cellulose ring formation, and the box labeled (b) is indicative of SYP clump formation. All experiments were done at 24°C.

I began to see the formation of cellulose–dependent ring formation as early as 4hrs (the red box labeled “a” in Fig. 12), while SYP- dependent clumps start to form around 7hrs (the red box labeled “b” in Fig. 12). I also found that the optimal timepoint for shaking biofilms under TPC is roughly 16hrs after inoculation (Fig. 12, bottom). Although anywhere from 14 – 18hrs is sufficient to see robust clumps, the trees are the strongest around 16hrs (Fig. 12). Lastly, timepoints taken around 24hrs display almost complete turbidity, denoting possible dispersion occurring (Fig. 12), making it suboptimal for imaging TPC – induced shaking biofilms.

I wanted to determine the specificity of pABA and its ability to induce biofilm formation. To do this, I looked at different pABA derivates, with calcium, to determine the ability of differently substituted benzoic acids to induce biofilm formation in ES114. The derivatives I used were: 4 – acetamidobenzoic acid, 4 – aminosalicylic acid, 4 – aminobenzamide, and anthranilic acid.

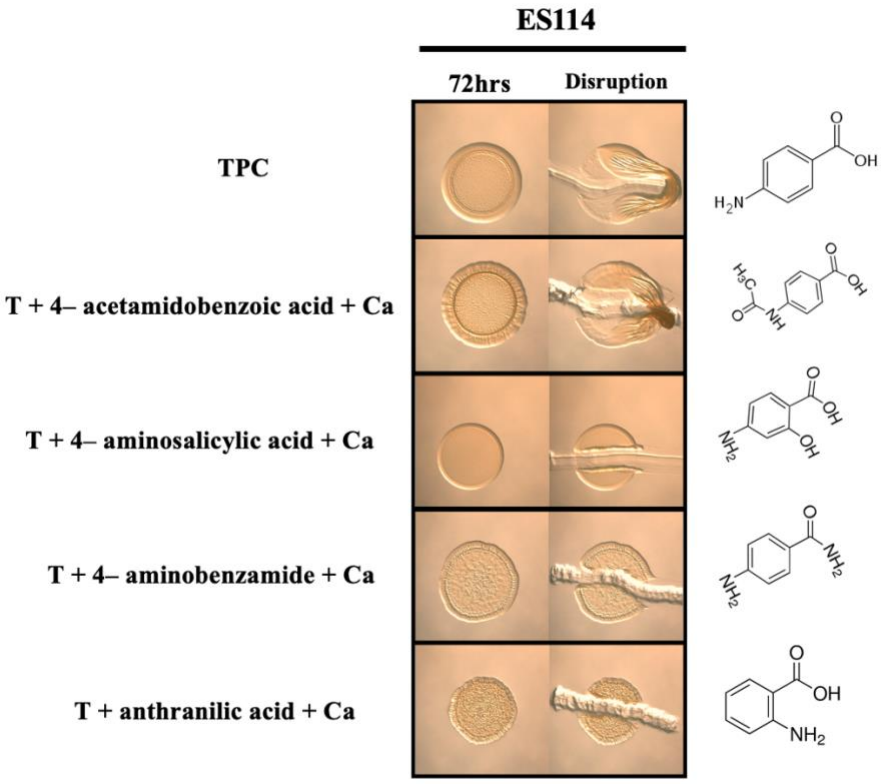

Figure 13. Induction of ES114 Biofilms is Specific to the Carboxyl – Group. Colony biofilm formation was assessed following growth of ES114 on tTBS + pABA/calcium (TPC), tTBS + 4 – acetamidobenzoic acid/calcium, tTBS + 4 – aminosalicylic acid/calcium, tTBS + 4 – aminobenzamide/calcium, and tTBS + anthranilic acid/calcium. Pictures were taken using a dissecting light microscope at 72 hrs. Each colony was disrupted using a toothpick after 72 hrs. Benzoic acid structures are shown on the right side, next to the colony pictures.

The ability of pABA to induce biofilm formation seems to be dependent on the carboxy group. 4 – acetamidobenzoic acid is also able to induce biofilm formation, when calcium was present, whereas none of the other acids permitted ES114 to form cohesive biofilms (Fig. 13). Notably, 4 – acetamidobenzoic acid is the only other acid in this group that has its carboxy group not obstructed (sterically hindered) or changed, when compared to pABA (Fig. 13; right). The ability of 4 – acetammidobenzoic acid to induce biofilm formation indicates that the carboxy group may be what is crucial for the ability of TPC to trigger ES114 to form a biofilm.

As mentioned above, two main polysaccharides contribute to ES114 biofilm formation. Previous work has identified the *syp* locus as a key factor for producing robust biofilms in genetically modified strains of ES114 (Shibata et al. 2012; Yip et al. 2006). To determine if pABA/calcium-induced biofilm formation depends on SYP, I evaluated a *sypR* deletion mutant that is unable to synthesize SYP.

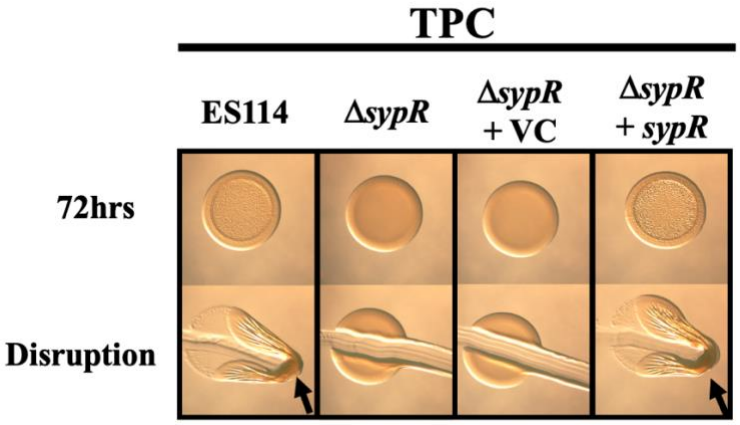

Figure 14: pABA- and Calcium-Induced ES114 Biofilms Require Syp. Colony biofilm formation was assessed following growth of the indicated strains on tTBS + pABA/calcium (TPC). Pictures were taken at 72hrs, and after 72hrs, each colony was disrupted using a toothpick and photographed. The following strains were tested: ES114, Δ*sypR* (KV5195), Δ*sypR* + vector control (VC), Δ*sypR* + *sypR*, a plasmid-based *sypR* complement. Arrows indicate where "pulling" and clumps, indicating cohesion, were observed (Dial, Speare, et al. 2021).

The Δ*sypR* mutant displayed a complete abrogation of biofilm formation, which could be restored by complementation through introduction of *sypR* on a plasmid (Fig. 14). Notably, the corresponding vector control for *sypR* did not restore biofilm formation (Fig. 14). These data indicate that pABA/calcium-induced biofilm are Syp-dependent, providing support to previous data that demonstrated that sticky biofilms produced by genetically modified strains depend on Syp.

Cellulose, encoded by the *bcs* locus, contributes to biofilm formation, which can be seen in shaking biofilms via the ring on the tube above the liquid (Tischler et al. 2018). I, therefore,

explored the impact that *bcs* has in ES114 – induced biofilm formation under pABA/calcium conditions.

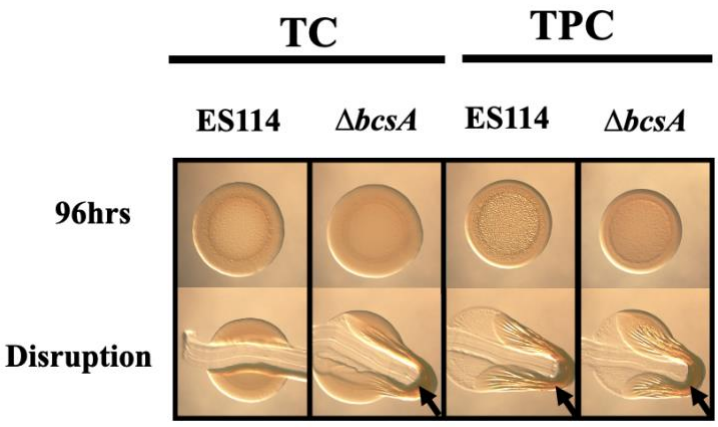

Figure 15. Disruption of Cellulose Synthesis Promotes Cohesive Biofilm Formation by ES114. Colony biofilm formation was assessed following growth of ES114 and Δ*bcsA* (KV8616) on tTBS + calcium (TC) and tTBS + pABA/calcium (TPC). Pictures were taken using a dissecting light microscope at 96 hrs. Each colony was disrupted using a toothpick after 96 hrs. Arrows indicate where "pulling," indicating cohesion, was observed (Dial, Speare, et al. 2021).

A Δ*bcsA* mutant, defective in the production of cellulose, did not diminish biofilm formation induced by pABA/calcium (Fig. 15, right), which is not unexpected given the importance of SYP in cohesive biofilm formation. However, the *bcsA* mutant formed a cohesive biofilm on TC, albeit less than the biofilm formed under pABA/calcium (Fig. 15, left). These results suggest that *bcsA*, or cellulose production, inhibits *syp*-dependent biofilm formation under tTBS agar conditions. The crosstalk between these two pathways will be explored further in subsequent sections.

To identify the underlying mechanisms for pABA/calcium - induced biofilm formation and determine if the upregulation of SYP depended on the induction of *syp* transcription, I asked if pABA/calcium could enhance *syp* promoter activity using a P*sypA-lacZ* fusion strain after 22hrs. Concurrently, I also explored the impact of tTBS conditions on *bcs* promoter activity using a P*bcsQ* – *lacZ* fusion strain; I monitored β-galactosidase activity after 4hrs of incubation.

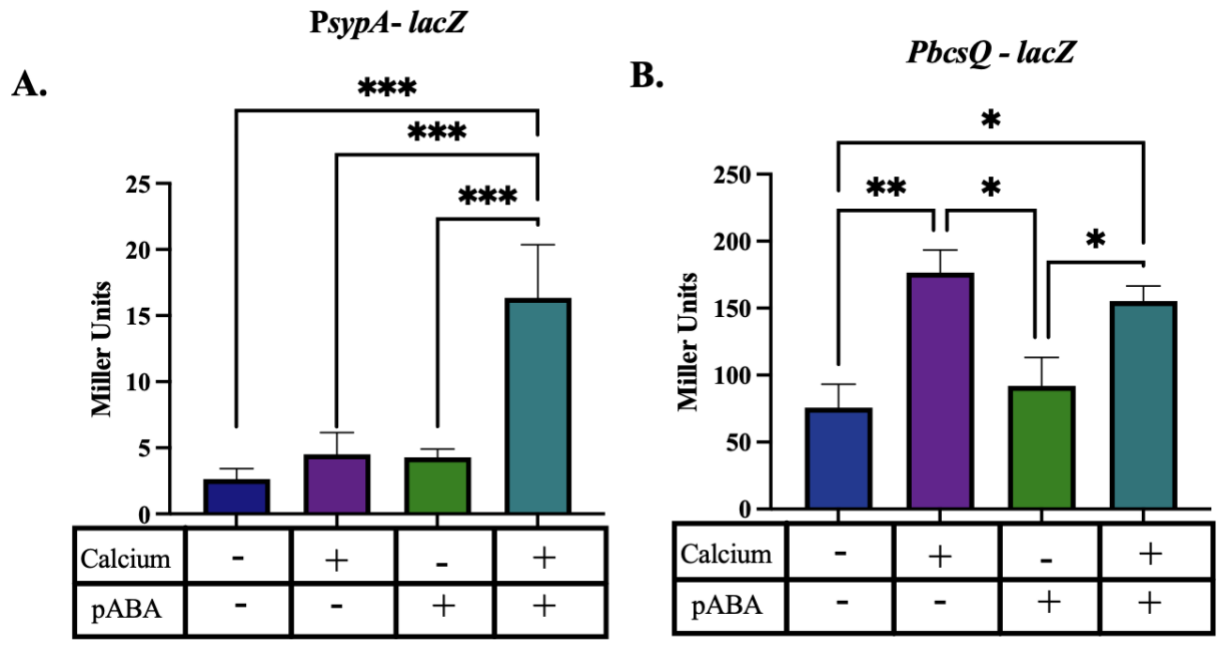

Figure 16. pABA/calcium Induces *syp* Transcription. *sypA* promoter activity (Miller units) was measured using a P*sypA-lacZ* fusion strain (KV8079) following subculture for 22 hrs in tTBS, tTBS + calcium, tTBS + pABA and tTBS + pABA/calcium. *bcsQ* promoter activity (Miller units) was measured using a P*bcsQ-lacZ* fusion strain (KV8078) following a 4hr subculture in tTBS, tTBS + calcium, tTBS + pABA, and T + pABA/calcium. Statistics were performed via a one-way ANOVA Tukey's multiple comparisons test, where Miller units are the dependent variable (Dial, Speare, et al. 2021). *P < 0.04 and **P = 0.0060 ***P < 0.0006.

Basal levels of *sypA* promoter activity (5 Miller units) occurred in tTBS without supplementation (Fig. 16, left). There was no substantial impact on *syp* transcription after adding calcium or pABA alone. However, upon addition of both pABA and calcium, I saw a significant increase in *sypA* promoter activity (~ 3 – fold increase). This increase in *sypA* promoter activity can, at least partially, account for biofilm formation under these conditions. Conversely, under these conditions, the addition of calcium caused an increase in *bcs* promoter activity, similar to that previously reported in LBS conditions (Fig. 16, right) (Tischler et al. 2018). However, adding pABA did not impact *bcs* promoter activity alone or in the context of calcium relative to the appropriate no-pABA controls. The lack of *bcsQ* activity was not surprising as biofilm data

suggested no impact of cellulose on pABA/calcium-induced wrinkled colony formation, and the transcriptional data supports that conclusion.

Transcriptomics Reveals Global Gene Expression Change due to pABA/calcium Conditions.

In order to fully understand the impact pABA has on the physiology of *V. fischeri,* one of our collaborators offered to perform a comparative transcriptome analysis. Lauren Speare, Garrett C. Sharpe, Scott M. Gifford and Alecia N. Septer from UNC – Chapel Hill performed the comparative transcriptome analysis and subsequent data mining. This analysis was done under the following conditions at 24°C: tTBS, tTBS with calcium, and tTBS with pABA/calcium. Cells were harvested and RNA isolated at two time points: at 4hrs when calcium–induced cellulose rings begin to form and 8hrs when SYP – dependent "trees" begin to form. Furthermore, for each 8hr timepoint, the planktonic and sessile cells were separated, and their transcriptomes were sequenced separately. The transcriptome data were analyzed using a principal coordinate analysis (PcoA) to determine how different the transcriptional profiles are among the different treatment groups.

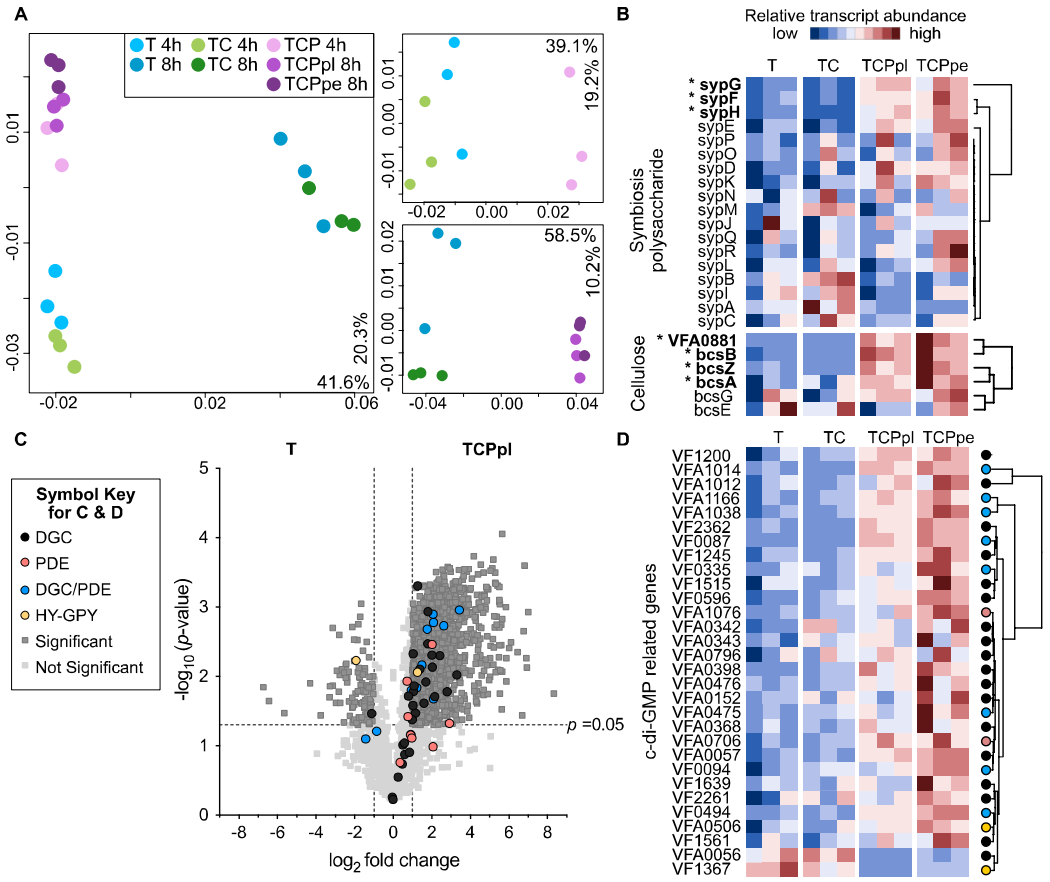

Figure 17. pABA/calcium Conditions Promote Global Changes in Gene Expression. (A) Principal coordinate analysis (PCoA) plots displays differences in ES114 transcriptomes incubated in different media types at 4 and 8 hrs (left), 4 hrs only (right, top), or 8 hrs only (right bottom). ES114 cells were incubated in tTBS (T, blue), tTBS + 10 mM $CaCl_2$ (TC, green), or tTBS + pABA/calcium (TCP, purple). Cells in TCP were either collected from suspension and considered "planktonic" (TCPpl) or collected from the biofilm pellet at the bottom of the tube (TCPpe). Samples were collected after either 4 (lighter shade) or 8 hrs (darker shade) of incubation. Percentages on each axis indicate the amount of variation explained by each axis; p-values. Calculated via PERMANOVA. (B) Heatmap of hierarchical clustering results for ES114 8 hr transcriptomes. Each row represents a gene from either the symbiosis polysaccharide (top) or cellulose biosynthesis (bottom) gene clusters; each column represents a sample. The square color in the heatmap indicates the relative transcript abundance for a given transcript across samples: red indicates high abundance, and blue indicates low abundance. Asterisks indicate genes with significantly higher relative transcript abundance in TCPpl and TCPpe relative to T and TC treatments. (C) Volcano plot showing the $\log_2$ fold change in transcript abundance between ES114 cultures incubated in tTBS (T) or tTBS 10 mM Calcium 9.7 mM pABA planktonic cells (TCPpl) for 8 hours. Transcripts with a negative $\log_2$ fold change value are more abundant in tTBS (left), and transcripts with a positive $\log_2$ fold change value are more abundant in tTBS Calcium pABA (right). The symbol indicates the functional assignment of the gene/transcript of interest: dark gray (DGC), red (PDE), yellow (HD-GYP), and blue (DCG/PDE). Data points above the dashed horizontal line had significant *P* –values between treatments (DESeq analysis; FDR $P<0.05$), and those outside of the vertical dashed lines had a

magnitude fold change of > |1| log_2 between treatments (gray squares). (D) Heatmap of hierarchical clustering results for the relative transcript per CFU abundance for ES114 8 hr transcriptomes. Each row represents a gene related to c-di-GMP production significantly differentially expressed in DESeq analysis (FDR $P<0.05$); each column represents a sample (Dial, Speare, et al. 2021).

PCoA performed on all treatments revealed that ES114 transcriptomes were influenced by both time and the presence/absence of pABA (Fig. 17A). When samples were analyzed independently at each time point, samples clustered based on whether pABA was present, with the presence/absence of pABA explaining 39.1% and 58.5% of the variation in the data at 4 and 8hrs, respectively (Fig. 17A). The transcriptome analysis was catered to focus on transcriptional changes for biofilm-related genes across the 8hr treatments when pABA had its most considerable effect. A hierarchical clustering analysis indicates that cells grown in pABA/calcium conditions are enriched for transcripts in most, but not all, *syp* and *bcs* genes compared to the tTBS control (Fig. 17B). The genes that were the most significantly enriched are as follows: *sypF, sypG, sypH, bcsA, bcsB, bcsZ,* as well as *VF_A0881*, which encodes a cellulose synthase protein. The upregulation of polysaccharide-related genes indicate that the transcriptome analysis supports my initial hypothesis and data thus far that pABA/calcium contributes to enhanced transcription of the *syp* and *bcs* gene clusters. However, calcium is likely the key player for *bcs* here and not pABA, as indicated by Figures 14 and 15 and the work discussed in future sections.

For a more comprehensive look at how cells respond to pABA/calcium, transcriptomes from the 8hr timepoint from the tTBS control and pABA/calcium were compared. pABA/calcium conditions resulted in over a thousand changes in gene expression, with the enrichment of transcripts for 688 genes and depletion of transcripts for 659 genes compared to the tTBS control (Fig. 17C). We decided to focus on the other key signal in biofilm formation: c-

di-GMP. When all 50 genes encoding proteins related to c-di-GMP synthesis and degradation were mapped onto a volcano plot, 30 genes were significantly differentially expressed between treatments (Fig. 17C). A hierarchical clustering analysis further explored the relative transcriptional changes for these 30 genes across all treatments at the 8hr timepoint. Transcripts for 28 of the 30 genes were enriched in the pABA/calcium condition (Fig. 17D), including 26 genes that encode putative DGCs or dual-function enzymes that could contribute to a global increase in c-di-GMP with pABA addition. Notably, only two genes had transcripts that were significantly decreased in pABA/calcium, a predicted DGC, and a predicted PDE (Fig. 17D). Taken together, pABA exerts a considerable impact on *V. fischeri* gene expression globally, with enrichment in transcripts associated with biofilm–related genes.

pABA Upregulates c-di-GMP while Causing a Slight Growth Defect and Cellular Aggregation.

Due to c-di-GMP having a strong connection with biofilm formation and so many c-di-GMP-related genes being enriched in the transcriptome analysis, I hypothesized that c-di-GMP might play a role in pABA/calcium-induced phenotypes.

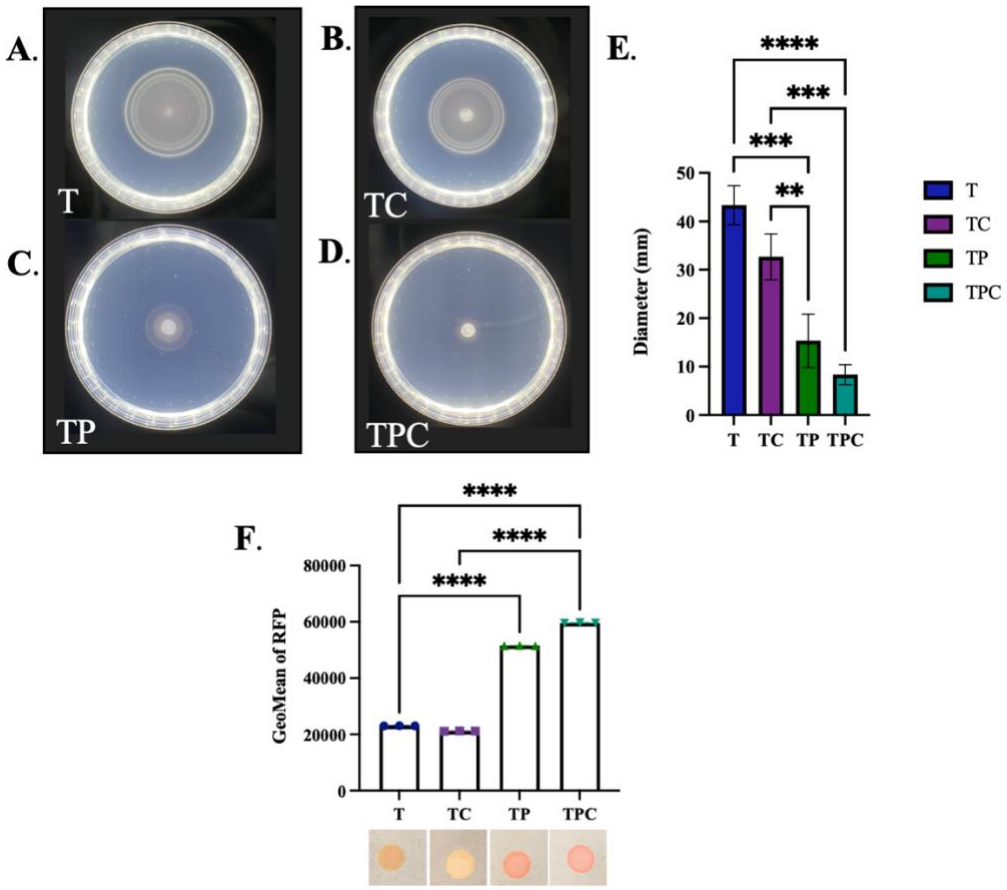

Figure 18. pABA Impacts Motility and c-di-GMP Production. (A-D) Migration of ES114 was evaluated using soft-agar motility plates supplemented with calcium, pABA, or both. Pictures were taken after 6 hrs, and representative images are shown. A. tTBS (T) B. tTBS + calcium (TC) C. tTBS + pABA (TP) and D. tTBS + pABA/calcium (TPC). (E) Migration was evaluated by measuring the outer diameter of the migrating cells. Statistics for E were performed via a one-way ANOVA with Tukey's multiple comparisons test, where diameter was the dependent variable. **P = 0.0049, ***P < 0.0005 and ****P < 0.0001 (F) Levels of c-di-GMP were estimated using ES114 containing c-di-GMP biosensor plasmid pFY4535. Flow cytometry measured RFP from the same strain grown in T, TC, TP, or TPC liquid cultures. The cells were first gated using AmCyan and then on RFP. Statistics for F were performed via a one-way ANOVA with Tukey's multiple comparisons test. **** P < 0.0001. A culture of this strain was spotted on tTBS plates containing calcium, pABA, or pABA/calcium, and the resulting RFP was visualized. Representative pictures are shown.

As described earlier, c-di-GMP is a second messenger that promotes biofilm formation and inhibits motility. Therefore, I determined if pABA supplementation would impact the motility of ES114. ES114, without supplementation, migrates rapidly in a semisolid medium,

reaching a diameter of around 45mm within 6hrs (Fig. 18A, B, and E). In contrast, when pABA was added to the medium, the migration slowed dramatically, and ES114 only reached a diameter of 8mm within the same 6hr window (Fig. 18C and E). These results indicate that c-di-GMP may be involved.

To determine if pABA addition increases c-di-GMP levels, I used a c-di-GMP biosensor that contains *rfp* (encoding red fluorescent protein) under the control of a c-di-GMP riboswitch (Zamorano-Sanchez et al. 2019). Increased levels of c-di-GMP will bind to the riboswitch and produce RFP, which can then be visualized and quantified. The addition of pABA to ES114 containing the biosensor produced a visibly and measurably significant increase in RFP production relative to unsupplemented cultures (Fig. 18F), indicating an upregulation in c-di-GMP production. This upregulation of RFP/c-di-GMP is consistent with the impact of pABA on biofilm formation and motility. While the addition of calcium alone did not significantly impact c-di-GMP levels, there was a trend upwards when both pABA and calcium were present (Fig. 18F).

Due to the global change in gene expression and pABA being, intrinsically, an acid, I wanted to ensure that the observed effects were not just attributed to the impact of pABA on the growth of ES114. Therefore, I monitored growth of ES114 in tTBS alone or with pABA/calcium supplementation.

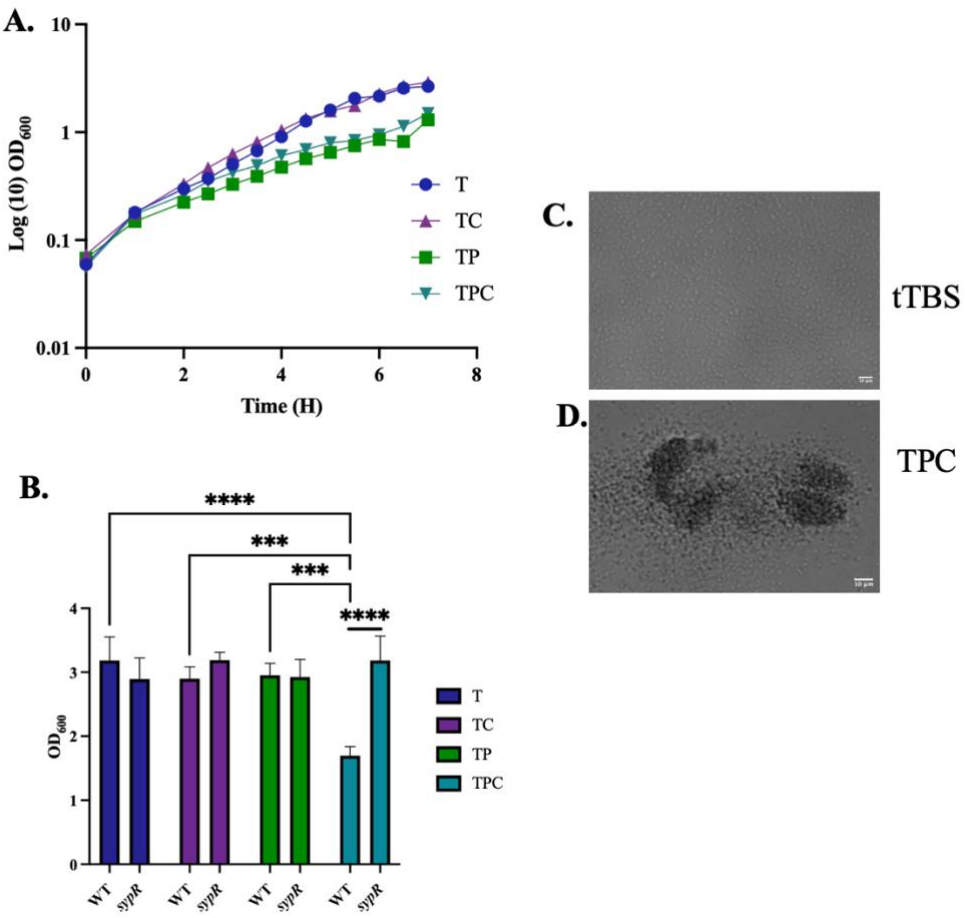

Figure 19. pABA Impacts Growth and Cellular Aggregation. (A) Growth of WT ES114 was evaluated over time in tTBS (T), tTBS + Calcium (TC), tTBS + pABA (TP), and tTBS + pABA/calcium (TPC) over the course of 7hrs by monitoring the OD_{600} using a spectrophotometer. (B) Growth of WT ES114 and Δ*sypR* in T, TC, TP, and TPC after 19hrs monitored via OD_{600} using a spectrophotometer. Statistics for B were performed via a two-way ANOVA with Tukey's multiple comparisons test, where OD was the dependent variable. ***P < 0.0002 and ****P < 0.0001 for comparisons between media conditions and a 2-way ANOVA using Šídák's multiple comparison test **** P < 0.0001 for comparisons between strains. (C-D) Picture of ES114 aggregation in T and TPC after the growth curve at 7 hrs**.**

The addition of calcium to the media exerted no impact on ES114 growth; pABA addition (with or without calcium) modestly diminished the OD of the cultures, suggesting a slight growth defect (Fig. 19A). However, cells grown under pABA conditions achieved the same OD as those grown in tTBS within 19hrs (Fig. 19B). While this was not the case for cells grown in pABA/calcium, the apparent growth defect under that condition could be attributed to the

formation of aggregates, which were observed in the cultures containing pABA/calcium (Fig. 19C and D). To test further whether cellular aggregation caused the decrease in OD, I used a mutant unable to produce *syp* biofilms, Δ*sypR*, and this strain under the same growth conditions was able to reach the same OD under pABA/calcium (Fig. 19B). This indicates that biofilm formation accounted for the decreased OD observed in WT at 19hrs. These data suggest that while pABA-induced cells exhibit a growth defect early in growth, they eventually catch up, and any remaining growth defect can be attributed to biofilm formation. Further, the observed biofilm phenotypes in pABA/calcium conditions are related to forming a biofilm rather than a growth defect.

Summary.

I found that yeast extract inhibits the Δ*binK* mutant biofilm formation and that pABA seems to be the inhibitory component. After discovering that pABA/calcium induces biofilm formation of ES114, I decided to focus on this result, and I set out to determine the various effects this condition had on ES114 physiology. In this section, I described the optimal conditions under which pABA/calcium induces biofilm formation and that this can occur under multiple assay conditions. I also showed that these biofilms are due to the upregulation and subsequent formation of *syp* – dependent biofilms rather than cellulose while uncovering a potential crosstalk between the two polysaccharides. Further, work revealed that pABA-induced gene expression changes globally, and many of those changes are directly linked to biofilm–related genes such as *syp*, *bcs*, and c-di-GMP. Lastly, pABA induces significant expression/production of c-di-GMP, and while it caused a slight growth defect during exponential growth, the cells eventually catch up to their non-treated counterparts, and any remaining growth defect can be attributed to the formation of cellular aggregates.

In the next section, I will tease apart the relationship between SYP and cellulose. I will also uncover the primary Syp regulator responsible for the observed biofilm phenotypes and the potential mechanism through which this occurs.

Genetic Analysis Revealed that the Hybrid Sensor Kinase, RscS, is Required for pABA/calcium-Induced Biofilm Formation.

Introduction.

As mentioned, the main polysaccharide for pABA/calcium-induced biofilms is SYP, which is also critical for efficient squid colonization (Visick, Stabb, and Ruby 2021). As detailed in the introduction, *syp* transcription is tightly controlled by several two-component regulators (Fig. 6). Correspondingly, I wanted to know if any of these regulators were responsible for inducing pABA/calcium biofilm formation or if pABA/calcium was working through unknown mechanisms to induce *syp* transcription.

I also found that, while cellulose, the other main polysaccharide in *V. fischeri*, did not impact pABA/calcium biofilm formation, the deletion of a cellulose synthase gene upregulated biofilm formation on calcium alone. It remains to be seen if biofilms formed by a Δ*bcsA* mutant under calcium conditions are *syp* dependent or occur due to an unknown polysaccharide. Still, there is a potential for crosstalk between the two polysaccharides SYP and cellulose competing for glucose subunits.

Three regulators, to date, have been identified to control *bcs* transcription/cellulose production, as detailed in the introduction. Two of these, VpsR and CasA, have a direct and indirect impact, respectively, on *bcs* transcription (Tischler et al. 2021). Therefore, to uncover if cellulose regulation/transcription contributes to SYP production, *vpsR* and *casA* mutants are potent tools.

In this section, I will go through all of the known regulators of biofilm formation in *V. fischeri* before discussing the central regulator(s) involved in pABA/calcium biofilm formation: SypF and RscS. I will also begin to detail the connection between cellulose and SYP synthesis by looking at two regulators of cellulose transcription: VpsR and CasA. I determined, through genetic manipulation, that RscS is the primary TCS responsible for the observed biofilm formation induced by pABA/calcium. I also hypothesized, and supported my hypothesis, that RscS is sensing the pABA environment to induce ES114 biofilm formation.

The Syp Regulatory Network is Crucial for pABA-Induced Biofilm Formation and Cellulose Inhibits SYP Production.

The central sensor and response regulator responsible for *syp* transcription and SYP production are SypF and SypG (respectively). These two regulators are, therefore, perfect options to delete to ascertain if the pABA/calcium upregulation of *syp* transcription is occurring through the canonical signaling pathway/ TCS network. Hence, I started my SYP regulator experimentation with *sypF* and *sypG* mutations, looking at biofilm formation and *syp* transcription.

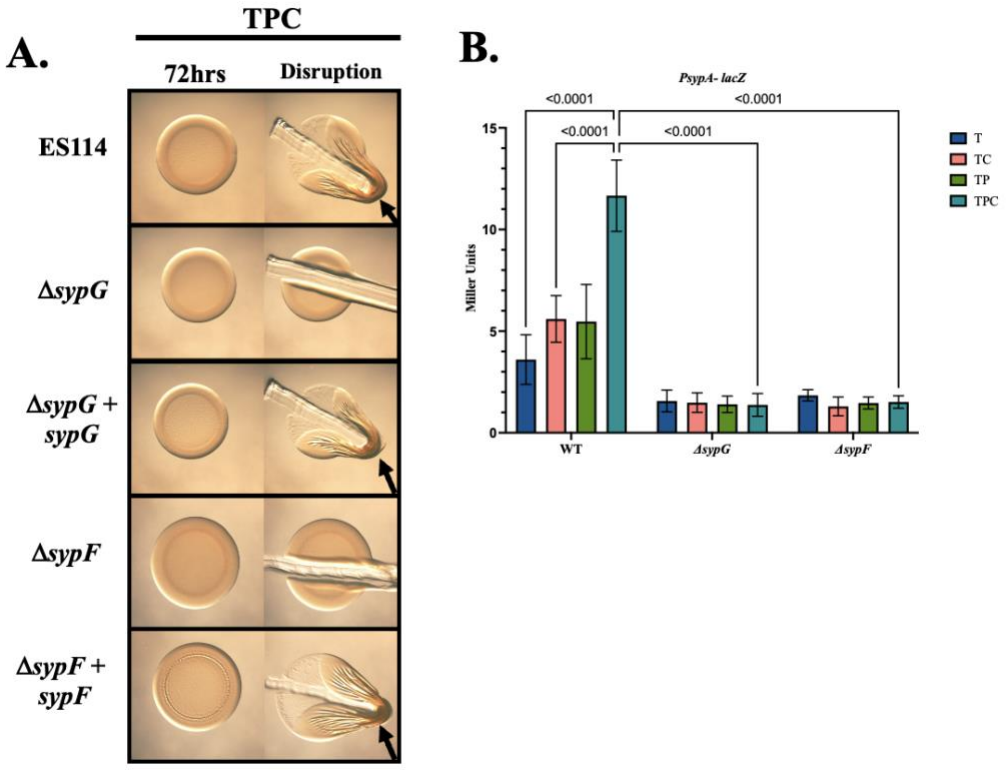

Figure 20. SypF and SypG are Required for pABA/calcium-Induced SYP Production and *syp* Transcription. (A) Colony biofilm formation by WT ES114, the Δ*sypG* mutant (KV1787), the *sypG* complement (KV6475), the Δ*sypF* mutant (KV5367), and the *sypF* complement (KV6659) were evaluated following growth on tTBS with 10mM calcium and 9.7mM pABA (TPC). Pictures were taken using a dissecting light microscope at 72hrs. Each colony was disrupted using a toothpick after 72hrs. Pictures are representative of 3 separate experiments. Arrows indicate where "pulling", indicating cohesion, was observed. (B) *sypA* promoter activity (Miller units) was measured using a P*sypA- lacZ* fusion strain (KV8079) where either *sypG* or *sypF* were deleted (KV10307 and KV10317, respectively) following subculture for 22hrs in tTBS (T), tTBS + calcium (TC), tTBS + pABA (TP) and tTBS + pABA/calcium (TPC). Statistics for panel B were performed via a two-way ANOVA Tukey's multiple–comparison test, where Miller units was the dependent variable.

I found that not only did the deletion of either *sypG* or *sypF* completely abrogate biofilm formation, but these deletions also prevented *sypA* transcription (Fig. 20A and B). I could also fully complement both *sypG* and *sypF,* further supporting the impact of SypG and SypF on pABA/calcium-induced biofilm formation (Fig. 20A). These data support the hypothesis that the

TCS network is responsible for pABA/calcium-induced biofilm formation but the exact regulator responsible is still unclear.

Since both RscS and HahK also contribute phosphoryl groups to the HPT domain of SypF (Fig. 6), any or all of these regulators could be contributing to the observed phenotype shown in Fig. 20A and B. RscS, as detailed in the introduction, sits at the top of the Syp TCS hierarchy. It was also the first regulator to be discovered in this network and is critical for squid colonization (Visick and Skoufos 2001). Therefore, I looked at an Δ*rscS* mutant under pABA calcium conditions.

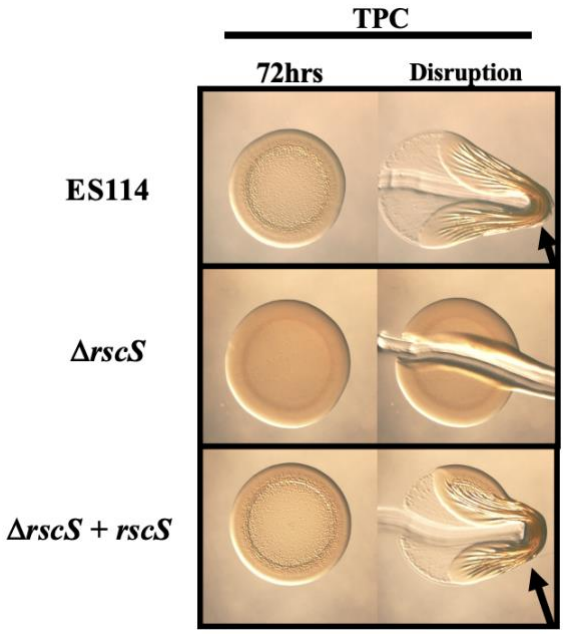

Figure 21. RscS is Critical for pABA/calcium-Induced Biofilm Formation on Solid Agar. Colony biofilm formation by WT ES114, the Δ*rscS* mutant (KV10130), and the *rscS* complement (KV10166) were evaluated following growth on tTBS + pABA/calcium (TPC). Pictures were taken using a dissecting light microscope at 72hrs. Each colony was disrupted using a toothpick after 72hrs. Pictures are representative of 3 separate experiments. Arrows indicate where "pulling," indicating cohesion, was observed.

Deletion of *rscS* results in a complete disruption of biofilm formation and could be fully complemented via an *rscS* gene at a non-native site in the chromosome (Fig. 21). This result is the first time that an Δ*rscS* mutant displayed a phenotype without any other genetic manipulation

under laboratory conditions. These data support the hypothesis that RscS is a key regulator responsible for pABA/calcium-induced biofilm formation.

Previously, HahK was considered to play a more prominent role in biofilm formation than RscS (Tischler et al. 2018). There could also be more than one, possibly all known regulators, responsible for the pABA/calcium observed phenotypes. I, therefore, next looked at the impact that HahK and its partner regulator, HnoX **(**Fig. 6), had on pABA/calcium-induced biofilm formation.

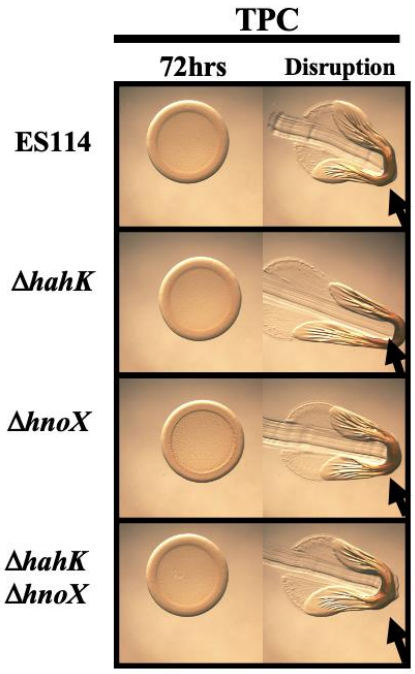

Figure 22. HahK and HnoX are not Required for TPC Biofilms. (A) Colony biofilm formation by WT ES114, the Δ*hahK* mutant (KV7964), the Δ*hnoX* mutant (KV8025), and the Δ*hahK* Δ*hnoX* double mutant (KV8484) were evaluated following growth on tTBS + pABA /calcium (TPC). Pictures were taken using a dissecting light microscope at 72hrs. Each colony was disrupted using a toothpick after 72hrs. Pictures are representative of 3 separate experiments. Arrows indicate where "pulling," indicating cohesion, was observed.

I found that, under pABA/calcium conditions, neither HahK nor HnoX have any impact on ES114 biofilm formation (Fig. 22). These data, combined with Figs 20 and 21, support the notion that RscS and SypF are the main contributors to biofilm formation, working through the

response regulator SypG. To further this hypothesis that RscS, and not HahK, is responsible for ES114 biofilm formation under pABA/calcium conditions, as well as determine if this regulation happens at the level of transcription, I also looked at *sypA* transcription when either *rscS* or *hahK* was deleted.

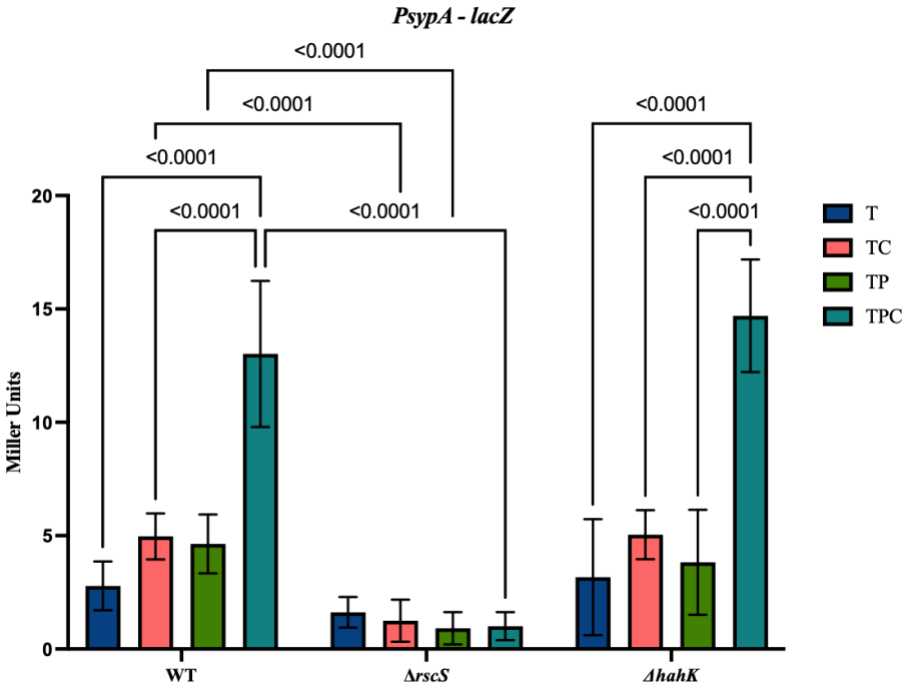

Figure 23. RscS Impacts *syp* Transcription to Upregulate Biofilm Formation. *sypA* promoter activity (Miller units) was measured using a *PsypA- lacZ* fusion strain (KV8079) where either *rscS* or *hahK* were deleted (KV9653 and KV10304, respectively) following subculture for 22hrs in tTBS (T), tTBS + calcium (TC), tTBS + pABA (TP) and tTBS + pABA/calcium (TPC). Statistics were performed via a two-way ANOVA with Tukey's multiple–comparison test, where Miller units was the dependent variable.

I found that the deletion of *rscS* completely abrogated *sypA* transcription; in fact, some of the values were below the limit of detection (Fig. 23). Conversely, deletion of *hahK* had no impact on *sypA* transcription under any condition. These data support the hypothesis that RscS, not HahK, is the primary regulator responsible for pABA/calcium-induced biofilm formation. The interplay between RscS and SypF will be evaluated in the next section.

Next, I determined if there is a relationship between SYP and cellulose production. To determine if the coherent biofilms seen in Fig. 15 (in the Δ*bcsA* mutant) were, in fact, SYP – dependent, I assessed a *bcsA sypQ* double mutant. This double mutant is unable to produce either polysaccharide; therefore, if the Δ*bcsA* biofilm formed under calcium conditions is, in fact, SYP, then deletion of *sypQ* will render a Δ*bcsA* mutant unable to form a biofilm on TC.

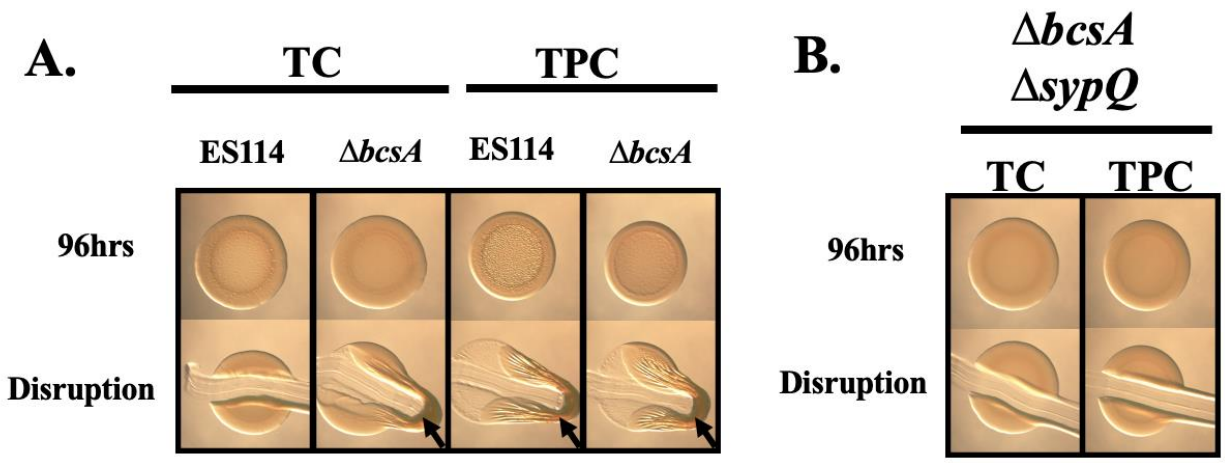

Figure 24. Cellulose Inhibits SYP – Production. (A) Colony biofilm formation was assessed following growth of ES114 and Δ*bcsA* (KV8616) (from Fig. 14, above) or (B) Δ*bcsA* Δ*sypQ* (KV9380) on tTBS + calcium (TC) and tTBS + pABA/calcium (TPC). Pictures were taken using a dissecting light microscope at 96 h. Each colony was disrupted using a toothpick after 96 h. Arrows indicate where "pulling," indicating cohesion, was observed**.**

The double mutant failed to produce a coherent biofilm under calcium conditions (Fig. 24B). These data indicate that the observed biofilm in Fig. 23A is SYP – dependent and further implicates cellulose inhibiting the production of SYP. To further explore the connection between SYP and cellulose, I assessed the various regulators of *bcs* transcription: VpsR and CasA.

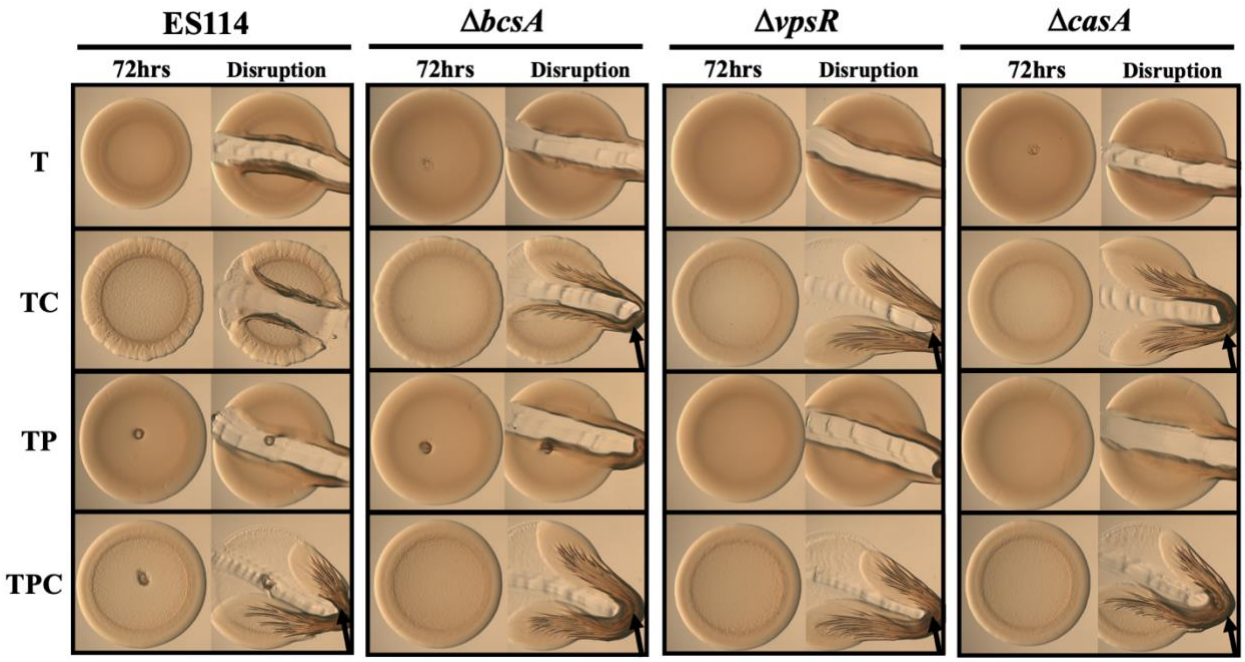

Figure 25. VpsR and CasA Inhibit SYP Production. Colony biofilm formation was assessed following growth of ES114, Δ*bcsA* (KV8616), Δ*vpsR* (KV9341), and Δ*casA* (KV8920) on tTBS (T), tTBS + calcium (TC), tTBS + pABA (TP) and tTBS + pABA/calcium (TPC). Pictures were taken using a dissecting light microscope at 96 h. Each colony was disrupted using a toothpick after 96 h. Arrows indicate where "pulling," indicating cohesion, was observed**.**

Perhaps unsurprisingly, due to VpsR and CasA controlling Bcs production, a Δ*vpsR* and Δ*casA* mutant displayed cohesive biofilm production on TC compared to WT (Fig. 25). Furthermore, the Δ*vpsR* and Δ*casA* mutants have stickier colonies when compared to the Δ*bcsA* mutant (Fig. 25). The hierarchy proposed is that both CasA and VpsR work to induce *bcs* transcription (Tischler et al. 2021); therefore, the greater induction of TC biofilms via the Δ*casA* and Δ*vpsR* mutants correlate to this network. These data support the hypothesis that cellulose production and/or transcription inhibits SYP production and or *syp* transcription and that there is a crosstalk between the two. While it is evident, based on figures 24 and 25, that a connection between the two polysaccharides exists, further work will need to be done in order to fully unravel the interplay between the two and determine the exact mechanism(s).

RscS is the Main Regulator Involved in pABA/calcium-induced Biofilm Formation.

As detailed above, RscS donates a phosphoryl group to the HPT domain of SypF in order to phosphorylate SypG and eventually upregulate *syp* transcription (Norsworthy and Visick 2015). Therefore, at this point, either SypF or RscS could be the primary regulator responsible for pABA/calcium-induced *syp* transcription and SYP production. In order to determine which regulator is truly responsible and possibly sensing pABA, I used a mutant of SypF that only contained the HPT domain. If SypF is the primary sensor, then complementing with just the SypF HPT will not rescue biofilm formation. Further, if the SypF HPT domain complements a Δ*sypF* mutant, then either HahK and/or RscS would need to be responsible for sensing the signal and relaying a response to it. Furthermore, under conditions in which only SypF-HPT is present, if I still see biofilm formation when *hahK/hnoX* is deleted, then RscS must be the regulator contributing phosphoryl groups to SypF.

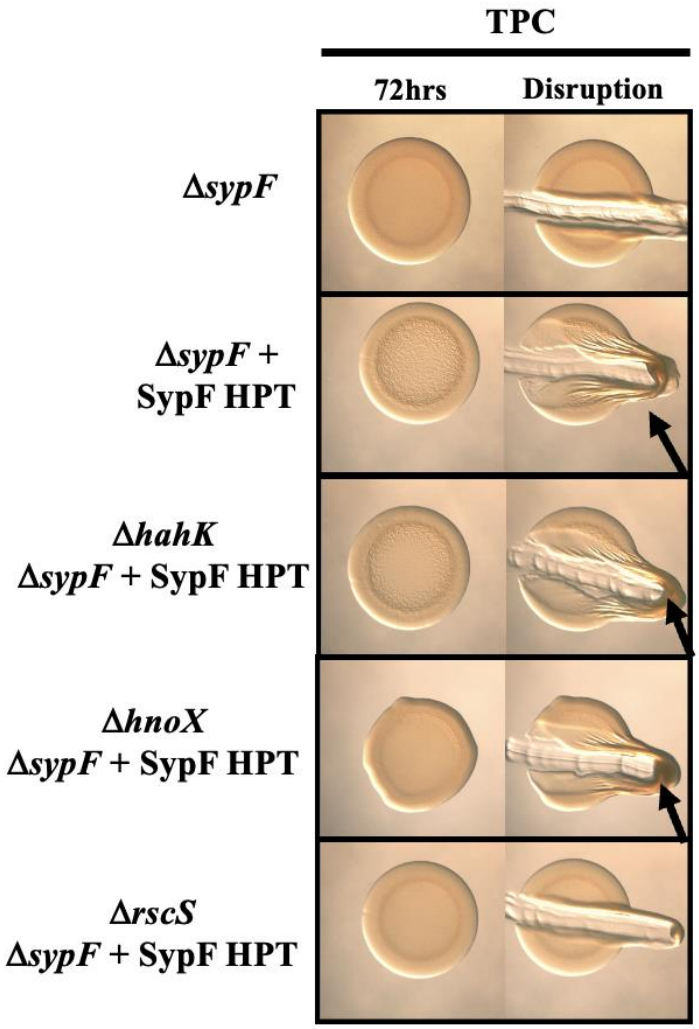

Figure 26. RscS is the Main Regulator Responsible for pABA/calcium-Induced Biofilm Formation. Colony biofilm formation by the Δ*sypF* mutant (KV5367), the *sypF* mutant complemented with only the SypF HPT domain (KV7226), Δ*hahK* Δ*sypF* complemented with SypF HPT (KV9968), Δ*hnoX* Δ*sypF* complemented with SypF-HPT (KV10226) and Δ*rscS* Δ*sypF* complemented with SypF-HPT (KV9953) were evaluated following growth on tTBS + pABA/calcium (TPC). Pictures were taken using a dissecting light microscope at 72hrs. Each colony was disrupted using a toothpick after 72hrs. Pictures are representative of 3 separate experiments. Arrows indicate where "pulling," indicating cohesion, was observed.

I saw that the SypF HPT domain alone could partially complement a Δ*sypF* mutant, indicating that either RscS or HahK is the primary regulator responsible for pABA/calcium-induced biofilm formation (Fig. 26). Only the Δ*rscS* mutant in the Δ*sypF* + SypF HPT mutant

background exhibited a disruption in biofilm formation (Fig. 26). These data, and the data above, support my hypothesis that RscS is the leading player in pABA/calcium-induced biofilm formation. In the next section, I will explore the exact role of RscS in WT ES114 biofilm formation under these new conditions. I hypothesize that RscS is sensing the pABA condition to upregulate *syp* transcription and eventual SYP-dependent biofilm formation.

RscS Senses the pABA/calcium Condition to Induce *syp* Transcription and Biofilm Formation.

In order to test my hypothesis that RscS is sensing pABA, I began by deleting one of the sensor domains of RscS. RscS contains two putative sensory domains: the periplasmic loop domain, which sits in the periplasmic space, and a PAS domain spanning the lipid bilayer and extending into the cytoplasm. Based on the ability of pABA to cross the lipid bilayer (Maynard et al. 2018), I hypothesize that pABA crosses the lipid bilayer and signals within the periplasmic space, as well as crossing the second lipid bilayer to elicit the other transcriptional effects shown in Fig. 23. Therefore, I decided to delete just the periplasmic loop of RscS. If pABA is signaling through that domain in order to promote biofilm formation, I would see an abrogation of biofilm formation. This construct was made in a non-native site on the chromosome in a background that has *rscS* deleted; hence, the only RscS present lacks a periplasmic loop.

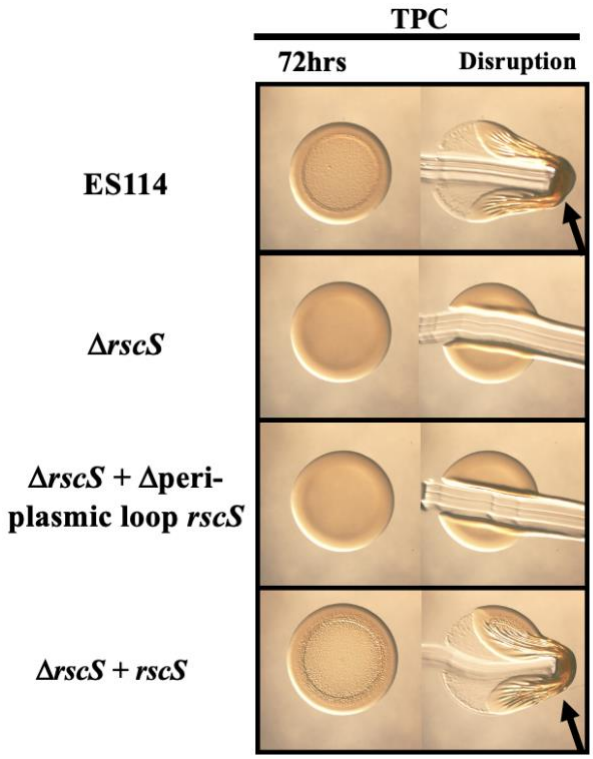

Figure 27. The Periplasmic Loop of RscS is Essential for TPC-Mediated Biofilm Formation. Colony biofilm formation by WT ES114, the Δ*rscS* mutant (KV10130), the Δ*rscS* mutant complemented with an *rscS* missing its periplasmic loop (KV10303), and the *rscS* complement (KV10166) were evaluated following growth on tTBS + pABA/calcium (TPC). Pictures were taken using a dissecting light microscope at 72hrs. Each colony was disrupted using a toothpick after 72hrs. Pictures are representative of 3 separate experiments. Arrows indicate where "pulling," indicating cohesion, was observed.

I found that when Δ*rscS* was complemented with a version of *rscS* lacking its periplasmic loop, pABA no longer induced biofilm formation (Fig. 27). In fact, the mutant lacking the periplasmic loop phenocopied a clean Δ*rscS* deletion versus the WT or full *rscS* complementation which exhibited cohesive biofilms (Fig. 27). However, there is one major caveat to this result: I do not know if RscS is being produced. Due to the low copy number of RscS naturally, as a sensor kinase, visualization via western blot is challenging. Consequently, I made the construct the same way as done previously in the Visick lab, and that was shown to produce an active RscS from a multi-copy plasmid (Geszvain and Visick 2008). Given these

previous results, I hypothesize that the Δperiplasmic loop *rscS* is being produced, but I cannot know for sure without western data.

I decided to support my hypothesis further that RscS is sensing pABA by employing more genetic tools. First, I utilized a plasmid that contains a WT *rscS* (RscS+; pLMS33). I put this plasmid, as well as a vector control plasmid, into WT ES114, resulting in *rscS* overexpression that does not overwhelm the system. For example, the strain containing the pLMS33 plasmid does not result in biofilm formation under LBS conditions, whereas other strains containing RscS+ constructs can form cohesive biofilms on LBS ((Yip et al. 2006) Fig. 28).

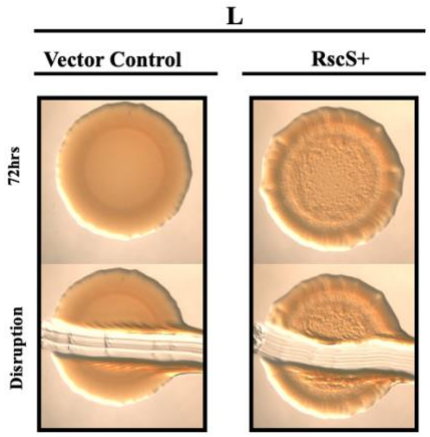

Figure 28. RscS + does not Induce Biofilm Formation on LBS Alone. Colony biofilm formation of ES114 + vector control (pKV69) or ES114 + wild-type *rscS* on a plasmid (pLMS33; RscS+) were assessed following growth on LBS (L). Pictures were taken using a dissecting light microscope at 72hrs. Each colony was disrupted using a toothpick after 72hrs. Pictures are representative of 3 separate experiments.

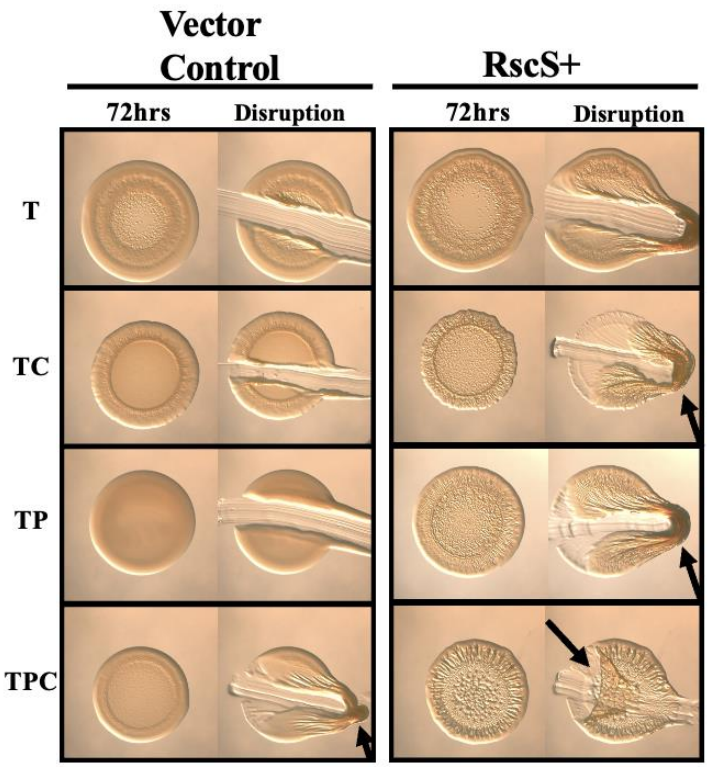

Figure 29. Multi-copy RscS Induces Biofilm Formation on pABA Media. Colony biofilm formation of ES114 + vector control (pKV69) or ES114 + wild-type *rscS* on a plasmid (pLMS33; RscS+) were assessed following growth on tTBS (T), tTBS + calcium (TC), tTBS + pABA (TP) and tTBS + pABA/calcium (TPC). Pictures were taken using a dissecting light microscope at 72hrs. Each colony was disrupted using a toothpick after 72hrs. Pictures are representative of 3 separate experiments. Arrows indicate where "pulling," indicating cohesion, was observed.

I found that the RscS+ plasmid induces biofilm formation on all media types: T, TC, TP, and TPC. Notable is its ability to promote biofilm formation on TP alone, as well as the further induction on TPC when compared to the vector control on TPC (Fig. 29). The highlight is the ability of extra copies of RscS to induce biofilm formation on a condition that, otherwise, does not support biofilm formation: TP. In order to support these data, I also assessed *sypA* transcription under these conditions with WT *rscS* on a plasmid.

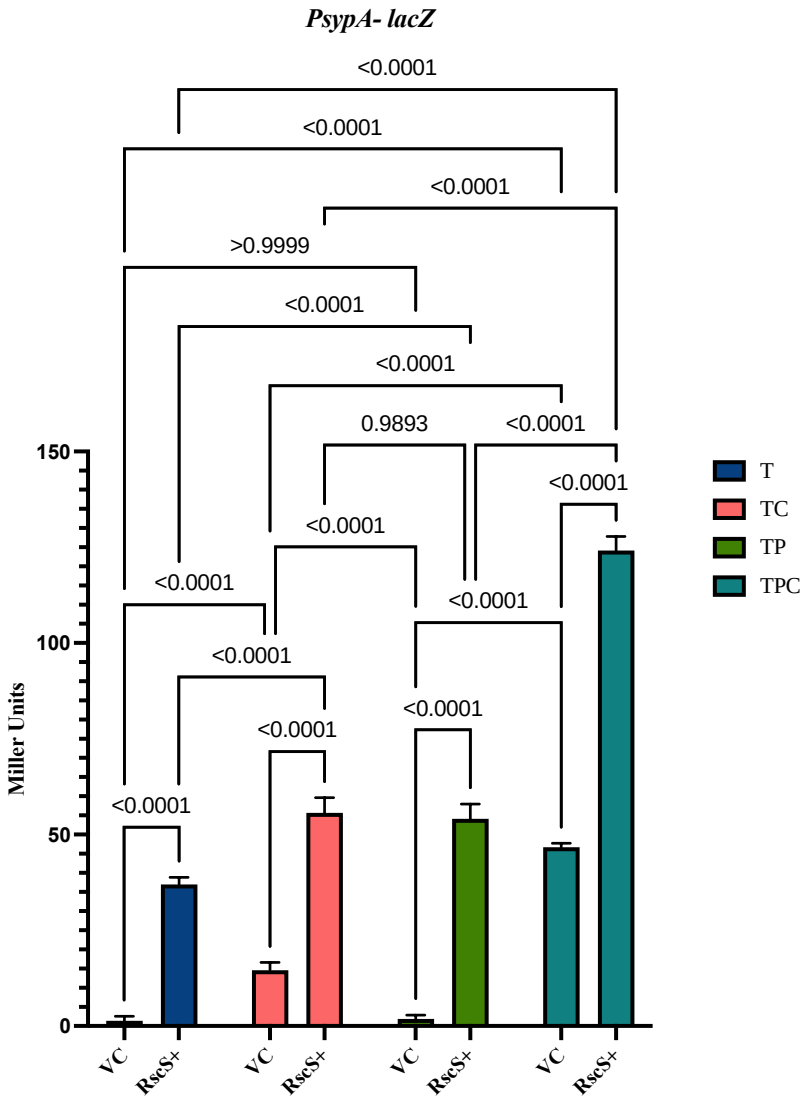

Figure 30. Multi-copy RscS Induces *syp* Transcription. *sypA* promoter activity (Miller units) was measured using P*sypA-lacZ* fusion strain KV8079 that contained either the Vector control (VC; pKV69) plasmid or the RscS+ plasmid (pLMS33) following a 22hr subculture in tTBS (T), tTBS + calcium (TC), tTBS + pABA (TP) and tTBS + pABA/calcium (TPC). Statistics were performed via a two-way ANOVA using Tukey's multiple–comparison test, where Miller units was the dependent variable.

The RscS+ plasmid induced a significant increase in *syp* transcription across all conditions when compared to VC (Fig. 30). There was also a significant increase when the strain containing RscS+ is in tTBS conditions was compared to the strain containing RscS+ in TP (Fig. 30). This increase in *syp* transcription of RscS+ in pABA supports my hypothesis of RscS sensing the

pABA condition to some extent. Also, under TPC conditions with strains that contained the RscS+ plasmid I saw the most significant increase in *syp* transcription that seems to be additive of both RscS+ under TC and TP conditions (Fig. 30). I did see a significant increase under TC conditions alone. My hypothesis here is that calcium induces SypF into a kinase rather than its default net phosphatase state and this, along with the increase in numbers of RscS, results in an increase in *syp* transcription and biofilm production. In contrast, under TP conditions, SypF still acts as a net phosphatase, so the ability of RscS+ to induce *syp* transcription and biofilm formation is directly due to the ability of RscS to sense/respond to pABA.

Previously, I saw that pABA/calcium-induced biofilms relies on SypF and, specifically, the HPT domain of SypF (Fig. 26). Therefore, I wondering if the RscS+-induced biofilms also depend on the HPT domain of SypF. To test this, I put the RscS+ plasmid (pLMS33) into a Δ*sypF* mutant and a Δ*sypF* mutant complemented with just the HPT domain of SypF.

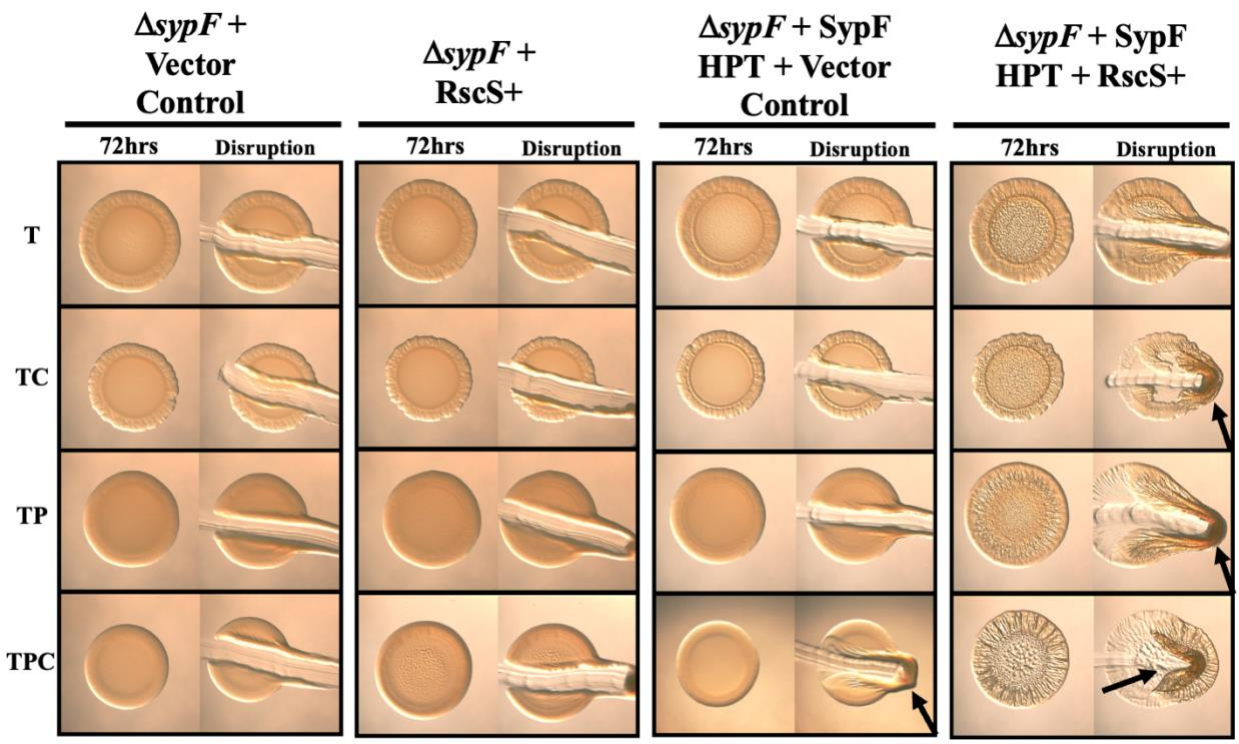

Figure 31. RscS+ Induction of Biofilm Formation Relies on the SypF HPT Domain. Colony biofilm formation of Δ*sypF* (KV5267) + vector control (pKV69), Δ*sypF* (KV5367) + wild-type *rscS* on a plasmid (pLMS33; RscS+), Δ*sypF* + SypF HPT (KV7226) + vector control (pKV69), and Δ*sypF* + SypF HPT (KV7226) + wild-type *rscS* on a plasmid (pLMS33; RscS+) were assessed following growth on tTBS (T), tTBS + calcium (TC), tTBS + pABA (TP) and tTBS + pABA/calcium (TPC). Pictures were taken using a dissecting light microscope at 72hrs. Each colony was disrupted using a toothpick after 72hrs. Pictures are representative of 3 separate experiments. Arrows indicate where "pulling," indicating cohesion, was observed.

The overexpression conditions, RscS+ plasmid, showed a dependence on just the SypF HPT domain similar to what I saw in the non-overexpression condition (Fig. 26 compared to Fig. 31). Although the strain with the RscS+ plasmid in the Δ*sypF* mutant background showed a lack of biofilm formation, complementation with just the SypF HPT domain was enough to rescue biofilm formation to that of the RscS+ plasmid in WT ES114. Therefore, the RscS+ plasmid relies on the SypF HPT domain to promote biofilm formation under all conditions, including pABA alone. I also wanted to test the possibility that the pABA-induced biofilm formation was due to RscS sensing pABA and having more signal input rather than just more sensor kinase

eliciting more signaling. To test this, I looked at a strain that carries pCLD54, which expresses WT *sypF* on a multi-copy plasmid, on pABA media to determine if SypF+ would induce biofilm formation as well.

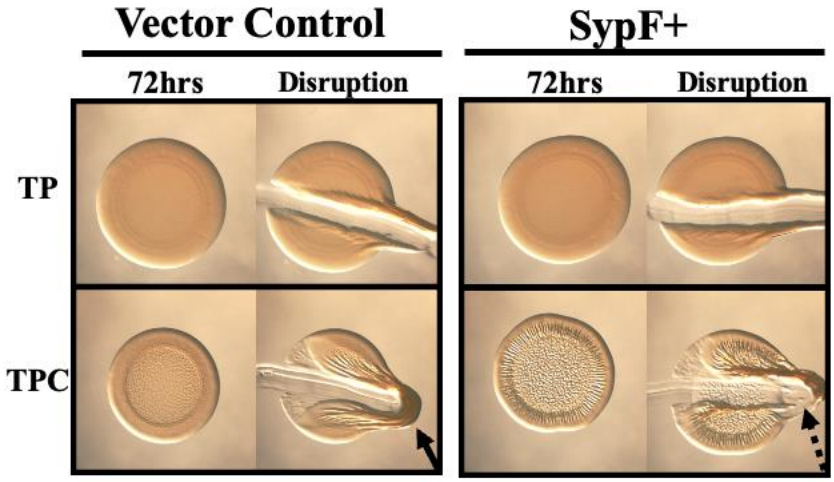

Figure 32. SypF+ does not Induce Biofilm Formation on tTBS + pABA Media. Colony biofilm formation of ES114 + vector control (pKV69) or ES114 + wild-type *sypF* on a plasmid (pCLD54; SypF+) were assessed following growth on tTBS + pABA (TP) and tTBS + pABA/calcium (TPC). Pictures were taken using a dissecting light microscope at 72hrs. Each colony was disrupted using a toothpick after 72hrs. Pictures are representative of 3 separate experiments. Arrows indicate where "pulling," indicating cohesion, was observed. Dotted arrows represent where "pulling" was observed but to a lesser extent than the solid arrows

I saw that the addition of more sensor kinase via a multi-copy plasmid does not induce biofilm formation on pABA alone (Fig. 32). The inability of SypF+ to induce biofilm formation under pABA conditions indicates that the results I saw in figures 29 and 30 may be due to RscS sensing the pABA condition. Further, the RscS+ might be able to relay more of a signal input due to the increase in numbers of sensing modules present. I also saw that SypF+ inhibited pABA/calcium-induced biofilm formation through an unknown mechanism. Future work will need to be done to follow up exactly how SypF is inhibiting biofilm formation under these conditions.

To further test the possibility that RscS can sense pABA, and the reliance of RscS on the HPT domain of SypF, I generated an RscS-SypF chimera ((Norsworthy and Visick 2015) and Fig. 6) in which the HPT domain of RscS was replaced with that of SypF and expressed from the chromosome at a non-native site under the control of the *rscS* promoter. In this setup, RscS is forced to signal through the HPT domain of SypF to phosphorylate downstream response regulators such as SypG. I first tested if this chimera was functional by complementing the individual Δ*rscS* and Δ*sypF* mutants.

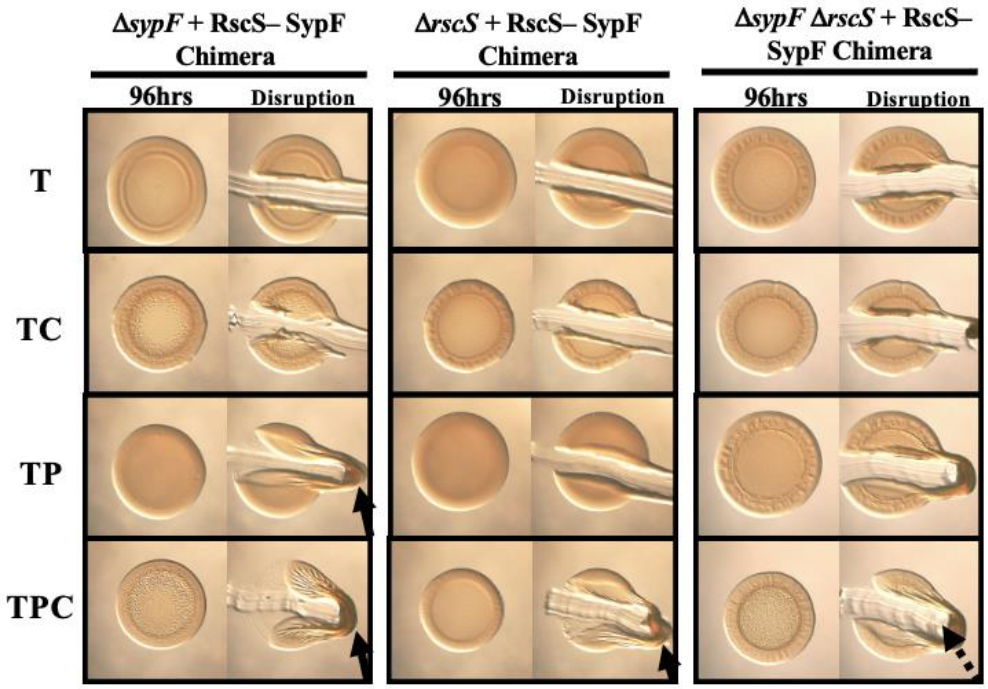

Figure 33. The RscS – SypF Chimera can Complement Various *syp* Regulators. Colony biofilm formation of Δ*sypF* Δ*rscS* + RscS – SypF chimera (KV10351; left), Δ*sypF* + RscS - SypF chimera (KV10355; middle), and the Δ*rscS* + RscS – SypF chimera (KV10302; right) were evaluated following growth on tTBS (T), tTBS. +calcium (TC), tTBS + pABA (TP) and tTBS + pABA/calcium (TPC). Pictures were taken using a dissecting light microscope at 72hrs. Each colony was disrupted using a toothpick after 72hrs. Pictures are representative of 3 separate experiments. Arrows indicate where "pulling," indicating cohesion, was observed. Dotted arrows represent where "pulling" was observed but to a lesser extent than the solid arrows.

The chimera complemented both deletion mutants, indicating that the chimera is functional and that the HPT domain of RscS is not necessary under these conditions to relay its

signal(s) to control biofilm formation (Fig. 33). Of note, the chimera not only complements the Δ*sypF* mutant but also promotes biofilm formation on pABA alone, much like pLMS33 does (Fig. 29). These data indicate two things: 1. Supporting the hypothesis that the full-length SypF default status is a net phosphatase and inhibits biofilm formation under pABA conditions in the absence of calcium, and 2. Expression from two copies of *rscS* can induce biofilm formation on pABA alone when only the SypF – HPT domain is present.

When I assessed the ability of the chimera to complement the Δ*rscS* Δ*sypF* double mutant, I observed only relatively weak biofilm formation (Fig. 33). I hypothesized that biofilm formation on TPC relies on coordinate signaling, presumably through the use of two sensor kinases; in the double mutant strain, there is only one sensory input due to the chimera. Therefore, I constructed a strain that contains the chimera at the non-native position and at the RscS native site in the chromosome.

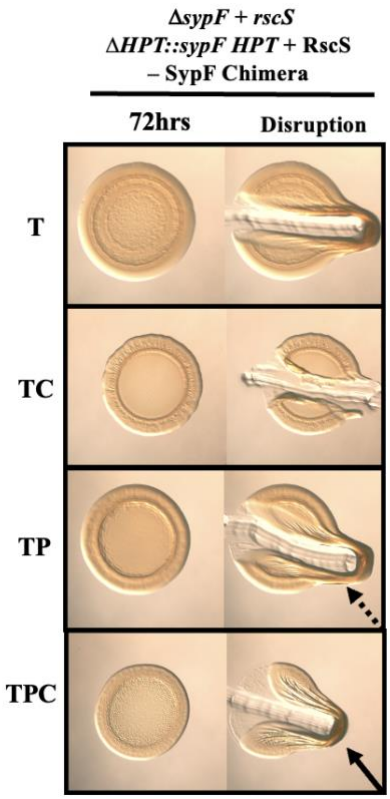

Figure 34. Two Copies of the RscS – SypF Chimera Induces Biofilm Formation on TP and TPC. Colony biofilm formation of Δ*sypF* + 2 copies of the RscS – SypF chimera (KV10397; *rscS* Δ*HPT::sypF HPT* + RscS – SypF chimera) was evaluated following growth on tTBS (T), tTBS. +calcium (TC), tTBS + pABA (TP) and tTBS + pABA/calcium (TPC). Pictures were taken using a dissecting light microscope at 72hrs. Each colony was disrupted using a toothpick after 72hrs. Pictures are representative of 3 separate experiments. Arrows indicate where "pulling," indicating cohesion, was observed. Dotted arrows represent where "pulling" was observed but to a lesser extent than the solid arrows.

The presence of two copies of the chimera not only fully complemented the double mutant but also modestly promotes biofilm formation on pABA alone (Fig. 34). These data further demonstrate the importance of RscS in recognizing the pABA signal and also indicate that there is a need for two coordinate sensors to elicit biofilm formation in ES114.

RscS seems to be responsible for pABA – dependent phenotypes; however, it is still unclear if RscS directly senses pABA conditions. To further explore the possibility that RscS responds to pABA, I used *V. fischeri* strain KB2B1 as a heterologous system. KB2B1 is another

wild-type strain isolated from *E. scolopes* and has been termed "dominant" due to its ability to dominate in colonization relative to ES114 (Bongrand et al. 2016). KB2B1 also contains a degenerate *rscS* (Rotman et al. 2019). Therefore, I decided to use KB2B1 as a heterologous system to determine if the ES114 RscS senses pABA. First, I characterized KB2B1 on LBS and tTBS plus calcium, pABA, and pABA/calcium (Fig. 35).

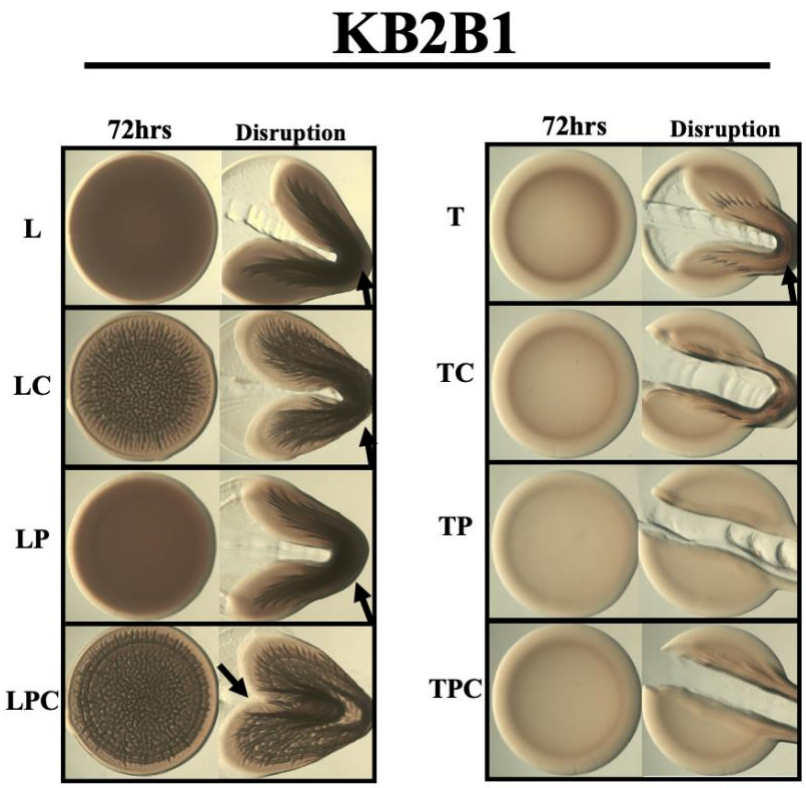

Figure 35. KB2B1 Readily Forms a Biofilm on all LBS Media but not all tTBS Media. Colony biofilm formation by WT KB2B1 was evaluated following growth on LBS (L), LBS + calcium (LC), LBS + pABA (LP), LBS + pABA/calcium (LPC), tTBS (T), tTBS + calcium (TC), tTBS + pABA (TP) and tTBS + pABA/calcium (TPC). Pictures were taken using a dissecting light microscope at 72hrs. Each colony was disrupted using a toothpick after 72hrs. Pictures are representative of 3 separate experiments. Arrows indicate where "pulling," indicating cohesion, was observed**.**

KB2B1 readily forms a biofilm under tTBS and LBS conditions but fails to do so when either calcium or pABA is added to tTBS (Fig. 35 and (Rotman et al. 2019)). Therefore, I reasoned that if the RscS from ES114 can promote biofilm formation in response to pABA, then

inserting the *rscS* gene into the KB2B1 chromosome might permit KB2B1 to form a biofilm in response to pABA.

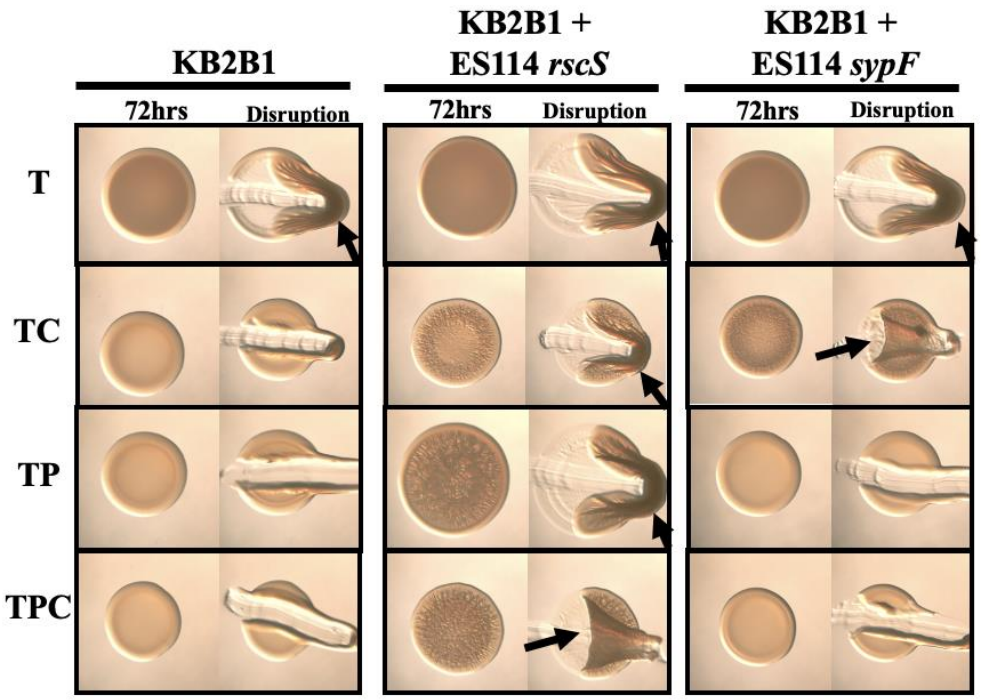

Figure 36. ES114 RscS Responds to pABA in a Heterologous System. Colony biofilm formation by WT KB2B1 (left), KB2B1 + ES114 *rscS* (middle; CD84), and KB2B1 + ES114 *sypF* (right; KV13089) was evaluated following growth on tTBS (T), tTBS + calcium (TC), tTBS + pABA (TP) and tTBS + pABA/calcium (TPC). Pictures were taken using a dissecting light microscope at 72hrs. Each colony was disrupted using a toothpick after 72hrs. Pictures are representative of 3 separate experiments. Arrows indicate where "pulling," indicating cohesion, was observed.

Indeed, I saw a significant increase in biofilm formation when KB2B1 expressing RscS from ES114 was grown on plates that contained either pABA alone or in conjunction with calcium (Fig. 36) I also saw that the biofilm formed by KB2B1 expressing RscS from ES114 on TP was larger than on TC or TPC, where the TP biofilm was a quarter centimeter larger than the other colonies. Finally, pABA-induced biofilm formation was not due just to the presence of an extra sensor kinase as the expression of $sypF_{ES114}$ at the same non-native site in KB2B1 did not permit biofilm formation on pABA or pABA/calcium conditions (Fig. 36). Of note, $SypF_{ES114}$

did promote biofilm formation upon calcium supplementation; further investigation will need to be done to determine SypF's role with respect to calcium. Some of this work is represented in Appendix A figure 50. The specific *rscS*$_{ES114}$-dependent increase in biofilm formation under a condition that generally does not permit KB2B1 to form a biofilm supports the conclusion that RscS is responsible for sensing pABA and/or pABA conditions. I wanted to ensure that the results seen in figure 35 were due to the RscS from ES114 and that the non-functional RscS in KB2B1 was truly having no effect on biofilm formation. To test this, I did the same experiment, except I deleted remnants of *rscS* out of KB2B1.

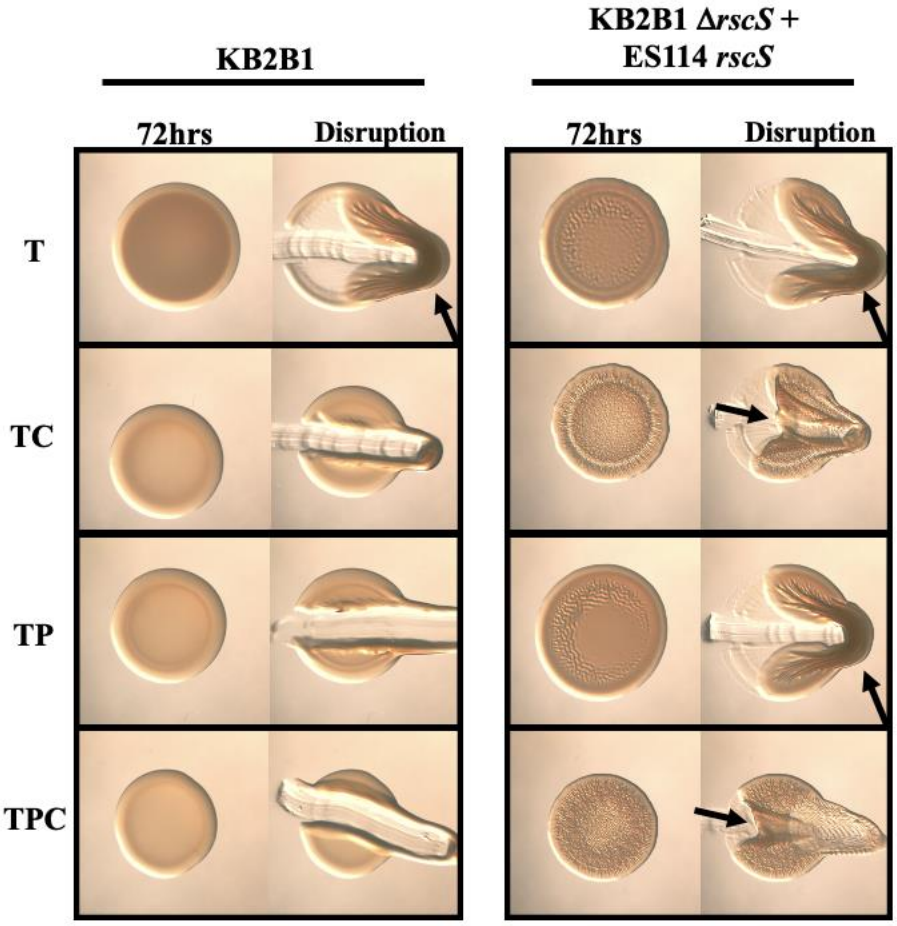

Figure 37. Induction of Biofilm Formation by KB2B1 is Solely due to ES114 *rscS*. Colony biofilm formation by WT KB2B1 and KB2B1 Δ*rscS* + ES114 *rscS* (KV10388) were evaluated following growth on tTBS (T), tTBS + calcium (TC), tTBS + pABA (TP) and tTBS + pABA/calcium (TPC). Pictures were taken using a dissecting light microscope at 72hrs. Each colony was disrupted using a toothpick after 72hrs. Pictures are representative of 3 separate experiments. Arrows indicate where "pulling," indicating cohesion, was observed**.**

I saw that deletion of *rscS* from KB2B1 elicited no effect on RscS from ES114's ability to induce biofilm formation under pABA conditions in KB2B1 (Fig. 37). These data indicate that the ES114 RscS – induced biofilm formation is truly due to ES114 RscS potentially sensing pABA and inducing biofilm formation.

Summary.

The ability of pABA/calcium to induce biofilm formation relies on the polysaccharide SYP. Several two-component systems regulate SYP production; therefore, I was curious if any of these regulators played a role in inducing SYP – dependent biofilm formation under pABA/calcium conditions. I found, perhaps not surprisingly, that pABA/ calcium biofilm relied on the central regulator SypF and the corresponding response regulator SypG. Further, just the HPT domain of SypF was necessary for biofilm formation, and specifically, RscS was the sensor kinase responsible for SYP-dependent biofilm formation under pABA/calcium.

I hypothesize that RscS senses pABA. I utilized a mutant missing its sensory domain, overexpression of RscS, an RscS-SypF chimera, and a heterologous system, all of which support my hypothesis that RscS senses pABA and/or the pABA condition. Lastly, I found a crosstalk between the two major polysaccharides in *V. fischeri:* SYP and cellulose. It seems that cellulose inhibits the production of SYP; however, future work will need to be done to thoroughly flush out how the two interplay and how, exactly, cellulose is inhibiting SYP.

c-di-GMP is Involved in SYP-Dependent Biofilm Formation and is Upregulated via Syp Regulators.

Introduction.

c-di-GMP is a ubiquitous second messenger used to transition from a sessile to a planktonic state of bacterial life and vice versa. Cells with low levels of c-di-GMP are poised to be planktonic, whereas high levels of c-di-GMP promote biofilm formation. The production of many polysaccharides in different bacterial species is linked to the levels of c-di-GMP (Romling, Galperin, and Gomelsky 2013) including cellulose production in *V. fischeri* (Tischler et al. 2021). However, while cellulose is related to the levels of c-di-GMP, the link between the major

V. fischeri polysaccharide, SYP, and c-di-GMP levels has yet to be fully connected (Dial, Speare, et al. 2021; Isenberg et al. 2022). Further, a link between SYP and c-di-GMP might also point towards the SYP TCSs controlling the levels of c-di-GMP, possibly through DGC/PDE up/down-regulation, respectively.

In the last section, I will establish a link between c-di-GMP and SYP production/SYP-dependent biofilm formation. I will then begin to dive into the link between SYP regulators and the levels of c-di-GMP. However, a complete connection has yet to be established, and future/further work will need to be done to determine which regulators and DGC/PDEs are responsible for the upregulation of SYP biofilm formation and c-di-GMP levels.

SYP – Dependent Biofilm Formation Relies on c-di-GMP Levels but not at the Level of Transcription.

I saw an upregulation in the levels of c-di-GMP due to pABA and pABA/calcium conditions. I also know that pABA/calcium induces SYP – dependent biofilm formation and RNA-seq analysis revealed global changes in c-di-GMP and biofilm related genes. Moreover, a role for c-di-GMP in *syp*-dependent biofilm formation has not been previously reported; therefore, I wondered if there was a link between these SYP-dependent biofilms and the levels of c-di-GMP. To test this possibility, I overexpressed the gene for a c-di-GMP phosphodiesterase (PDE), *VF_0087*, which was previously shown to be effective in decreasing c-di-GMP levels of strain KB2B1 (Dial, Eichinger, et al. 2021). First, I asked if overexpression of *VF_0087* abolished or diminished the pABA-induced increase in c-di-GMP using the biosensor.

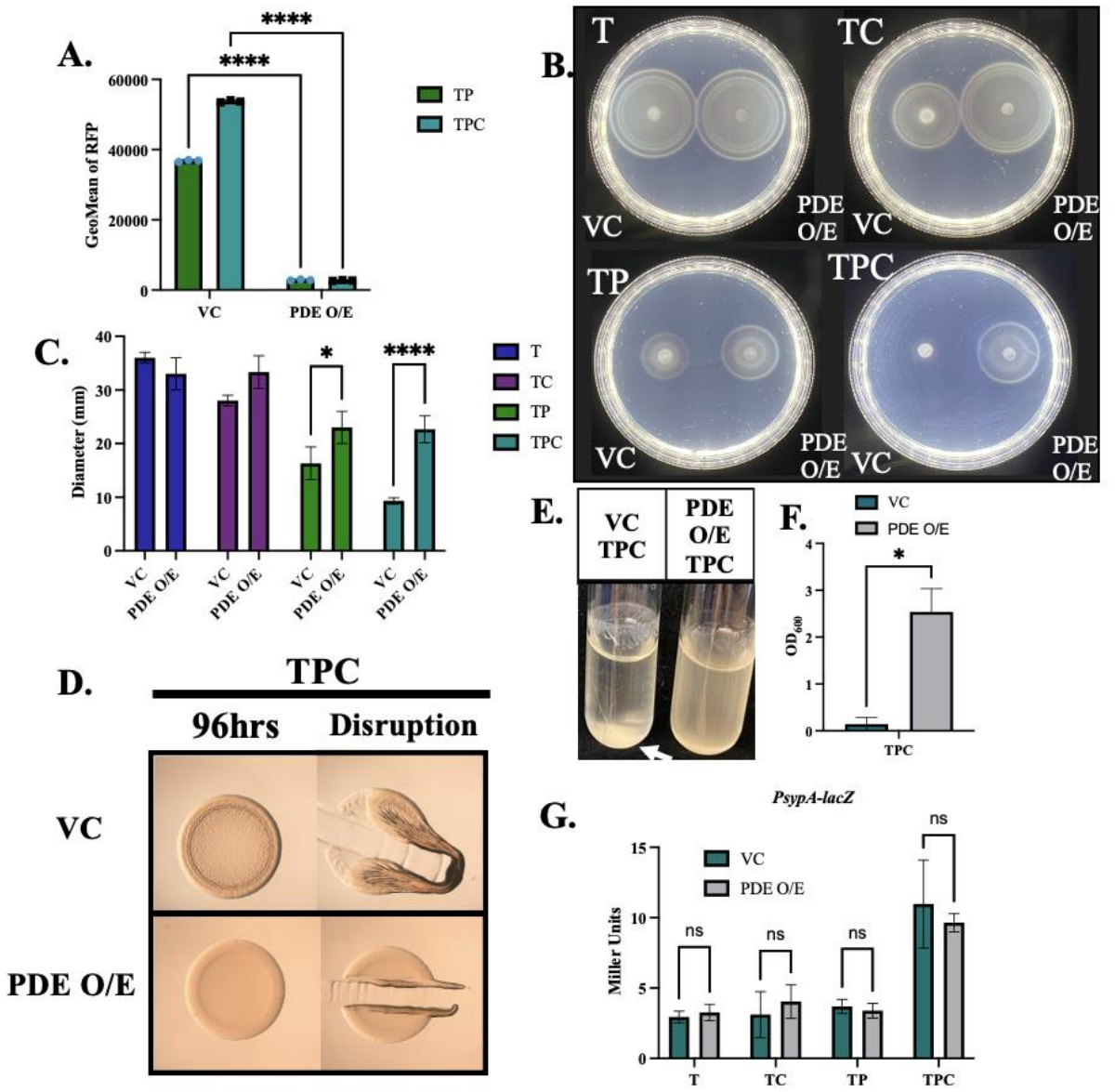

Figure 38. SYP – Dependent Biofilm Formation is Linked to c-di-GMP Post-Transcriptionally. (A) The levels of RFP from strains carrying c-di-GMP biosensor pFY4535 and either the vector control or a plasmid (pKV302) that overexpresses phosphodiesterase (PDE) *VF_0087* were measured using flow cytometry following growth in either tTBS + pABA (TP) or tTBS + pABA/calcium (TPC). The cells were first gated on AmCyan and then on RFP. Statistics for A were performed via a one-way ANOVA using Tukey's multiple comparisons test. **** P < 0.0001. (B & C) Migration of ES114 carrying vector control (VC) or PDE overexpressing plasmid pKV302 (PDE O/E) was evaluated using tTBS soft-agar motility plates (T) supplemented with calcium (TC), pABA (TP), or both (TPC). Pictures were taken after 6hrs, and representative images are shown. Migration was evaluated by measuring the outer diameter of the migrating cells. Statistics for C were done via a 2-way ANOVA using Šídák's multiple comparison test, where diameter was the dependent variable. *P = 0.0137 and ****P < 0.0001 (D) Colony biofilm formation was assessed following growth of ES114 carrying the vector

control (VC) or pKV302 (PDE O/E) on TPC. Pictures were taken at 96 h before and after disrupting the spots with a toothpick. (E & F) The same strains in D were grown in tTBS liquid medium containing pABA/calcium with shaking. Pictures were taken at 19 h, and the OD_{600} was measured as an indicator of biofilm formation. Arrows indicate where "pulling" and clumps, indicating cohesion, were observed. Statistics for F were performed using a paired T-test, where OD_{600} was the dependent variable. *P = 0.0136 (G) *sypA* promoter activity (Miller units) was measured using P*sypA*-*lacZ* fusion strain KV8079 that contained either the VC plasmid or the PDE O/E plasmid following a 22 h subculture in either T, TC, TP or TPC. Statistics for G were performed via a two-way ANOVA using Šídák's multiple comparison test, where Miller units was the dependent variable (Dial, Speare, et al. 2021).

I found that overexpression of *VF_0087* significantly decreased the levels of RFP, indicating decreased levels of c-di-GMP (Fig. 38A). Second, I asked if overexpression of *VF_0087* increased migration of ES114 through soft agar supplemented with pABA, due to the severe defect in motility I saw in earlier experimentation (Fig. 18A-E) and found that it partially rescued ES114's pABA-induced migration defect (Fig. 38B & C) and fully rescued ES114's calcium-induced migration defect. Notably, the overexpression of *VF_0087* substantially decreased c-di-GMP levels without fully restoring motility, suggesting that pABA might impact migration through more than one factor. Third, I asked if overexpression of *VF_0087* could inhibit biofilm formation induced by pABA/calcium. Whereas the vector control strain produced cohesive colony biofilms, the PDE-overproducing strain failed to form a biofilm on tTBS plates supplemented with pABA/calcium (Fig. 38D). Fourth, I looked at whether PDE overexpression would also inhibit biofilm formation in shaking cultures. I observed a trend similar to that on plates, with the vector control strain producing clumps, rings, and trees and the *VF_0087*-overexpressing strain lacking these biofilms (Fig. 38E-F). Finally, I asked if *VF_0087* overexpression affected *syp*-dependent biofilms by controlling *sypA* promoter activity. Although I found that PDE overexpression did not impact *sypA* promoter activity at 22 h (Fig. 37G), c-di-GMP may exert its effect on SYP biofilm by mediating transcriptional changes of other

important *syp* genes and/or at a post-transcriptional level. These data reveal that pABA-induced c-di-GMP is a key underlying mechanism controlling the ability of ES114 to form *syp*-dependent biofilms.

SYP Regulators also Impact c-di-GMP Levels within the Cell.

Due to the impact of c-di-GMP on SYP-dependent biofilm formation, I next wanted to know which SYP regulator might impact c-di-GMP levels to promote biofilms. Although c-di-GMP levels did not impact *syp* transcription, which SYP regulators typically control, we have also seen regulation post-transcriptionally via SypE (Morris, Darnell, and Visick 2011; Morris and Visick 2013a). The prominent regulator to look at is RscS due to the importance, and sensing ability, of RscS in the pABA/calcium condition.

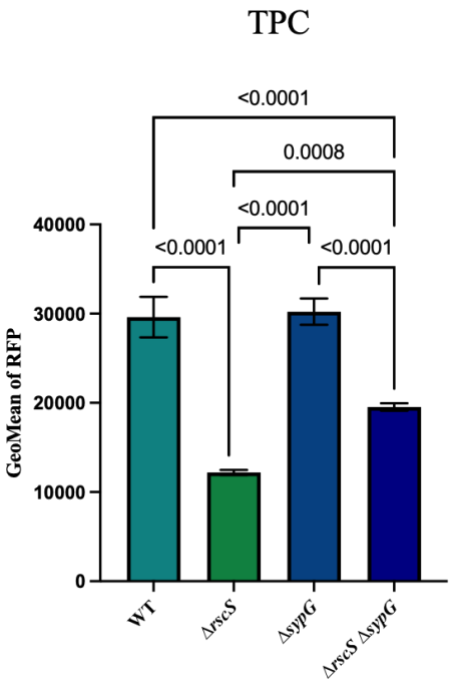

Figure 39. c-di-GMP Levels Rely on RscS but not SypG. The levels of RFP from strains carrying c-di-GMP biosensor pFY4535 were measured using flow cytometry following growth in tTBS + pABA/calcium (TPC). The strains tested were ES114, Δ*rscS* (KV10130), Δ*sypG* (KV1787), and Δ*rscS* Δ*sypG* (KV10182). The cells were first gated on AmCyan and then on RFP. Statistics for A were performed via a one-ANOVA using Tukey's multiple comparisons test.

I found that an Δ*rscS* mutant had significantly decreased the levels of c-di-GMP; however, there was not a complete abrogation suggesting other mechanisms, besides RscS/the SYP regulators, are responsible for the increase in c-di-GMP via pABA/calcium conditions (Fig. 39). Because RscS would need to, presumably, work through a response regulator, I also looked at the c-di-GMP levels when I deleted *sypG*. I saw no change in c-di-GMP levels when *sypG* was deleted as the levels of RFP were similar to WT (Fig. 39). A double *rscS sypG* mutant displayed an intermediate phenotype between an Δ*rscS* signal mutant and a Δ*sypG* signal mutant (Fig. 39). This intermediate phenotype suggests that RscS is not fully working through SypG in order to upregulate c-di-GMP levels under pABA/calcium conditions.

Previously, the Visick lab has shown a link between RscS and the response regulator SypE (Morris, Darnell, and Visick 2011). I wondered if, since RscS is not working through SypG to upregulate c-di-GMP levels, RscS might be working through SypE. Also, SypE is known to work post-transcriptionally (Morris and Visick 2013a) and based on the data above (Fig. 38), if RscS is working through SypE rather than SypG, it would explain why c-di-GMP levels do not impact *syp* transcription. I decided to look at both a Δ*sypE* mutant and a Δ*sypA* mutant, as there is a tight interplay between the two SYP regulators.

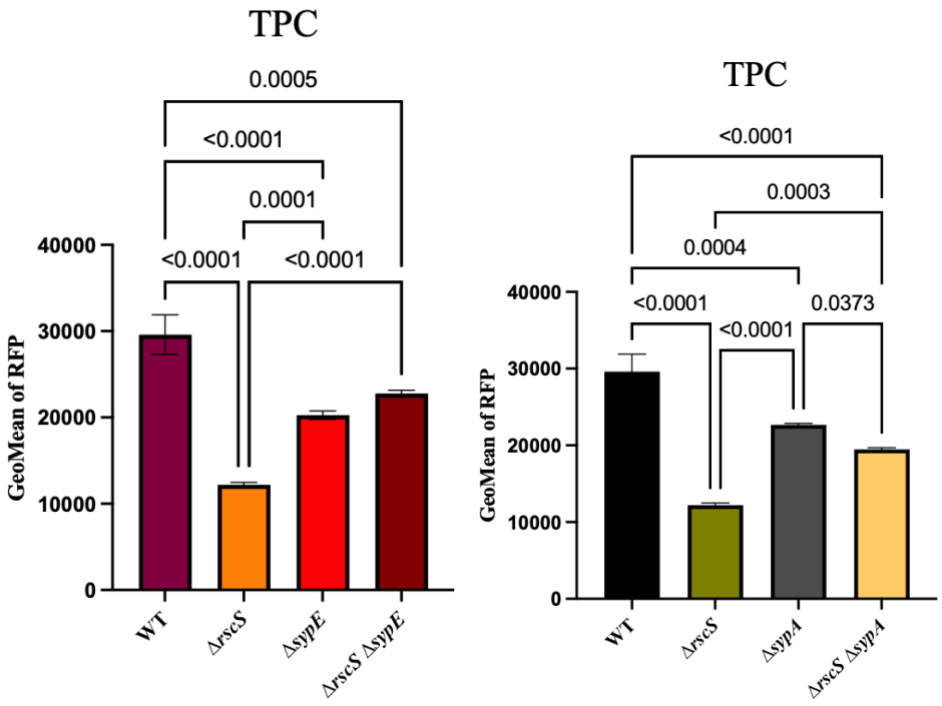

Figure 40. RscS Might be Working Post-Transcriptionally through SypE/A to Upregulate c-di-GMP Levels. The levels of RFP from strains carrying c-di-GMP biosensor pFY4535 were measured using flow cytometry following growth in tTBS + pABA/calcium (TPC). The strains tested were ES114, Δ*rscS* (KV10130), Δ*sypE* (KV10163; left), Δ*rscS* Δ*sypE* (KV10182; left), Δ*sypA* (KV9189; right), and Δ*rscS* Δ*sypA* (KV10183; right). The cells were first gated on AmCyan and then on RFP. Statistics for A were performed via a one–way ANOVA using Tukey's multiple comparisons test.

Upon deletion of either *sypE* or *sypA,* I saw a significant decrease in c-di-GMP levels compared to WT (Fig. 40 left and right). However, I also saw a significant increase in RFP production when the single mutants were compared to an Δ*rscS* mutant alone (Fig. 40). Further, I saw that an Δ*rscS* Δ*sypE* double mutant had increased c-di-GMP levels (Fig. 40, left), although not significantly. In contrast, the Δ*rscS* Δ*sypA* mutant displayed an intermediate phenotype (Fig. 40, right), much like the Δ*rscS* Δ*sypG* double (compare Fig. 39 with Fig. 40). I cannot fully conclude that RscS is working through SypE/A to induce c-di-GMP levels and subsequent biofilm formation. I believe there is a connection between RscS and the levels of c-di-GMP as

indicated by the significant decrease in c-di-GMP levels in an Δ*rscS* mutant; however, more work will need to be done in order to determine the exact mechanisms of this upregulation.

Summary.

In summary of my last results section, I found a link between the levels of c-di-GMP and SYP-dependent biofilm formation. PDE overexpression disrupts SYP-dependent biofilms; however, this dependence of SYP biofilms on c-di-GMP is not happening at the level of transcription but rather post-transcriptionally. RscS was shown to have a crucial role in biofilm formation and the increase in c-di- GMP levels due to pABA. I hypothesized that RscS is working, post-transcriptionally, through SypE to upregulate c-di-GMP levels, but the data only partially support this conclusion. More investigation is needed to determine precisely how pABA/RscS is upregulating the levels of c-di-GMP and how this small molecule interacts with SYP.

CHAPTER FOUR

DISCUSSION

Introduction.

My dissertation initially aimed to examine the *agaR* gene and how it contributes to biofilm formation but detoured once I uncovered conditions that induced biofilm formation in ES114. Previously, the work to determine the regulators that impact ES114 biofilm formation used genetically modified strains. In 2018, Louise Lie discovered that calcium, a small molecule, induced biofilm formation in a Δ*binK* mutant (Tischler et al. 2018). Although still genetically modified, it does not rely on overexpression for phenotypic exploration (overexpression of *rscS, sypG* and/or Δ*sypE*). The finding that calcium, as well as other salts, impacted biofilm formation (Marsden et al. 2017), led me to believe that there might be a condition that would help elucidate how *agaR* affects biofilm formation. These modifications, ultimately, helped me uncover conditions that induced WT ES114 biofilms. The inability of WT ES114 to form a biofilm in the laboratory has been a significant gap in the field. It is evident that ES114 can form a biofilm *in vivo*, as it was isolated from squid, and WT ES114 forms aggregates during colonization experiments (Yip et al. 2005). The work with *agaR* led to me finding new conditions that promote biofilm formation in *V. fischeri* and therefore the aim of my dissertation swiveled to determine the mechanisms behind ES114 biofilm formation

In this section, I will expand on my findings that yeast extract inhibits the Δ*binK* mutant biofilm and that pABA, a component of yeast extract, seems to be the inhibitory component for the Δ*binK* mutant while inducing biofilm formation in ES114. Importantly, two molecules,

pABA and calcium, are required for WT biofilm formation, and RscS and SypF are the central regulators involved in this signal transduction. Further, I propose that RscS is responsible for sensing the pABA input, while SypF might be responsible for sensing the calcium signal. I will discuss the impact of the SYP and cellulose crosstalk and how that might play a role in colonization. C-di-GMP is an important second messenger that, until recently, had seemingly no impact on SYP production; I will explore what my data suggest about the link between the two. Lastly, I will discuss the use of KB2B1 as a heterologous system as well as the potential roles of these molecules during squid colonization via ES114 and KB2B1.

Yeast Extract Inhibits Biofilm formation.

The first experiment I did to uncover a condition promoting biofilm was eliminating the yeast extract from LBS (tTBS). Removing the yeast extract yielded a condition in which the Δ*binK* mutant could form a biofilm without calcium supplementation, which is required under LBS conditions (Tischler et al. 2018). The promotion of biofilm formation under this new condition is not entirely surprising, as Dr. Anne Marsden examined different salt and media concentrations and found different biofilm phenotypes depending on the nutrient content within the media (Marsden et al. 2017). However, her work was done utilizing a strain that overexpresses *rscS* and, therefore, overrides the underlying signals of the system. Therefore, using a genetically modified strain that does not produce biofilms without extra supplementation allowed me to uncover this condition that had been previously overlooked.

There is some evidence that yeast extract broadly inhibits biofilm formation in bacterial species outside of *V. fischeri.* Specifically, extracts from *Charophyta*, *Chlorophyta,* and Cyanobacteria were tested against several bacterial and yeast species (Cepas et al. 2019). Extracts from *Charophyta* inhibited the biofilm formation of *E. coli*, *P. aeruginosa*,

Staphylococcus aureus, *Staphylococcus epidermidis*, and yeast species *Candida parapsilopsis* (Cepas et al. 2019). Further, when looking at all yeast extracts, the broadest effects were noted against biofilms formed by *Enterobacter cloacae*, a related species to *V. fischeri* (Cepas et al. 2019). Although not obtained from a manufacturer, the impact of raw yeast extract inhibiting many bacterial species cannot be understated. It might point to a physiological reason, such as yeast species needing to inhibit biofilm formation for productive growth and nutrient acquisition. Further, Cepas et al. found a specific component of these yeast extracts to be inhibitory to biofilm formation: fatty acids (FA) (Cepas et al. 2019). Other studies have shown that the FA oleic acid (*cis* – 9 – octadecenoic acid) inhibits biofilm formation and cell viability in *S. aureus* (Stenz et al. 2008). Similarly, in *P. aeruginosa cis* – 2 – decanoic acid induces biofilm dispersal (Davies and Marques 2009). All of this points to yeast extract generally having anti-biofilm properties and potentially playing an active role in inducing biofilm dispersal.

LBS is a largely undefined medium made up of tryptone, yeast extract, and salt, where tryptone and yeast extract come from manufacturers and are often batch specific. Therefore, determining the difference between LBS and the newly termed tTBS would have been arduous. Luckily, Dr. Karen Visick previously had obtained lists of the contents of Difco tryptone and yeast extract, and comparisons revealed several differences, such as sugars and vitamins. I originally began my experimentation by examining the impact of potential sugar content, which will be discussed in Appendix A, while simultaneously examining vitamins. The vitamin concentrations in tryptone, relative to yeast extract, are more limited and have been studied before (Khedr 2000); therefore, my work focused on the different vitamins present in tryptone versus yeast extract. Of these vitamins, I tested: nicotinic acid, choline, inositol, para–

aminobenzoic acid, pyridoxine, folic acid, and thiamine. From these vitamins only one, pABA, inhibited the Δ*binK* mutant biofilm formation on tTBS.

pABA Inhibits Δ*binK* Biofilms while Inducing SYP – Dependent Biofilm Formation in WT.

Through the use of tTBS media, I found that pABA inhibited the biofilm formed by a Δ*binK* mutant; in these experiments, I always utilized WT ES114 as a negative control. Surprisingly, I found that a combination of pABA and calcium (pABA/calcium)- induced WT biofilm formation on tTBS, something we had never seen before in the laboratory setting. This is a bit of a contradiction; can pABA inhibit while also inducing? However, notably, calcium needs to be present in order to allow for pABA biofilm induction, an important distinction. I will discuss further, below, the roles I hypothesize both SypF and RscS are playing under pABA/calcium conditions. Briefly, my data support the conclusion that RscS senses pABA and SypF is senses calcium, ultimately upregulating *syp* transcription and biofilm formation. Focusing on SypF, we propose that SypF acts as a net phosphatase (Thompson et al. 2018) until calcium signaling induces kinase activity. Therefore, in the Δ*binK* mutant background, while SypF is present, and acts as a net phosphatase. pABA signaling alone is not enough to induce biofilm formation unless two sensor kinase genes (such as two *rscS* genes) are present.

While HahK is dispensable for pABA/calcium-induced biofilm formation, it still plays a role under the Δ*binK* mutant biofilm conditions (Tischler et al. 2018). Further, HahK is negatively regulated by the nitric oxide (NO)-binding protein HnoX (Thompson et al. 2019); therefore, it is possible that BinK and/or yeast extract could alter the amounts of intrinsically produced NO, which in turn would impact the ability of HahK to contribute to biofilm induction (Fig. 41). I hypothesize that, under tTBS conditions, in a Δ*binK* mutant background HahK is not inhibited and, in conjunction with RscS, can induce biofilm formation without the need for

calcium (Fig. 41; Top). However, under pABA conditions, more NO could be produced (Vasilieva et al. 2016), inhibiting HahK and, subsequently, Δ*binK* mutant biofilms (Fig. 41; Bottom). This all remains speculation, and more work will need to be done looking at NO levels under pABA conditions to ascertain if HahK is being inhibited. Further, examining the impact of Δ*hnoX* and Δ*hahK* mutations in the Δ*binK* mutant background on all media types (T, TC, TP, and TPC) could support my hypothesis.

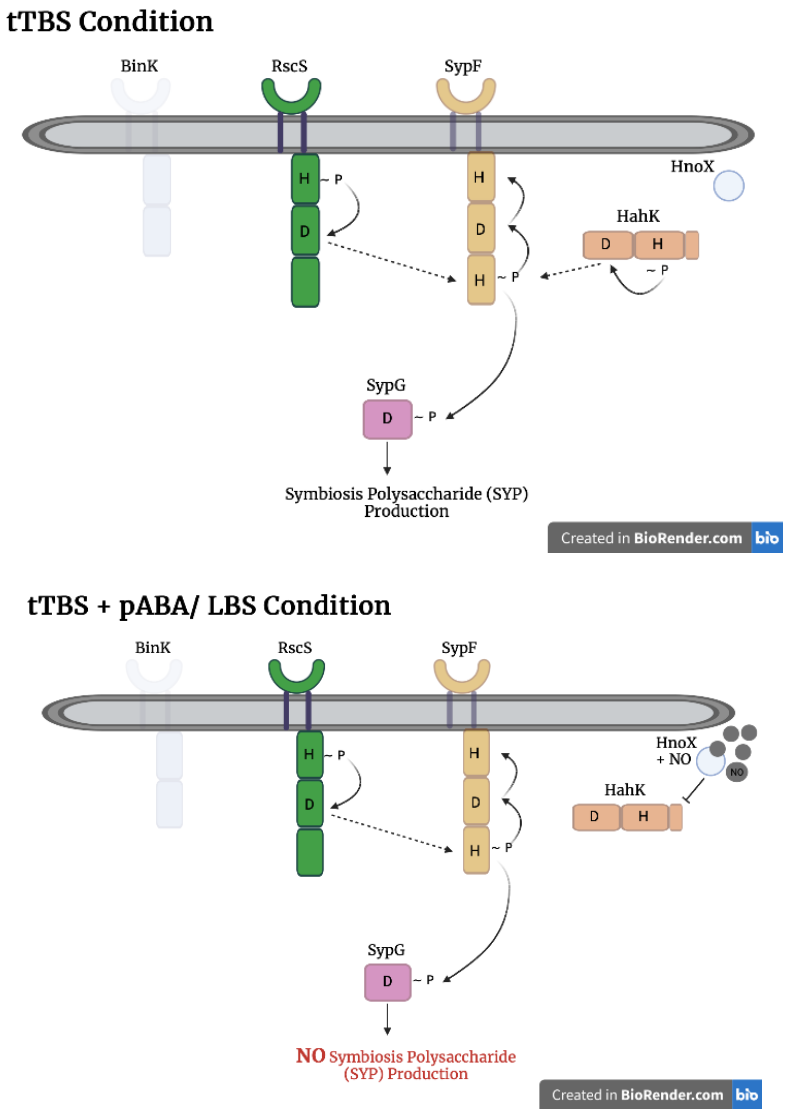

Figure 41. Model of the tTBS Conditions Versus pABA/LBS Condition. Top. The SYP regulatory network where *binK* has been deleted (transparent), SypF is acting as a phosphatase, and HnoX is not functional. The two positive signals from RscS and HahK work together to promote biofilm formation. **Bottom.** Same as the top except for nitric oxide (NO; grey circles) is present in abundance, thereby activating HnoX and inhibiting HahK, leaving only one sensor kinas RscS as a positive signal, leading to no SYP production. Both images were created in BioRender.

The ability of pABA to induce biofilms appears to be specific. pABA is a vital metabolite crucial to folic acid synthesis; however, folic acid cannot induce biofilm formation in WT ES114. It is possible that the range of folic acid is different than pABA; however, I did test a

wide range of folic acid concentrations and none induced biofilm formation. Similarly, when I tested analogs of pABA, only the compounds that contained benzoic acids, where the carboxyl group was not sterically hindered, promoted biofilm formation. These data indicate that pABA, specifically the benzoic acid/carboxyl group, is crucial for biofilm induction. There are other examples of benzoic acids acting as signaling molecules for chemotaxis and biofilm formation.

Halomonas titanicae contains several receptors that bind to benzoic acid and benzoate derivatives (Gasperotti et al. 2021). When *H. titanicae* receptors are introduced into a heterologous system, namely *E. coli*, they promote chemotaxis towards both benzoic acid and 2 – hydroxybenzoate (Gasperotti et al. 2021). The ability of *H. titanicae,* a Gram-negative bacterium isolated from a hydrocarbon–contaminated sea harbor, to perform chemotaxis to a specific benzoic acid might indicate an evolutionary advantage. The PcaY_PP chemoreceptor in *Pseudomonas putida* recognizes and binds to 17 different C6 – rings containing carboxylic acid (Fernandez et al. 2017; Gavira et al. 2021). In *Comamonas testosterone,* 2,6 – dihydroxybenzoate and 2 – hydroxybenzoate not only directly bind to a *C. testosterone* chemoreceptor but also alter the kinase activity of CheA (Huang et al. 2016), further showing that benzoates can influence signal transduction. Lastly, benzoic acid stimulates *E. coli* to form biofilms, irrespective of concentrations (Synowiec et al. 2021).

pABA itself has also been shown to induce biofilm formation in another species. In the oral microenvironment, *S. gordonii* produces and secretes pABA into the environment during multispecies biofilm formation. The presence of pABA induces *P. gingivalis* to metabolize the molecule, which leads to increased expression and production of fimbrial adhesins necessary for colonization and productive biofilm formation. pABA also increased colonization and virulence of *P. gingivalis* in a mouse model (Kuboniwa et al. 2017). This study, besides ours, remains the

only study displaying that pABA can promote biofilm formation. The above studies provide support for a benzoic acid binding to and signaling through sensory domains, and my work suggests that pABA itself has a similar role.

pABA Causes Global Transcriptional Changes.

The transcriptomics analysis of ES114 in the pABA condition showed a significant up/down-regulation of a multitude of genes, including those related to biofilm formation/polysaccharide production, as well as the production of c-di-GMP. Interestingly, in the Kuboniwa study of *P. gingivalis*, they found, through proteomics, that pABA resulted in changes in the levels of hundreds of proteins (Kuboniwa et al. 2017). Taken together, these data indicate a substantial response to pABA and imply that pABA has numerous effects on cell physiology. These responses include the induction of biofilm behaviors in both *P. gingivalis* (Kuboniwa et al. 2017) and *V. fischeri.* However, where *V. fischeri* receives the pABA signal is still undetermined but will be discussed later.

Similar to *S. gordonii*, *E. coli* can secrete and uptake pABA (Maynard et al. 2018). In *E. coli*, the AbgT family of transporters is responsible for the uptake of pABA in its glutamine–bound form (pABA-glu); these transporters also cleave the glu residue upon cell entrance. However, pABA can also freely diffuse through the *E. coli* membrane (Maynard et al. 2018) and is assumed to be able to freely diffuse into *V. fischeri*. In the transcriptomic data, I saw an enrichment in gene transcription of the AbgT family of transporters, specifically the transporter gene *VF_0639*, under pABA conditions. However, the deletion of this transporter gene and that encoding another known AbgT transporter resulted in no change in biofilm formation (Appendix A; Fig. 47). Therefore, it seems more likely that pABA freely diffuses across the membrane to elicit the global effects within the cell. This possibility seems the most likely since pABA

appears to be signaling through RscS, whose sensor domain(s) lie within the periplasm. Hence, transport across both membranes through the AbgT transporter would not allow the RscS signal cascade to occur. The lack of phenotype points to the *abgT* genes being dispensable for biofilm formation but it remains possible that AbgT has other effects on pABA-induced physiological changes besides biofilm formation.

The transcriptomic data also revealed an upregulation of genes related to pABA metabolism, including *pabC*. Most of these genes, with the exception of *pabC*, however, are essential, and therefore more intricate genetic manipulation will need to be done to study them, such as using CRISPR interference for a knockdown rather than a knockout (Peters et al. 2016). We could also try using an inducible system to insert our essential gene of interest on a plasmid and induce its expression to delete the gene from the genome (Boneca et al. 2008). Then, we can limit the inducible agent and measure biofilm outcome. However, this would have to be further optimized due to the variability of shaking biofilm phenotypes.

Not all genes related to pABA metabolism are essential. Indeed, I could delete the *pabC* gene in *V. fischeri*. PabC converts 4 – amino – 4- deoxychorismate, an intermediate molecule, into pABA (Basset et al. 2004). The deletion of *pabC* from *V. fischeri* yielded no biofilm–dependent phenotypes (Appendix A; Fig. 48). I hypothesize that pABA needs to be in its benzoic acid form, with the carboxyl – group unhindered, to promote biofilm formation. If so, no metabolism of pABA would be needed to induce ES114 to form biofilms.

RscS Senses the pABA Condition, and SypF Might be Essential for Calcium Signaling.

Overall, my data, including Appendix Figure 50, provide strong evidence that pABA is signaling through RscS and calcium is signaling through SypF (Fig. 36 and Fig. 41). Further, it is these two signals (pABA and calcium) and two sensor kinases that coordinately upregulate *syp*

transcription and SYP biofilm formation. RscS and SypF contain sensory domains located within the periplasmic space, and presumably both pABA and calcium can freely diffuse across the lipid bilayer into the periplasmic space to signal through these sensor kinases (Tischler et al. 2021; Maynard et al. 2018). More work will need to be done to determine if pABA and calcium are binding to RscS and SypF, respectively. For example, crystal structures with RscS or SypF and their respective molecules as well as ITC binding assays could help prove binding between these molecules and sensor kinases. Further, in relation to SypF and calcium, similar mutants as was made in RscS, such as the deletion of the periplasmic loop, could be constructed to help further my hypothesis. However, there are several examples of known small molecules analogous to pABA binding to either the PAS domain or periplasmic-loop – like domain of other proteins in other species.

In both *Halorhodospira halophila* and *Rhodospirillum centenum*, 4 – hydroxycinnamic acid has been shown to bind directly to and act as a ligand for the PAS domain (Mix et al. 2016). For *P. putida* and *P. mendocina*, both of which encode proteins with PAS 4 domains, aromatic hydrocarbons bind to the TodS sensor kinase to drive phosphorylation/signal transduction (Busch et al. 2009; Busch et al. 2007; Lacal et al. 2006; Silva-Jimenez et al. 2012; Koh et al. 2016). Although pABA is not an aromatic hydrocarbon, the structures are similar, and pABA could bind similarly to RscS as toluene binds to TodS (Koh et al. 2016; Busch et al. 2009). *Xanthomonas campestris* pv. *Campestris* also encodes proteins with a PAS 4 domain that binds to different dodecanoic acids via the sensor kinase RpfS, which results in signal transduction and a functional response (An et al. 2014). *Erthrobacter litoralis*, which contains a PAS 9 domain in the sensor kinase EL346, binds to riboflavin, which activates signal transduction (Rivera-Cancel et al. 2014). Lastly, in *Xanthomonas campestris* pv. *campestris*, which encodes a transmembrane

SK with an N-terminal segment in the periplasm with sensor function akin to the periplasmic loop of RscS, this transmembrane SK has been shown to bind to a diffusible signal factor (namely a medium–chain fatty acid) similar to pABA (Cai et al. 2017). Although these molecules are pABA analogs, these data support that pABA-like molecules, across a wide variety of taxonomies, can bind to and signal through domains similar to the ones that RscS contains.

Calcium is also a potent regulator of numerous systems. One of the most heavily examined regulatory networks stimulated by calcium is the Gac/Rsm pathway in *P. aeruginosa* (Broder, Jaeger, and Jenal 2016). In this network, calcium binds to the periplasmic sensory domain of LadS to activate kinase activity. LadS activates the Gac/Rsm pathway, leading to chronic infection and drug tolerance by reducing *P. aeruginosa* growth rate (Broder, Jaeger, and Jenal 2016). In a species closely related to *V. fischeri*, *V. cholerae*, calcium binds to the loop that forms the upper wall of the ligand binding pocket in sensory protein Mlp24 (Takahashi et al. 2019). This binding/activation of Mlp24 leads to chemotactic behaviors in *V. cholerae*, specifically to various amino acids (Takahashi et al. 2019). Mlp24 seems to be regulated by two signals: calcium and amino acids, where calcium acts as the co-signal for the primary signal of amino acids. This coordinate signaling is similar to how I propose calcium works in conjunction with pABA, detailed further in the next section. Expanding on the idea of calcium working in conjunction with another molecule to elicit an effect, in *Bacillus subtilis* both cadmium and calcium complex to signal through MntR (Kliegman et al. 2006). MntR is a manganese transport regulator and, upon activation, represses the transcription of genes related to the uptake of manganese (Kliegman et al. 2006). These examples show that calcium is a signaling molecule in

various organisms and that calcium often works in conjunction with other molecules to initiate its effects.

These data, along with the work in my dissertation, support the notion that pABA might signal through RscS, initiating autophosphorylation and subsequent signal transduction. Concurrently, calcium could signal through SypF, activating its kinase activity to phosphorylate SypG, which would upregulate *syp* transcription and SYP production (Fig. 42). Further, the regulation of *syp* seems to rely on at least two sensor kinases receiving their respective signals to induce biofilm formation. This redundant regulation is seen in numerous bacterial species when controlling energetically taxing processes and likely occurs in *V. fischeri*. Additionally, mutations in SypF, RscS and even the RscS-SypF chimera in the HATPase, REC and HPT domains would be useful to help determine if the HKs are dimerizing and/or cross phophorylating in order to upregulate *syp*. Lastly, deletions in the kinase domains of RscS and SypF where the REC/HATPase domain can take phosphoryl groups but cannot act as a kinase would help clarify the signal transduction pathway occurring under pABA/calcium conditions.

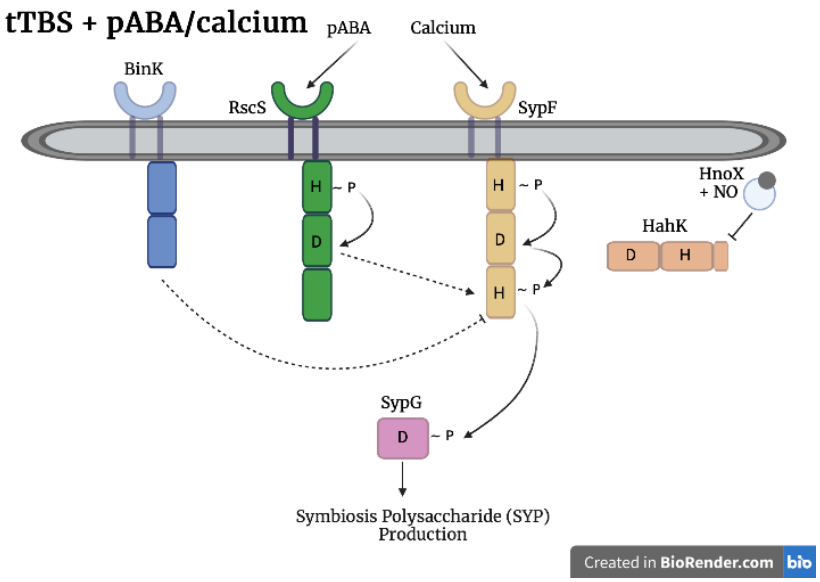

Figure 42. Model that pABA and Calcium Work Together to Induce Biofilm Formation. The SYP regulatory network where pABA is signaling through RscS and calcium is signaling through SypF, turning SypF into a kinase to activate *syp* transcription and SYP production. Image created in BioRender.

ES114 Biofilms Need Coordinate Signals for Biofilm Formation and Squid Colonization.

As described in the last section and Figure 42, RscS and SypF coordinately regulate *syp* transcription and SYP production. There are a couple of other examples of this regulation in other bacterial species, as well as *V. fischeri* itself. I already outlined that LadS in *P. aeruginosa* responds to the small molecule calcium (Broder, Jaeger, and Jenal 2016). Further, LadS counteracts the activities of another sensor kinase within the same pathway, RetS. The LadS and RetS signals converge by controlling the transcription of RsmZ, a small regulatory RNA (Ventre et al. 2006; Goodman et al. 2004). This regulatory network controls the expression of the type III secretion system, biofilm formation, antibiotic resistance, and eventual chronic infection (Ventre et al. 2006; Goodman et al. 2004; Broder, Jaeger, and Jenal 2016).

The quorum sensing mechanism in *V. fischeri* is described in-depth in the introduction. However, it remains an important example of coordinate signaling to initiate a response, in this case, luminescence. AinR and LuxP/Q recognize their respective autoinducers to

dephosphorylate LuxU and, subsequently, LuxO (Verma and Miyashiro 2013). This phosphorylation cascade eventually leads to the bioluminescent behaviors of *V. fischeri*. Therefore, even in the same organism, coordinate signaling plays a vital role in gene regulation.

I hypothesize that this coordinate signaling, or redundant regulation, is necessary during *V. fischeri* squid colonization. There are times when *V. fischeri* must be poised to form a biofilm (or aggregate of cells) versus having flagella and being in a more planktonic state. The regulation via two signaling molecules ensures that both signals must be present to induce SYP production and eventual biofilm formation. There may be calcium microenvironments within the squid along with areas where benzoic acid-like compounds are present. Perhaps when both molecules are in a high enough abundance, *V. fischeri* begins to form a biofilm. I do not necessarily propose that pABA is the specific molecule needed to activate RscS; in fact, it could be any benzoic acid compound present in the squid that binds to RscS efficiently enough to induce *syp* transcription. However, pABA might be an essential nutrient in squid as it is in humans (Services 2020), it might be equally possible that pABA is the signaling molecule.

V. fischeri might be able to produce and excrete pABA much like its *E. coli* counterpart (Maynard et al. 2018) and, therefore, pABA/calcium could act as a type of quorum sensing molecule, such that when calcium is present, pABA excretion increases in order for biofilm formation to occur. The link between calcium and pABA production, as a form of quorum sensing, has yet to be determined, and whether or not there is pABA present within the squid is also an open area of research. Altogether, I purpose that the process of coordinate regulation is vital to squid colonization, and calcium, along with pABA (or a benzoic acid analog), are needed to induce SYP-dependent biofilm formation.

KB2B1 as a Heterologous System.

Utilizing KB2B1 as a heterologous system allowed us to show that RscS is sensing pABA and do it in a biologically relevant system. Initially, we discussed using *E. coli*, a relatively standard heterologous system, to show that RscS is truly sensing pABA, but *E. coli* came with several caveats/hurdles to overcome from the beginning. First, previously in the Visick lab, it had been observed that *rscS* expression via plasmid was toxic to *E. coli* cells. Second, the concentration of pABA I use to induce biofilm formation in *V. fischeri* causes a substantial growth defect in *E. coli*. These two factors would have caused many troubleshooting issues that might not have ever been resolved. The availability of another *V. fischeri* species that does not contain a functional RscS protein and does not produce biofilm formation when pABA is present presented the perfect opportunity to study if the RscS in ES114 was senses pABA. In this section, I will discuss the differences between KB2B1 and ES114 sensing pABA and/or calcium, as well as how KB2B1 can potentially be used as a standard heterologous system for ES114.

In ES114, the combination of pABA and calcium induces biofilm formation. Presumably, RscS senses pABA, autophosphorylates, and begins the signal transduction process. Simultaneously, calcium is thought to signal through SypF, changing this protein into a kinase, which eventually causes phosphorylation of SypG and upregulation of *syp* transcription and SYP production. Under LBS/tTBS conditions, without the addition of small molecules, ES114 does not produce biofilms. On the other hand, KB2B1 produces biofilms under all conditions except for TC, TP, and TPC. I propose that, under non-calcium and/or pABA conditions, KB2B1 is naturally primed for biofilm formation, and idea supported by KB2B1 being a hyper-aggregator strain of *V. fischeri* (Bongrand et al. 2016; Koehler et al. 2018). KB2B1 has evolved not to need

RscS, as the *rscS* allele in the KB2B1 genome is non-functional (Rotman et al. 2019), and therefore does not need the signal from pABA/benzoic acid.

Further, there are some point mutations within *sypF* of KB2B1; although we do not know what these mutations do on a functional level, they may alter SypF to be constantly in its net kinase state rather than its phosphatase state (Fig. 43, top). I hypothesize that the kinase state in KB2B1 is more robust, as KB2B1 can signal even on LBS where NO levels might be higher. It could also be the case that the intrinsically produced levels of NO via LBS are not significant enough to activate HnoX and inhibit HahK in KB2B1. Another alternative is that SypF might still sense calcium, but the outcome of calcium-sensing is opposite of what occurs in ES114. If so, then under calcium conditions in KB2B1 SypF would become a phosphatase, disrupting signal transduction and biofilm formation. This potential signaling mechanism might not be strong, as the calcium disruption of KB2B1 is variable. I propose that pABA could upregulate NO levels, activating HnoX and inhibiting HahK. If my hypothesis is correct either of these conditions (calcium or pABA) would cause an inhibition of biofilm formation, and both pABA and calcium would halt biofilm formation altogether (Fig. 43, bottom).

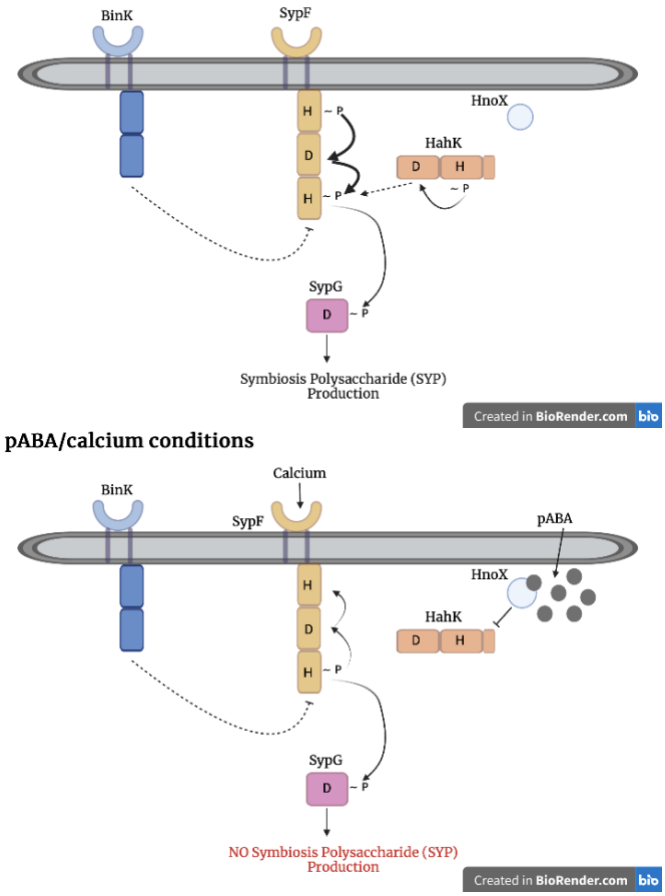

Figure 43. Model of SYP Regulation in KB2B1 under Various Conditions. Top. Under LBS or TBS conditions, SypF acts as a kinase, and HahK contributes to the phosphorylation of the HPT domain of SypF. KB2B1 contains a non-functional RscS; therefore, it has been omitted from the KB2B1 diagram. **Bottom.** Under pABA conditions, NO production is upregulated, activating HnoX and inhibiting HahK phosphorylation. When calcium is present, it signals through SypF changing SypF into its dephosphorylation state, opposite ES114. Image made in BioRender.

When the *rscS* from ES114 was put, in single copy, into the KB2B1 genome, I saw biofilm formation on all conditions, which suggests that RscS might also sense calcium. It should also be noted that the RscS from ES114 promotes better spreading of the biofilm colony of KB2B1 as the colony is visibly and measurably larger than any of its counterparts. This spreading could be due to increased growth on pABA, which could be measured via a growth curve, or the colony spreads better on the agar containing pABA which would result in the larger colony size. It might be the case that this extra sensor kinase allows the small signal going

through the native SypF, even when calcium is present, to be strong enough to induce biofilm formation; however, the native *sypF* will have to be deleted from KB2B1 and tested to determine if this is correct. Notably, the calcium-induced biofilm is weaker than the pABA-induced biofilm. Additionally, when the SypF from ES114 is added to the KB2B1 genome, the only condition for which this addition promotes biofilm formation to occur is with calcium supplementation. All of this is purely speculative at the moment; more work will need to be done to determine how calcium and pABA work in the context of KB2B1.

KB2B1 has the potential to become a powerful tool for studying ES114, as well as other strains of *V. fischeri*. Through an examination of the competence pathway (Cohen et al. 2021), work in the Visick lab has significantly increased our ability to transform this once-difficult strain of *V. fischeri.* Genetic manipulation of the KB2B1 genome, such as deleting KB2B1-specific genes, is still a work in progress, but deleting genes native to ES114 in KB2B1 is relatively straightforward. Furthermore, conjugating plasmids into KB2B1 is as achievable as it is in ES114. The relative ease of KB2B1 genetics opens the possibility of studying ES114-specific genes in a strain that exhibits the opposite phenotypes, such as biofilm formation (as mentioned), motility, luminescence, as well as c-di-GMP levels (Dial, Eichinger, et al. 2021). All of these phenotypes have specific partially or substantially, in the case of luminescence, understood mechanisms of action in ES114. The fact that they are so different in KB2B1 is intriguing, and not all of the factors that influence these phenotypes have been discovered. The opposition in KB2B1 makes it the perfect heterologous system for ES114-specific phenotypes.

SYP and Cellulose Crosstalk.

While determining which polysaccharide was responsible for pABA/calcium-induced biofilms, I found an unexpected phenotype: a Δ*bcsA* mutant displayed increased SYP production.

Specifically, when calcium was the only small molecule present, I saw an increase in SYP-dependent biofilm formation in a Δ*bcsA* mutant. These data suggest a crosstalk between the two pathways/polysaccharides. Through transcription assays (utilizing strains that could not produce SYP but could still produce cellulose), I could not find a reproducible result nor transcriptional link between SYP and cellulose; therefore, I propose that this crosstalk happens post-transcriptionally at the levels of subunits. Presently, the *V. fischeri* field does not know the exact structure of SYP; however, it is possible that it could be a glucose-containing polymer, which is also the essential subunit of cellulose. Hence, SYP and cellulose production might both hinge on the amount of glucose within the cell. For example, if *syp* transcription is upregulated, more glucose subunits would be required, less cellulose would be produced, and vice versa. This competition would explain why, when the cellulose synthase is deleted, I see an increase in the production of SYP while the transcription data is inconclusive. However, more work will need to be completed to determine the structure and subunits of SYP. We have some evidence that these two polysaccharides are connected higher, at the level of transcriptional regulation, through SypF and VpsR (Darnell, Hussa, and Visick 2008); however, my investigation was not fruitful in determining how this regulation is occurring under tTBS + calcium conditions.

The competition between polysaccharides is a phenomenon also seen in *P. aeruginosa*. When the exopolysaccharide PSL is no longer produced, there is an increase in the production of the other main polysaccharide PEL. Further, when PEL is absent, there is an increase in alginate production (Ghafoor, Hay, and Rehm 2011). Overall, it is suggested that this interconnection between these polysaccharides ultimately determines biofilm shape and function. In the *V. fischeri* system, it is possible that various polysaccharides must be produced depending on its localization within the squid. Therefore, this interconnection is important for steps in squid

colonization. More research will need to be done to untangle the SYP and cellulose regulatory networks completely.

The Link Between c-di-GMP and SYP – Dependent Biofilms.

Previously, a connection between the production of SYP and c-di-GMP levels was not well studied or established. Through the work presented here and in Dial et al. 2021, I established a connection between c-di-GMP and SYP production post–transcriptionally. There could still be a connection between the two at the levels of transcription, but our method of looking at the levels of *syp* transcription is not sensitive enough to catch any differences that might occur with and without PDE expression. Another way we should consider looking at *syp* transcription under c-di-GMP depleted conditions is through qRT-PCR. There are several examples of c-di-GMP regulating the production of various polysaccharides both transcriptionally and post-transcriptionally.

In *P. aeruginosa,* the binding of c-di-GMP to the transcriptional regulator FleQ promotes the transcription of *pel* and *psl* genes, which encode their respective polysaccharides. In this system, the role of c-di-GMP is to bind to and convert FleQ from a repressor to an activator, which then induces expression of Pel exopolysaccharide genes and subsequent biofilm formation (Hickman and Harwood 2008; Baraquet et al. 2012; Lee et al. 2007). Likewise, in the closely related species, *V. cholerae,* c-di-GMP binds to and regulates transcriptional regulators VpsR and VpsT. VpsR and VpsT regulate the expression of *vps* genes, which produce the main polysaccharide in *V. cholerae*; when c-di-GMP levels are high, *vps* gene transcription is upregulated, and subsequently, biofilm production (Zamorano-Sanchez et al. 2015).

However, all of these examples involve c-di-GMP regulating the levels of transcription. Although more work needs to be done to ensure that c-di-GMP is not affecting *syp* transcription,

I have other data that suggest that SYP production via c-di-GMP occurs post-transcriptionally. I found that RscS is crucial for c-di-GMP levels, and this dependence is not through SypG; however, evidence suggests that RscS works with SypE (Morris and Visick 2013a). The data I presented here somewhat support previous work. It might be that RscS works through the SypE/SypA arm to upregulate c-di-GMP levels and subsequent SYP production, but more work will need to be done in order to establish this connection more firmly. For example, constructing a new c-di-GMP reporter more compatible with *V. fischeri* is necessary as the current reporter is lost at a regular rate and confounds the RFP levels found through flow cytometry analysis.

There are several examples of c-di-GMP working post-transcriptionally to upregulate polysaccharide production. In fact, c-di-GMP was discovered through its role as an allosteric activator of cellulose synthase (Ross et al. 1987). In bacterial species such as *E. coli*, *Komagataeibacter xylinus*, and *Rhodobacter sphaeroides*, c – di – GMP regulates the expression of cellulose by binding to and activating the cellulose synthase complex BcsA – BcsB (Morgan, McNamara, and Zimmer 2014). This binding and subsequent activation results in the production and translocation of cellulose to the outer membrane, resulting in biofilm formation (Morgan, McNamara, and Zimmer 2014). Lastly, c-di – GMP upregulates the transcriptional regulator CsgD, transcriptionally, in both *E. coli* and *Salmonella enterica*. CsgD controls the expression of the *csgBAC* operon, which encodes the structural subunits of curli; therefore, if the *csgBAC* operon is upregulated, so is biofilm formation (Tagliabue et al. 2010; Sommerfeldt et al. 2009).

Conclusions.

The impact of studying biofilm formation in a more natural context cannot be overstated. This dissertation has introduced pABA/calcium as a condition that induces biofilm formation by WT ES114 *V. fischeri*. I have also established crosstalk between SYP and cellulose

polysaccharide production. Through the use of pABA/calcium conditions, I have identified a role for RscS, in which RscS senses pABA or the pABA condition to upregulate *syp* transcription and eventual biofilm formation. My work confirms the work thus far to uncover the mechanism(s) of RscS on SYP production. Lastly, I put forward the notion that to stimulate ES114 biofilms; there must be two coordinate signaling molecules or signal transduction events. Overall, I have provided the foundation for more advances in the SYP signal transduction network, exploiting a new heterologous system and exploring the relationship between c-di-GMP and SYP.

APPENDIX A
ADDITIONAL STUDIES

Sugar Uptake Genes Affect Biofilm Formation.

As described in the results section, I first looked at an *agaR* mutant's phenotypes that Dr. Alice Tischler had discovered through transposon mutagenesis. The *aga* operon is vital for sugar import, specifically the chitin subunit: N-acetylgalactosamine. LBS has an abundance of sugars; therefore, to determine if these sugars affect *agaR* mutant biofilm formation, I used a media with less sugar content: tTBS.

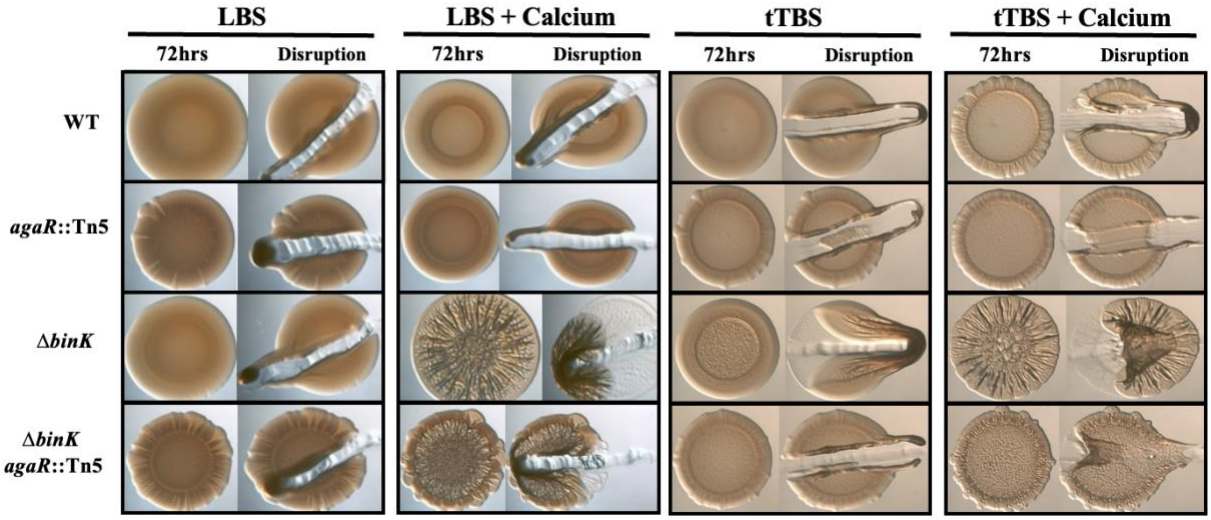

Figure 44. *agaR* Exhibits Varying Biofilm Phenotypes Depending on the Media. Colony biofilm formation by WT ES114, *agaR*::Tn*5* (AT61), the Δ*binK* mutant (KV7860), and Δ*binK agaR*::Tn*5* (AT37) were evaluated following growth on LBS, LBS + 10 mM calcium, tTBS, and tTBS + 10 mM calcium. Pictures were taken using a dissecting light microscope at 72 hrs. Each colony was disrupted using a toothpick after 72 hrs. Pictures are representative of 3 separate experiments.

On LBS media AT61 (ES114 with a Tn*5* transposon disruption in *agaR*) and AT37 (Δ*binK* mutant background with Tn*5* transposon in *agaR*) started to exhibit sectoring, signifying mutations occurring around the colony's edge (Fig. 44). The mutant containing a Δ*binK* mutation displayed cohesive biofilms on media containing calcium (Fig. 44) Interestingly, I noticed that the Δ*binK* mutant forms a biofilm on tTBS; however, the Δ*binK agaR*::Tn*5* mutant, *agaR*::Tn*5* mutant and WT, did not exhibit enhanced biofilm formation (Fig. 44). The inability of the Δ*binK*

agaR::Tn*5* mutant to form a biofilm on tTBS is possibly due to the inability of the mutant to uptake N-acetylgalactosamine. Further, with the discrepancy between the Δ*binK agaR*::Tn*5* mutant and the Δ*binK* mutant phenotype on tTBS (Fig. 43), I decided to explore if adding sugars back to tTBS would inhibit Δ*binK* tTBS biofilm formation.

Supplementation of Sugar Inhibits Δ*binK* Biofilm Formation.

The *aga* operon specifically uptakes N-acetylgalactosamine, and the inability of the Δ*binK agaR*::Tn*5* mutant to uptake this sugar, presumably, is why the Δ*binK* mutant and not the *agaR* Δ*binK* mutant formed a biofilm on tTBS. Therefore, when looking at the differences between LBS and tTBS, I decided to examine if various sugars would inhibit the Δ*binK* mutant biofilm phenotype. I looked at N-acetylglucosamine and N-acetylgalactosamine and two simple sugars, glucose and fructose, with or without calcium.

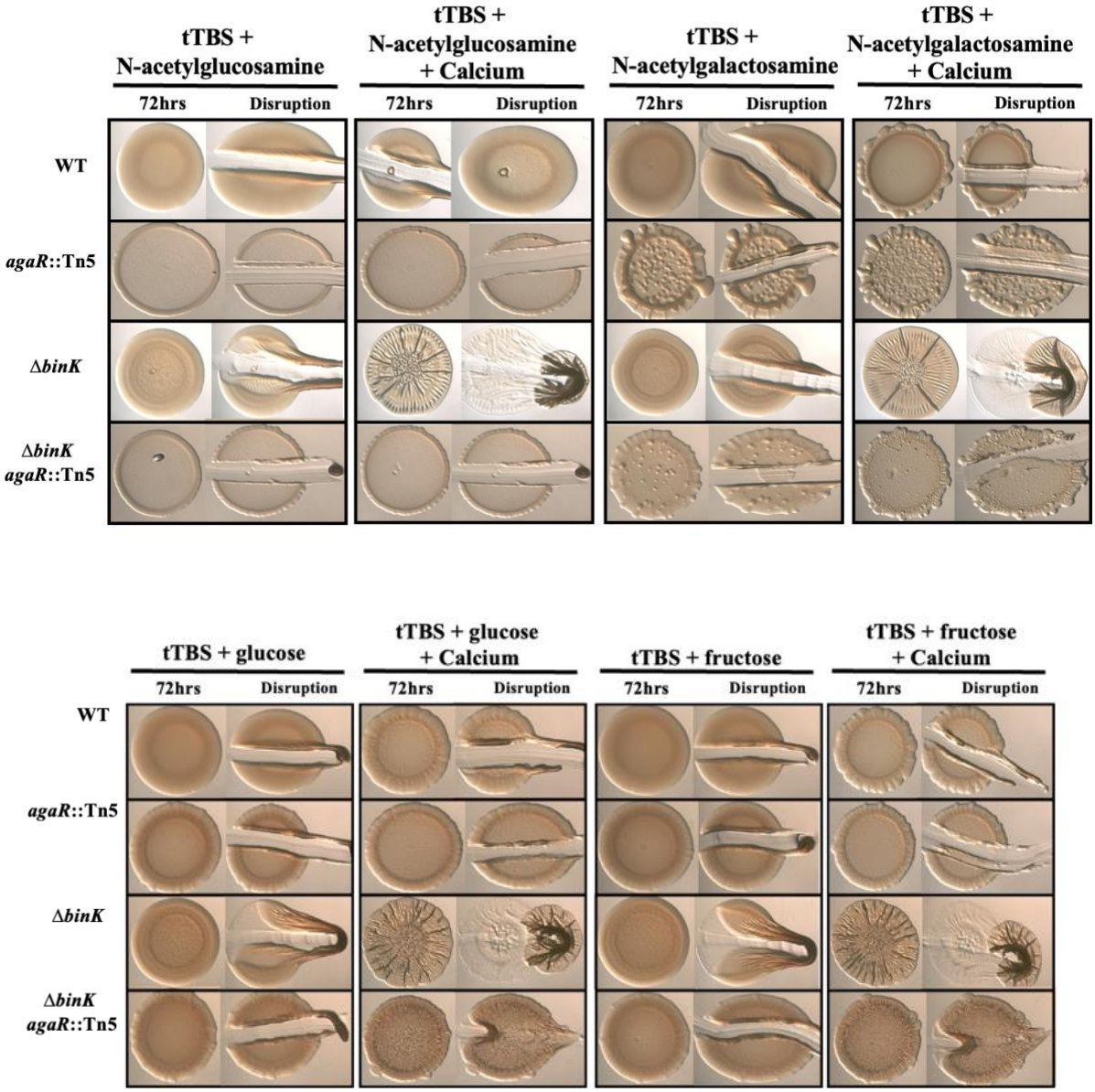

Figure 45. N-acetylglucosamine and N-acetylgalactosamine Inhibit Δ*binK* Biofilm Formation. Colony biofilm formation by WT ES114, *agaR*::Tn*5* (AT61), the Δ*binK* mutant (KV7860), and Δ*binK agaR*::Tn*5* (AT37) were evaluated following growth on tTBS + N-acetylglucosamine, tTBS + N-acetylglucosamine + calcium, tTBS + N-acetylgalactosamine, tTBS + N-acetylgalactosamine + calcium, tTBS + glucose, tTBS + glucose + calcium, tTBS + fructose, and tTBS + fructose + calcium. Pictures were taken using a dissecting light microscope at 72 hrs. Each colony was disrupted using a toothpick after 72 hrs. Pictures are representative of 2 separate experiments.

I found that both N-acetylglucosamine and N-acetylgalactosamine disrupted the Δ*binK* mutant biofilm formation, but neither glucose nor fructose had an effect on biofilm formation (Fig.

45). Further, both of the *agaR* mutants exhibited "bumpy" phenotypes, which could be supressor mutations arising that permits better growth under these conditions (Fig. 45; top**)**. However, more work would need to be done to determine if those bumps are truly suppressor mutants.

The effect that both N-acetylglucosamine and N-acetylgalactosamine have on Δ*binK* mutant biofilm formation led me to examine if the derivatives of these sugars, without the acetyl group, would also disrupt biofilms.

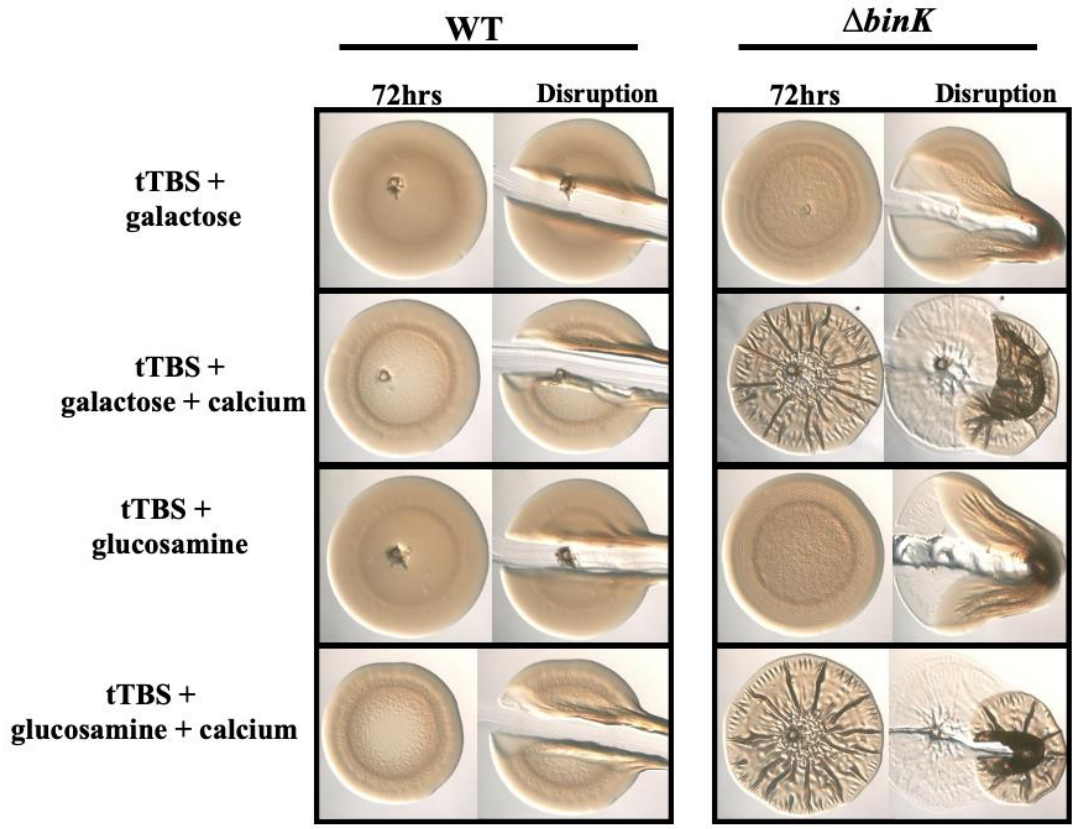

Figure 46. Sugar Derivatives do not Inhibit Δ*binK* Mutant Biofilm Formation. Colony biofilm formation by WT ES114 and the Δ*binK* mutant (KV7860) were evaluated following growth on tTBS + galactose, tTBS + galactose + calcium, tTBS + glucosamine, tTBS + glucosamine + calcium. Pictures were taken using a dissecting light microscope at 72 hrs. Each colony was disrupted using a toothpick after 72 hrs. Pictures are representative of 2 separate experiments.

Galactose and glucosamine did not disrupt the Δ*binK* mutant biofilm formation (Fig. 46), indicating that the effects observed in Figure 45 were, in fact, due to those specific sugars.

Further, it seems that the acetyl group is crucial for biofilm disruption; however, the exact mechanism of biofilm inhibition is still unknown.

Biofilm Formation on tTBS by the Δ*binK* mutant is possibly a starvation response.

I wanted to determine if it was the lack of nutrients that is responsible for the induction of biofilm formation by the Δ*binK* mutant. Therefore, I looked at media that contained either double the amount of tryptone, without yeast extract, or media that contained yeast extract only, without tryptone.

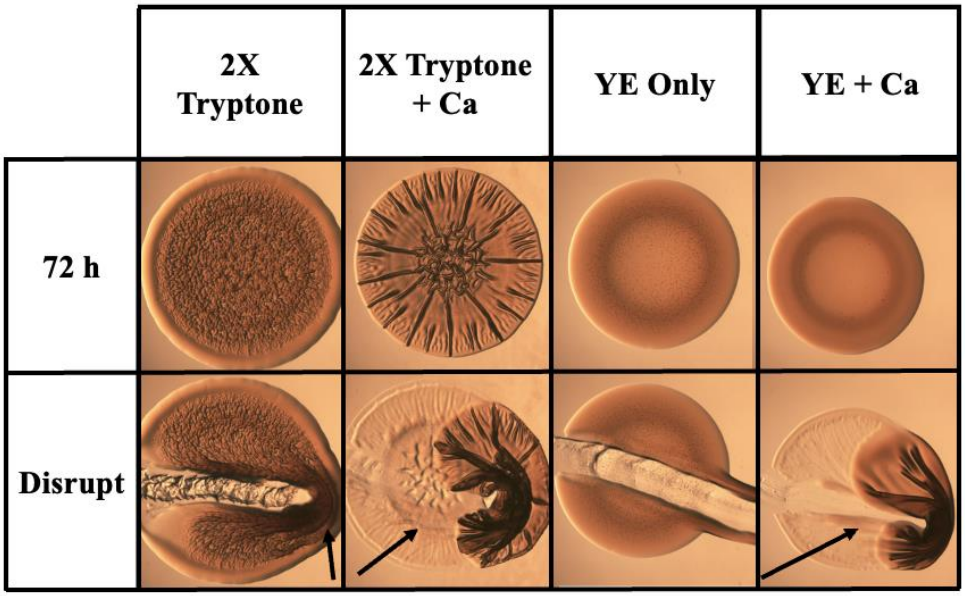

Figure 47. Yeast extract, but not tryptone, inhibits colony biofilms in the absence of calcium. Colony biofilm formation by the Δ*binK* mutant (KV7860) was evaluated following growth on 2X tryptone, 2X tryptone + 10 mM calcium, YE (LBS lacking tryptone), and YE + 10 mM calcium. Pictures were taken using a dissecting light microscope at 72 h before and after disruption using a toothpick. Pictures are representative of 3 separate experiments. Arrows indicate where "pulling," indicating cohesion, was observed.

I found that while the 2X tryptone media does induce biofilm formation by the Δ*binK* mutant the biofilm that forms are not as strong as that formed by the Δ*binK* mutant on tTBS (compare figure 47 with figure 46). Further, yeast extract alone does not induce biofilm formation by the Δ*binK* mutant without the addition of calcium. These data indicating that it is

not the lower nutrient content in tTBS *per se* that facilitates biofilm formation and that a nutrient(s) present in yeast extract is inhibitory to biofilm formation. However, as mentioned, the induction of biofilm formation on 2X tryptone is not as robust as that seen on tTBS; therefore, it is possible that a starvation response is partially responsible for the observed biofilm induction.

pABA Transporters and Synthesizers have no Impact on TPC Biofilm Formation

In figure 17, I saw that pABA has global effects on ES114 physiology, including pABA uptake and pABA synthesis. These upregulations could affect WT biofilm formation or c-di-GMP synthesis and were worth pursuing. I not only disrupted the transporter upregulated in the transcriptomics data (*VF_0639*) but also the *abgT* transporter with homology to the *abgT* transporter in *E. coli* (*VF_1410*).

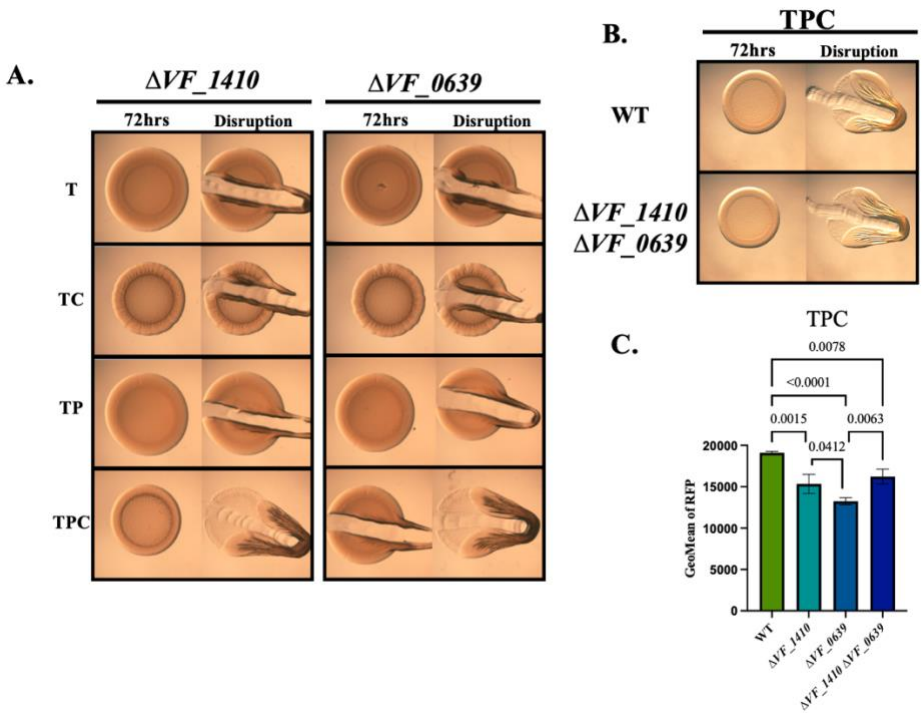

Figure 48. AbgT Transporters do not Affect Biofilm Formation but Impacts c-di-GMP Levels. (A) Colony biofilm formation by Δ*VF_1410* (KV9773) and Δ*VF_0639* (KV9794) were evaluated following growth on tTBS (T), tTBS + calcium (TC), tTBS + pABA (TP) and tTBS + pABA/calcium (TPC) **(B)** WT and the Δ*VF_1410* Δ*VF_0639* (CD25) double mutant were evaluated on TPC. Pictures were taken using a dissecting light microscope at 72hrs. Each colony was disrupted using a toothpick after 72hrs. **(C)** The levels of RFP from strains carrying c-di-GMP biosensor pFY4535 were measured in TPC.

Disruption of the genes for the AbgT transporters did not inhibit biofilm formation (Fig. 47A and B). I did see a significant decrease in the levels of c-di-GMP when *VF_0639* was deleted as well as when *VF_1410* or when both transporters were deleted (Fig. 47C). These results suggest that the uptake of pABA does not affect WT biofilm formation but does very modestly impact the ability of WT to induce c-di-GMP synthesis under TPC conditions. The exact mechanism through which TPC upregulates c-di-GMP is still unknown; however, these results suggest that pABA must be, at least partially, taken up to upregulate c-di-GMP levels.

The transcriptomics data also showed a significant increase in *pabC* transcription. PabC mediates the conversion of 4 – amino – 4- deoxychorismate, an intermediate molecule, into

pABA; this reaction is also reversible (Basset et al. 2004). I decided to examine if disrupting the synthesis of pABA would impact biofilm formation or c-di-GMP levels.

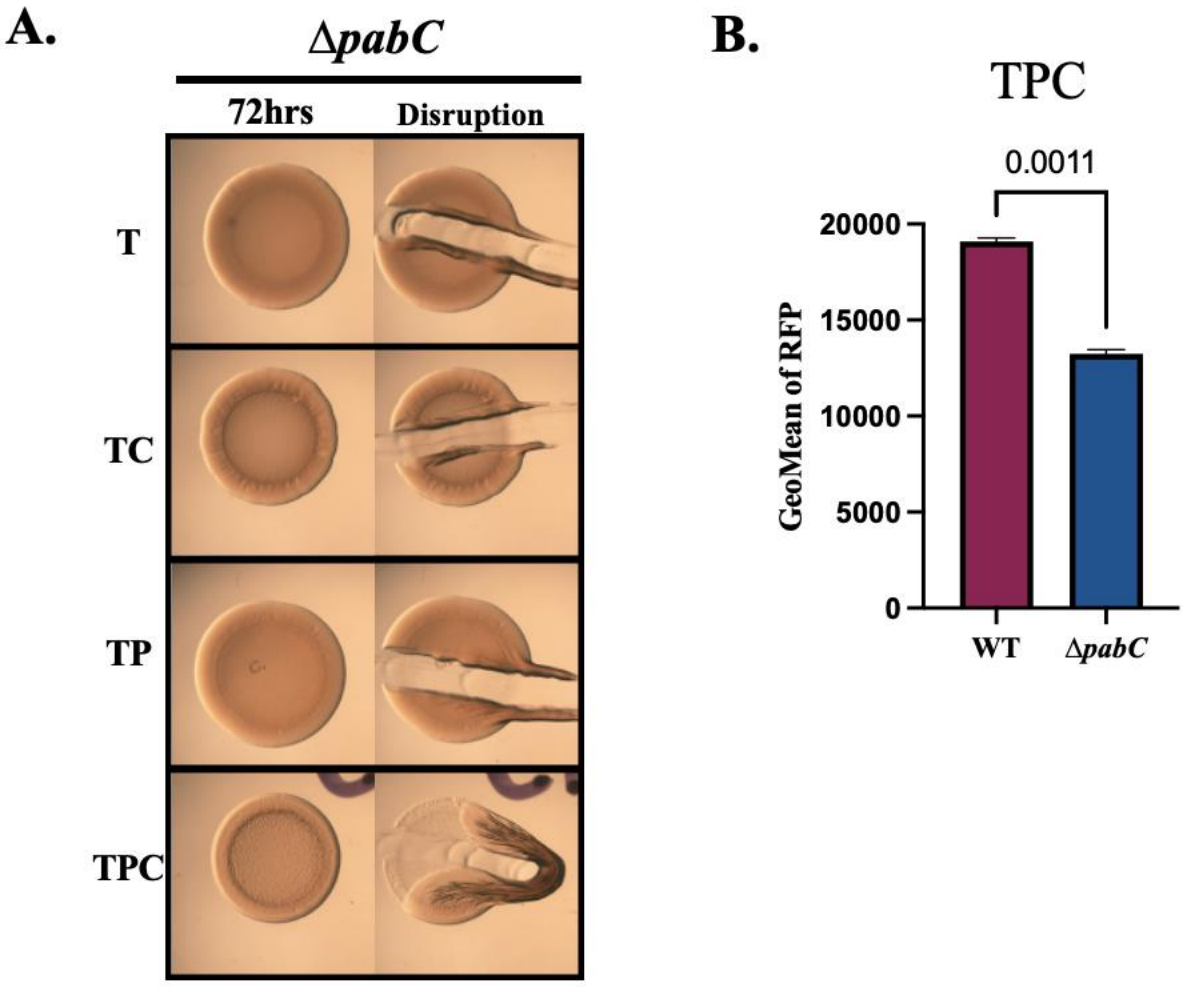

Figure 49. pABA Synthesis does not Affect Biofilm Formation but Impacts c-di-GMP Levels. (A) Colony biofilm formation by Δ*pabC* (KV9793) was evaluated following growth on tTBS (T), tTBS + calcium (TC), tTBS + pABA (TP), and tTBS + pABA/calcium (TPC). Pictures were taken using a dissecting light microscope at 72hrs. Each colony was disrupted using a toothpick after 72hrs. **(B)** The levels of RFP from strains carrying c-di-GMP biosensor pFY4535 were measured in TPC.

The disruption of *pabC* exhibited no impact on TPC-induced biofilms (Fig. 48A). However, the Δ*pabC* mutant did significantly decrease the levels of c-di-GMP within the cells (Fig. 48B). The decrease in c-di-GMP levels suggest that pABA synthase and/or pABA

metabolism impacts the synthesis of c-di-GMP. This decrease could occur from pABA metabolites impacting DGC and/or PDE function but more work will need to be done to determine the exact mechanism(s).

RscS is Crucial for Δ*binK*-Induced Biofilm Formation.

Given the importance of RscS on WT biofilm formation, I also wondered if the Δ*binK* mutant phenotype on tTBS depended on RscS. Further, I hypothesize that, under tTBS conditions, both RscS and HahK are the regulators supplying phosphoryl groups to the HPT domain of SypF, which eventually upregulates *syp* transcription and SYP production (Fig. 41). My hypothesis is that it takes two sensors signaling in order to induce SYP-dependent biofilm formation. Therefore, deletion of *rscS* in the Δ*binK* mutant background should render loss of biofilm formation on tTBS.

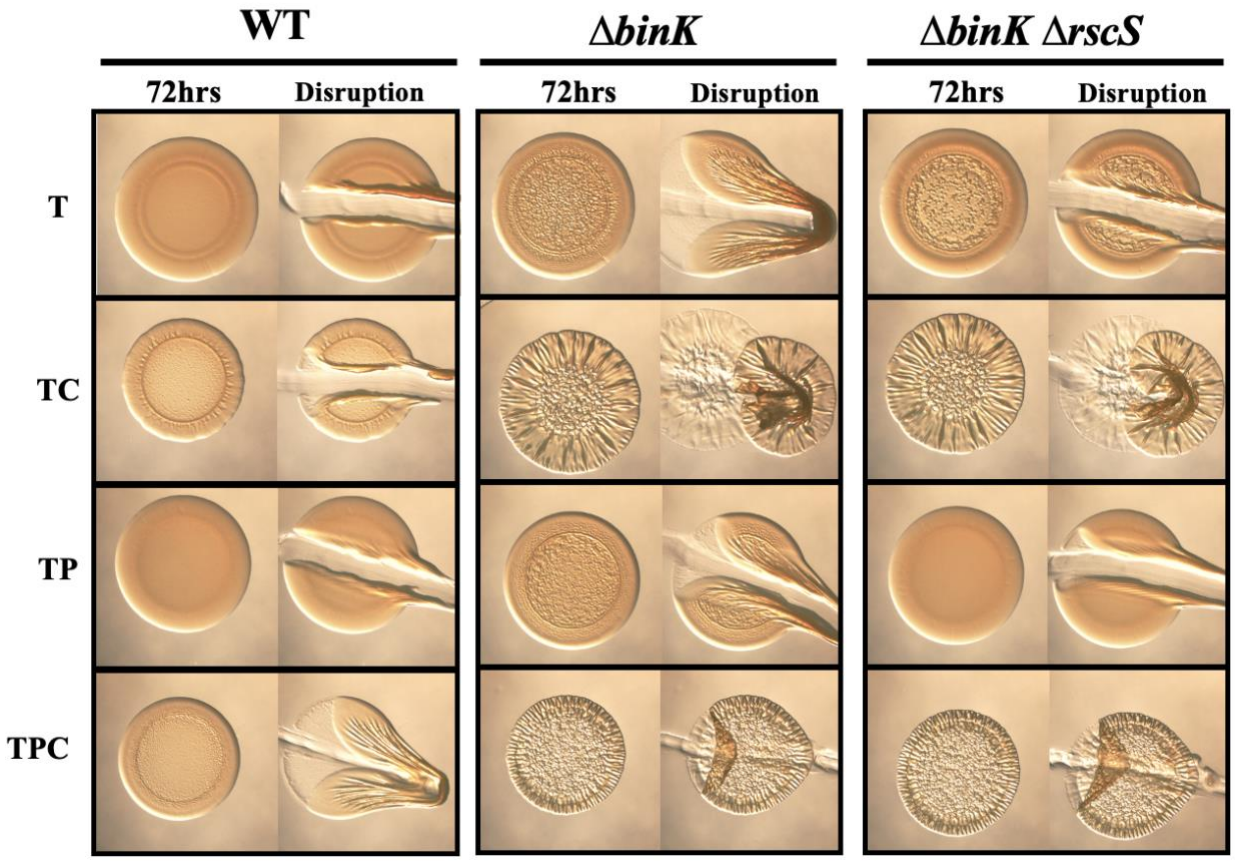

Figure 50. Δ*binK* Mutant Biofilm Formation on tTBS Relies on RscS. Colony biofilm formation by wild-type strain ES114, the Δ*binK* mutant (KV7860), and the Δ*binK* Δ*rscS* double mutant (KV7861) were assessed following growth on tTBS (T), tTBS + 10 mM calcium (TC), tTBS + 9.7 mM pABA (TP), and tTBS + pABA/calcium (TPC). Pictures were taken using a dissecting light microscope at 72 and 96 hrs. The colony was disrupted using a toothpick after 96hrs.

The Δ*binK* mutant forms a biofilm under tTBS, TC, and TPC conditions, with slight biofilm formation under TP (including colony architecture) but less than its tTBS counterpart (Fig. 49; middle). As displayed previously, biofilm formation only occurs on TPC for WT ES114 (Fig. 49; left). Due to the robust nature of calcium-mediated induction of biofilm formation, under any calcium conditions, the Δ*binK* mutant and the Δ*binK* Δ*rscS* mutant form cohesive biofilms (Fig. 49; middle and right). I propose this is due to the strong signal SypF is receiving from calcium to induce kinase activity, compounded by the fact that BinK is no longer shuttling phosphoryl groups

off of SypF to inhibit biofilm formation. Notably, the deletion of *rscS* rendered an abrogation of biofilm formation on tTBS in the Δ*binK* mutant (Fig. 49, right).

Further, any biofilm formation occurring under TP conditions in the Δ*binK* mutant background is lost when *rscS* is deleted (Fig. 49, right). The loss of any biofilm formation or architecture occurring under TP conditions in the Δ*binK* mutant background further supports my hypothesis that RscS is sensing pABA and is responsible for any pABA-induced biofilm phenotypes. The exact signal transduction scheme and if/how HahK plays into the Δ*binK* mutant biofilms have yet to be uncovered. However, I have laid the groundwork for another profitable project in the Visick lab.

SypF is Potentially Sensing Calcium.

To support my hypothesis that SypF might be sensing calcium, I tested a strain that expressed SypF from a multicopy plasmid (SypF+) in a wrinkled colony assay as well as at the level of *syp* transcription. I already looked at this plasmid under TP and TPC conditions (Fig. 32). However, I hypothesized that SypF might be sensing calcium (Fig. 42); therefore, I examined T and TC conditions and assessed *syp* transcription to determine if the induction of biofilms was happening at the level of transcription or post-transcriptionally.

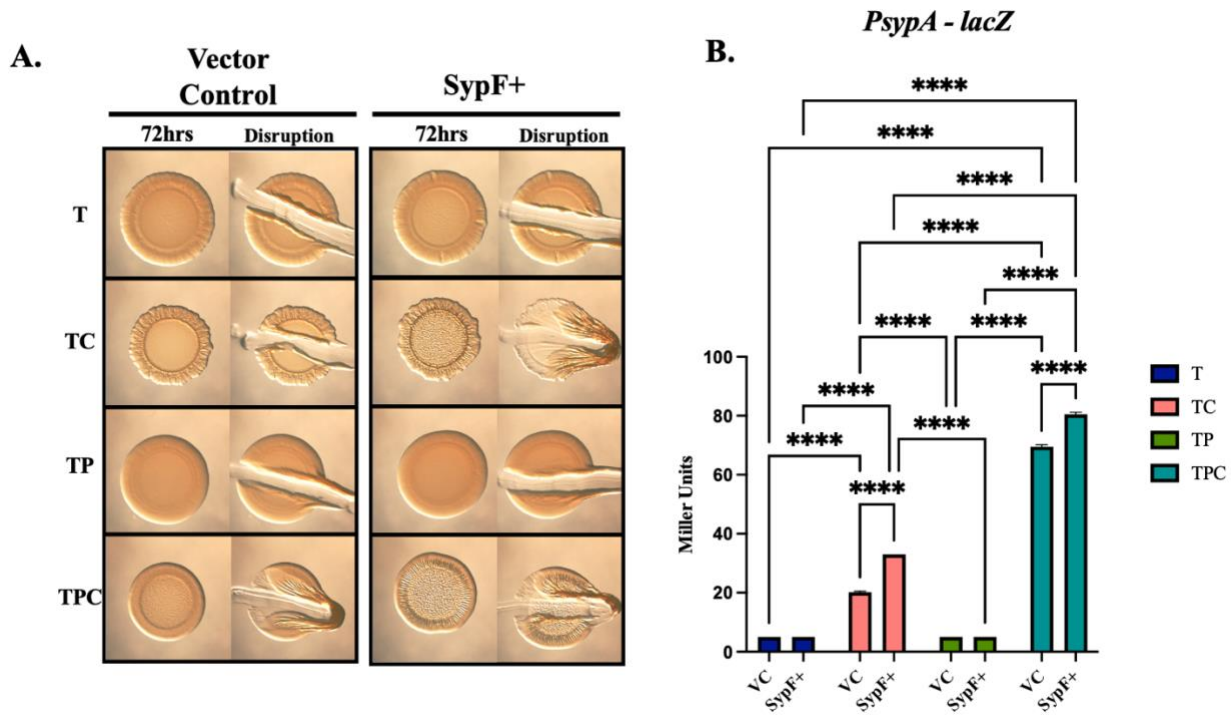

Figure 51. SypF+ Induces Biofilm Formation on tTBS Calcium. (A) Colony biofilm formation of ES114 + vector control (pKV69) or ES114 + wild type *sypF* on a plasmid (pCLD54; SypF+) were assessed following growth on tTBS, tTBS + calcium (TC), tTBS + pABA (TP) and tTBS + pABA/calcium (TPC) (also shown in Fig. 31). Pictures were taken using a dissecting light microscope at 72hrs. Each colony was disrupted using a toothpick after 72hrs. Pictures are representative of 3 separate experiments. (B) *sypA* promoter activity (Miller units) was measured using P*sypA-lacZ* fusion strain KV8079 that contained either the Vector control (VC; pKV69) plasmid or the SypF+ plasmid (pCLD54) following a 22hr subculture in tTBS (T), tTBS + calcium (TC), tTBS + pABA (TP) and tTBS + pABA/calcium (TPC). Statistics were performed via a two-way Tukey's multiple–comparison test, where Miller units was the dependent variable.

When the SypF+ plasmid was introduced into WT, I saw an increase in biofilm formation under TC conditions compared to the vector control (Fig. 50A). As noted previously, SypF+ does not induce biofilm formation under TP conditions and even seems to inhibit biofilm formation on TPC (Figs. 32 and 50A). The *syp* transcription data show a similar trend for TC conditions where there is a slight but significant increase in *syp* transcription when SypF+ is present (Fig. 50B). However, the TPC transcription data does not match the corresponding biofilm data. Under TPC conditions, I also saw a significant increase in *syp* transcription when

SypF+ was present (Fig. 50B), whereas the biofilm displays a seeming inhibition of TPC-induced biofilms. More work and various troubleshooting will need to be done to sort out this discrepancy; however, I believe the data shown support my hypothesis that SypF is sensing calcium. Again, this sets up another area of future research in determining if SypF indeed senses calcium, what domains are crucial, and if any direct binding of calcium by SypF occurs.

REFERENCE LIST

Ainsaar, K., K. Mumm, H. Ilves, and R. Horak. 2014. 'The ColRS signal transduction system responds to the excess of external zinc, iron, manganese, and cadmium', *BMC Microbiol*, 14: 162.

Altura, M. A., E. A. Heath-Heckman, A. Gillette, N. Kremer, A. M. Krachler, C. Brennan, E. G. Ruby, K. Orth, and M. J. McFall-Ngai. 2013. 'The first engagement of partners in the *Euprymna scolopes-Vibrio fischeri* symbiosis is a two-step process initiated by a few environmental symbiont cells', *Environ Microbiol*, 15: 2937-50.

Altura, M. A., E. Stabb, W. Goldman, M. Apicella, and M. J. McFall-Ngai. 2011. 'Attenuation of host NO production by MAMPs potentiates development of the host in the squid-vibrio symbiosis', *Cell Microbiol*, 13: 527-37.

An, S. Q., J. H. Allan, Y. McCarthy, M. Febrer, J. M. Dow, and R. P. Ryan. 2014. 'The PAS domain-containing histidine kinase RpfS is a second sensor for the diffusible signal factor of *Xanthomonas campestris*', *Mol Microbiol*, 92: 586-97.

Asmat, T. M., T. Tenenbaum, A. B. Jonsson, C. Schwerk, and H. Schroten. 2014. 'Impact of calcium signaling during infection of *Neisseria meningitidis* to human brain microvascular endothelial cells', *PLoS One*, 9: e114474.

Baraquet, C., K. Murakami, M. R. Parsek, and C. S. Harwood. 2012. 'The FleQ protein from *Pseudomonas aeruginosa* functions as both a repressor and an activator to control gene expression from the *pel* operon promoter in response to c-di-GMP', *Nucleic Acids Res*, 40: 7207-18.

Barraud, N., D. J. Hassett, S. H. Hwang, S. A. Rice, S. Kjelleberg, and J. S. Webb. 2006. 'Involvement of nitric oxide in biofilm dispersal of *Pseudomonas aeruginosa*', *J Bacteriol*, 188: 7344-53.

Basset, G. J., E. P. Quinlivan, S. Ravanel, F. Rebeille, B. P. Nichols, K. Shinozaki, M. Seki, L. C. Adams-Phillips, J. J. Giovannoni, J. F. Gregory, 3rd, and A. D. Hanson. 2004. 'Folate synthesis in plants: the p-aminobenzoate branch is initiated by a bifunctional PabA-PabB protein that is targeted to plastids', *Proc Natl Acad Sci U S A*, 101: 1496-501.

Bassis, C. M., and K. L. Visick. 2010. 'The cyclic-di-GMP phosphodiesterase BinA negatively regulates cellulose-containing biofilms in *Vibrio fischeri*', *J Bacteriol*, 192: 1269-78.

Beloin, C., S. Renard, J. M. Ghigo, and D. Lebeaux. 2014. 'Novel approaches to combat bacterial biofilms', *Curr Opin Pharmacol*, 18: 61-8.

Bilecen, K., and F. H. Yildiz. 2009. 'Identification of a calcium-controlled negative regulatory system affecting *Vibrio cholerae* biofilm formation', *Environ Microbiol*, 11: 2015-29.

Boettcher, K. J., and E. G. Ruby. 1990. 'Depressed light emission by symbiotic *Vibrio fischeri* of the sepiolid squid *Euprymna scolopes*', *J Bacteriol*, 172: 3701-6.

Boettcher, K. J., Ruby, E.G., and McFall-Ngai, M.J. . 1996. 'Bioluminescence in the symbiotic squid *Euprymna scolopes* is controlled by a daily biological rhythm', *Journal of Comparative Physiology A*, 170: 65-73.

Boneca, I. G., C. Ecobichon, C. Chaput, A. Mathieu, S. Guadagnini, M. C. Prevost, F. Colland, A. Labigne, and H. de Reuse. 2008. 'Development of inducible systems to engineer conditional mutants of essential genes of *Helicobacter pylori*', *Appl Environ Microbiol*, 74: 2095-102.

Bongrand, C., E. J. Koch, S. Moriano-Gutierrez, O. X. Cordero, M. McFall-Ngai, M. F. Polz, and E. G. Ruby. 2016. 'A genomic comparison of 13 symbiotic *Vibrio fischeri* isolates from the perspective of their host source and colonization behavior', *ISME J*, 10: 2907-17.

Bongrand, C., and E. G. Ruby. 2019. 'Achieving a multi-strain symbiosis: strain behavior and infection dynamics', *ISME J*, 13: 698-706.

Bourret, T. J., L. Liu, J. A. Shaw, M. Husain, and A. Vazquez-Torres. 2017. 'Magnesium homeostasis protects *Salmonella* against nitrooxidative stress', *Sci Rep*, 7: 15083.

Braithwaite, R. A., and L. A. McEvoy. 2005. 'Marine biofouling on fish farms and its remediation', *Adv Mar Biol*, 47: 215-52.

Brennan, C. A., C. R. DeLoney-Marino, and M. J. Mandel. 2013. 'Chemoreceptor VfcA mediates amino acid chemotaxis in *Vibrio fischeri*', *Appl Environ Microbiol*, 79: 1889-96.

Broder, U. N., T. Jaeger, and U. Jenal. 2016. 'LadS is a calcium-responsive kinase that induces acute-to-chronic virulence switch in *Pseudomonas aeruginosa*', *Nat Microbiol*, 2: 16184.

Brooks, J. F., 2nd, M. C. Gyllborg, D. C. Cronin, S. J. Quillin, C. A. Mallama, R. Foxall, C. Whistler, A. L. Goodman, and M. J. Mandel. 2014. 'Global discovery of colonization determinants in the squid symbiont *Vibrio fischeri*', *Proc Natl Acad Sci U S A*, 111: 17284-9.

Brooks, J. F., 2nd, and M. J. Mandel. 2016. 'The Histidine Kinase BinK Is a Negative Regulator of Biofilm Formation and Squid Colonization', *J Bacteriol*, 198: 2596-607.

Bryers, J. D. 2008. 'Medical biofilms', *Biotechnol Bioeng*, 100: 1-18.

Busch, A., M. E. Guazzaroni, J. Lacal, J. L. Ramos, and T. Krell. 2009. 'The sensor kinase TodS operates by a multiple step phosphorelay mechanism involving two autokinase domains', *J Biol Chem*, 284: 10353-60.

Busch, A., J. Lacal, A. Martos, J. L. Ramos, and T. Krell. 2007. 'Bacterial sensor kinase TodS interacts with agonistic and antagonistic signals', *Proc Natl Acad Sci U S A*, 104: 13774-9.

Cai, Z., Z. H. Yuan, H. Zhang, Y. Pan, Y. Wu, X. Q. Tian, F. F. Wang, L. Wang, and W. Qian. 2017. 'Fatty acid DSF binds and allosterically activates histidine kinase RpfC of phytopathogenic bacterium *Xanthomonas campestris* pv. campestris to regulate quorum-sensing and virulence', *PLoS Pathog*, 13: e1006304.

Cairns, L. S., V. L. Marlow, E. Bissett, A. Ostrowski, and N. R. Stanley-Wall. 2013. 'A mechanical signal transmitted by the flagellum controls signalling in *Bacillus subtilis*', *Mol Microbiol*, 90: 6-21.

Casper-Lindley, C., and F. H. Yildiz. 2004. 'VpsT is a transcriptional regulator required for expression of vps biosynthesis genes and the development of rugose colonial morphology in *Vibrio cholerae* O1 El Tor', *J Bacteriol*, 186: 1574-8.

Castillo, M. G., M. S. Goodson, and M. McFall-Ngai. 2009. 'Identification and molecular characterization of a complement C3 molecule in a lophotrochozoan, the Hawaiian bobtail squid *Euprymna scolopes*', *Dev Comp Immunol*, 33: 69-76.

Cepas, V., Y. Lopez, Y. Gabasa, C. B. Martins, J. D. Ferreira, M. J. Correia, L. M. A. Santos, F. Oliveira, V. Ramos, M. Reis, R. Castelo-Branco, J. Morais, V. Vasconcelos, I. Probert, E. Guilloud, M. Mehiri, and S. M. Soto. 2019. 'Inhibition of Bacterial and Fungal Biofilm Formation by 675 Extracts from Microalgae and Cyanobacteria', *Antibiotics (Basel)*, 8.

Chakraborty, S., M. Li, C. Chatterjee, J. Sivaraman, K. Y. Leung, and Y. K. Mok. 2010. 'Temperature and Mg2+ sensing by a novel PhoP-PhoQ two-component system for regulation of virulence in *Edwardsiella tarda*', *J Biol Chem*, 285: 38876-88.

Chambers, L. D., K. R. Stokes, F. C. Walsh, and R. J. K. Wood. 2006. 'Modern approaches to marine antifouling coatings', *Surface and Coatings Technology*, 201: 3642-52.

Chamnongpol, S., M. Cromie, and E. A. Groisman. 2003. 'Mg2+ sensing by the Mg2+ sensor PhoQ of *Salmonella enterica*', *J Mol Biol*, 325: 795-807.

Chang, W. S., M. van de Mortel, L. Nielsen, G. Nino de Guzman, X. Li, and L. J. Halverson. 2007. 'Alginate production by *Pseudomonas putida* creates a hydrated microenvironment and contributes to biofilm architecture and stress tolerance under water-limiting conditions', *J Bacteriol*, 189: 8290-9.

Cherepanov, P. P., and W. Wackernagel. 1995. 'Gene disruption in *Escherichia coli*: TcR and KmR cassettes with the option of Flp-catalyzed excision of the antibiotic-resistance determinant', *Gene*, 158: 9-14.

Chodur, D. M., P. Coulter, J. Isaacs, M. Pu, N. Fernandez, C. M. Waters, and D. A. Rowe-Magnus. 2018. 'Environmental Calcium Initiates a Feed-Forward Signaling Circuit That Regulates Biofilm Formation and Rugosity in *Vibrio vulnificus*', *mBio*, 9.

Christensen, D. G., A. E. Marsden, K. Hodge-Hanson, T. Essock-Burns, and K. L. Visick. 2020. 'LapG mediates biofilm dispersal in *Vibrio fischeri* by controlling maintenance of the VCBS-containing adhesin LapV', *Mol Microbiol*, 114: 742-61.

Christensen, D. G., J. Tepavčević, and K. L. Visick. 2020. 'Genetic Manipulation of *Vibrio fischeri*', *Curr Protoc Microbiol*, 59: e115.

Christensen, D. G., and K. L. Visick. 2020. '*Vibrio fischeri*: Laboratory Cultivation, Storage, and Common Phenotypic Assays', *Curr Protoc Microbiol*, 57: e103.

Chun, C. K., J. V. Troll, I. Koroleva, B. Brown, L. Manzella, E. Snir, H. Almabrazi, T. E. Scheetz, F. Bonaldo Mde, T. L. Casavant, M. B. Soares, E. G. Ruby, and M. J. McFall-Ngai. 2008. 'Effects of colonization, luminescence, and autoinducer on host transcription during development of the squid-vibrio association', *Proc Natl Acad Sci U S A*, 105: 11323-8.

Claes, M. F., and P. V. Dunlap. 2000. 'Aposymbiotic culture of the sepiolid squid *Euprymna scolopes*: role of the symbiotic bacterium *Vibrio fischeri* in host animal growth, development, and light organ morphogenesis', *J Exp Zool*, 286: 280-96.

Cohen, J. J., S. J. Eichinger, D. A. Witte, C. J. Cook, P. M. Fidopiastis, J. Tepavčević, and K. L. Visick. 2021. 'Control of Competence in *Vibrio fischeri*', *Appl Environ Microbiol*, 87.

Collins, A. J., T. R. Schleicher, B. A. Rader, and S. V. Nyholm. 2012. 'Understanding the role of host hemocytes in a squid/vibrio symbiosis using transcriptomics and proteomics', *Front Immunol*, 3: 91.

Conner, J. G., D. Zamorano-Sanchez, J. H. Park, H. Sondermann, and F. H. Yildiz. 2017. 'The ins and outs of cyclic di-GMP signaling in *Vibrio cholerae*', *Curr Opin Microbiol*, 36: 20-29.

Cunliffe, M., R. C. Upstill-Goddard, and J. C. Murrell. 2011. 'Microbiology of aquatic surface microlayers', *FEMS Microbiol Rev*, 35: 233-46.

Cutruzzola, F., and N. Frankenberg-Dinkel. 2016. 'Origin and Impact of Nitric Oxide in *Pseudomonas aeruginosa* Biofilms', *J Bacteriol*, 198: 55-65.

Darnell, C. L., E. A. Hussa, and K. L. Visick. 2008. 'The putative hybrid sensor kinase SypF coordinates biofilm formation in *Vibrio fischeri* by acting upstream of two response regulators, SypG and VpsR', *J Bacteriol*, 190: 4941-50.

Davey, M. E., and A. O'Toole G. 2000. 'Microbial biofilms: from ecology to molecular genetics', *Microbiol Mol Biol Rev*, 64: 847-67.

Davidson, S. K., T. A. Koropatnick, R. Kossmehl, L. Sycuro, and M. J. McFall-Ngai. 2004. 'NO means 'yes' in the squid-vibrio symbiosis: nitric oxide (NO) during the initial stages of a beneficial association', *Cell Microbiol*, 6: 1139-51.

Davies, D. G., and C. N. Marques. 2009. 'A fatty acid messenger is responsible for inducing dispersion in microbial biofilms', *J Bacteriol*, 191: 1393-403.

Deloney-Marino, C. R., and K. L. Visick. 2012. 'Role for *cheR* of *Vibrio fischeri* in the Vibrio-squid symbiosis', *Can J Microbiol*, 58: 29-38.

DeLoney-Marino, C. R., A. J. Wolfe, and K. L. Visick. 2003. 'Chemoattraction of *Vibrio fischeri* to serine, nucleosides, and N-acetylneuraminic acid, a component of squid light-organ mucus', *Appl Environ Microbiol*, 69: 7527-30.

Dial, C. N., S. J. Eichinger, R. Foxall, C. J. Corcoran, A. H. Tischler, R. M. Bolz, C. A. Whistler, and K. L. Visick. 2021. 'Quorum Sensing and Cyclic di-GMP Exert Control Over Motility of *Vibrio fischeri* KB2B1', *Front Microbiol*, 12: 690459.

Dial, C. N., L. Speare, G. C. Sharpe, S. M. Gifford, A. N. Septer, and K. L. Visick. 2021. 'Para-Aminobenzoic Acid, Calcium, and c-di-GMP Induce Formation of Cohesive, Syp-Polysaccharide-Dependent Biofilms in *Vibrio fischeri*', *mBio*, 12: e0203421.

Dobretsov, S., R. M. Abed, and M. Teplitski. 2013. 'Mini-review: Inhibition of biofouling by marine microorganisms', *Biofouling*, 29: 423-41.

Donlan, R. M. 2002. 'Biofilms: microbial life on surfaces', *Emerg Infect Dis*, 8: 881-90.

Donlan, R. M., and J. W. Costerton. 2002. 'Biofilms: survival mechanisms of clinically relevant microorganisms', *Clin Microbiol Rev*, 15: 167-93.

Dunn, A. K., D. S. Millikan, D. M. Adin, J. L. Bose, and E. V. Stabb. 2006. 'New rfp- and pES213-derived tools for analyzing symbiotic *Vibrio fischeri* reveal patterns of infection and *lux* expression in situ', *Appl Environ Microbiol*, 72: 802-10.

Elasri, M. O., and R. V. Miller. 1999. 'Study of the response of a biofilm bacterial community to UV radiation', *Appl Environ Microbiol*, 65: 2025-31.

Eto, D. S., H. B. Gordon, B. K. Dhakal, T. A. Jones, and M. A. Mulvey. 2008. 'Clathrin, AP-2, and the NPXY-binding subset of alternate endocytic adaptors facilitate FimH-mediated bacterial invasion of host cells', *Cell Microbiol*, 10: 2553-67.

Fernandez, M., M. A. Matilla, A. Ortega, and T. Krell. 2017. 'Metabolic Value Chemoattractants Are Preferentially Recognized at Broad Ligand Range Chemoreceptor of *Pseudomonas putida* KT2440', *Front Microbiol*, 8: 990.

Fishman, M. R., K. Giglio, D. Fay, and M. J. Filiatrault. 2018. 'Physiological and genetic characterization of calcium phosphate precipitation by Pseudomonas species', *Sci Rep*, 8: 10156.

Fishman, M. R., J. Zhang, P. A. Bronstein, P. Stodghill, and M. J. Filiatrault. 2018. 'Ca(2+)-Induced Two-Component System CvsSR Regulates the Type III Secretion System and the Extracytoplasmic Function Sigma Factor AlgU in *Pseudomonas syringae* pv. tomato DC3000', *J Bacteriol*, 200.

Flemming, H. C., T. R. Neu, and D. J. Wozniak. 2007. 'The EPS matrix: the "house of biofilm cells"', *J Bacteriol*, 189: 7945-7.

Flemming, H. C., and J. Wingender. 2010. 'The biofilm matrix', *Nat Rev Microbiol*, 8: 623-33.

Flemming, H. C., J. Wingender, U. Szewzyk, P. Steinberg, S. A. Rice, and S. Kjelleberg. 2016. 'Biofilms: an emergent form of bacterial life', *Nat Rev Microbiol*, 14: 563-75.

Galperin, M. Y., D. A. Natale, L. Aravind, and E. V. Koonin. 1999. 'A specialized version of the HD hydrolase domain implicated in signal transduction', *J Mol Microbiol Biotechnol*, 1: 303-5.

Gao, R., and A. M. Stock. 2009. 'Biological insights from structures of two-component proteins', *Annu Rev Microbiol*, 63: 133-54.

Garcia Vescovi, E., F. C. Soncini, and E. A. Groisman. 1996. 'Mg2+ as an extracellular signal: environmental regulation of *Salmonella* virulence', *Cell*, 84: 165-74.

Gasperotti, A. F., M. K. Herrera Seitz, R. S. Balmaceda, L. M. Prosa, K. Jung, and C. A. Studdert. 2021. 'Direct binding of benzoate derivatives to two chemoreceptors with Cache sensor domains in *Halomonas titanicae* KHS3', *Mol Microbiol*, 115: 672-83.

Gavira, J. A., M. A. Matilla, M. Fernandez, and T. Krell. 2021. 'The structural basis for signal promiscuity in a bacterial chemoreceptor', *FEBS J*, 288: 2294-310.

Geszvain, K., and K. L. Visick. 2008. 'The hybrid sensor kinase RscS integrates positive and negative signals to modulate biofilm formation in *Vibrio fischeri*', *J Bacteriol*, 190: 4437-46.

Ghafoor, A., I. D. Hay, and B. H. Rehm. 2011. 'Role of exopolysaccharides in *Pseudomonas aeruginosa* biofilm formation and architecture', *Appl Environ Microbiol*, 77: 5238-46.

Gjermansen, M., P. Ragas, C. Sternberg, S. Molin, and T. Tolker-Nielsen. 2005. 'Characterization of starvation-induced dispersion in *Pseudomonas putida* biofilms', *Environ Microbiol*, 7: 894-906.

Goodman, A. L., B. Kulasekara, A. Rietsch, D. Boyd, R. S. Smith, and S. Lory. 2004. 'A signaling network reciprocally regulates genes associated with acute infection and chronic persistence in *Pseudomonas aeruginosa*', *Dev Cell*, 7: 745-54.

Grab, D. J., E. Nyarko, O. V. Nikolskaia, Y. V. Kim, and J. S. Dumler. 2009. 'Human brain microvascular endothelial cell traversal by *Borrelia burgdorferi* requires calcium signaling', *Clin Microbiol Infect*, 15: 422-6.

Graf, J., P. V. Dunlap, and E. G. Ruby. 1994. 'Effect of transposon-induced motility mutations on colonization of the host light organ by *Vibrio fischeri*', *J Bacteriol*, 176: 6986-91.

Graf, J., and E. G. Ruby. 1998. 'Host-derived amino acids support the proliferation of symbiotic bacteria', *Proc Natl Acad Sci U S A*, 95: 1818-22.

Henke, J. M., and B. L. Bassler. 2004. 'Three parallel quorum-sensing systems regulate gene expression in *Vibrio harveyi*', *J Bacteriol*, 186: 6902-14.

Hickman, J. W., and C. S. Harwood. 2008. 'Identification of FleQ from *Pseudomonas aeruginosa* as a c-di-GMP-responsive transcription factor', *Mol Microbiol*, 69: 376-89.

Horton, R. M., H. D. Hunt, S. N. Ho, J. K. Pullen, and L. R. Pease. 1989. 'Engineering hybrid genes without the use of restriction enzymes: gene splicing by overlap extension', *Gene*, 77: 61-8.

Hu, L., R. B. Raybourne, and D. J. Kopecko. 2005. 'Ca2+ release from host intracellular stores and related signal transduction during *Campylobacter jejuni* 81-176 internalization into human intestinal cells', *Microbiology (Reading)*, 151: 3097-105.

Huang, Z., B. Ni, C. Y. Jiang, Y. F. Wu, Y. Z. He, R. E. Parales, and S. J. Liu. 2016. 'Direct sensing and signal transduction during bacterial chemotaxis toward aromatic compounds in *Comamonas testosteroni*', *Mol Microbiol*, 101: 224-37.

Hughes, C. S., E. Longo, M. K. Phillips-Jones, and R. Hussain. 2017. 'Characterisation of the selective binding of antibiotics vancomycin and teicoplanin by the VanS receptor regulating type A vancomycin resistance in the enterococci', *Biochim Biophys Acta Gen Subj*, 1861: 1951-59.

Hussa, E. A., C. L. Darnell, and K. L. Visick. 2008. 'RscS functions upstream of SypG to control the syp locus and biofilm formation in *Vibrio fischeri*', *J Bacteriol*, 190: 4576-83.

Hussa, E. A., T. M. O'Shea, C. L. Darnell, E. G. Ruby, and K. L. Visick. 2007. 'Two-component response regulators of *Vibrio fischeri*: identification, mutagenesis, and characterization', *J Bacteriol*, 189: 5825-38.

Isenberg, R. Y., D. G. Christensen, K. L. Visick, and M. J. Mandel. 2022. 'High Levels of Cyclic Diguanylate Interfere with Beneficial Bacterial Colonization', *mBio*, 13: e0167122.

Johnson, M. D., C. K. Garrett, J. E. Bond, K. A. Coggan, M. C. Wolfgang, and M. R. Redinbo. 2011. '*Pseudomonas aeruginosa* PilY1 binds integrin in an RGD- and calcium-dependent manner', *PLoS One*, 6: e29629.

Jones, B. W., and Nishiguchi, M.K. . 2004. 'Counterillumination in the Hawaiian bobtail squid, *Euprymna scolopes* Berry (Mollusca: Cephalopoda)', *Marine Biology*, 144: 1151 - 55.

Karatan, E., and P. Watnick. 2009. 'Signals, regulatory networks, and materials that build and break bacterial biofilms', *Microbiol Mol Biol Rev*, 73: 310-47.

Key, J., M. Hefti, E. B. Purcell, and K. Moffat. 2007. 'Structure of the redox sensor domain of *Azotobacter vinelandii* NifL at atomic resolution: signaling, dimerization, and mechanism', *Biochemistry*, 46: 3614-23.

Khan, N. A., Y. Kim, S. Shin, and K. S. Kim. 2007. 'FimH-mediated *Escherichia coli* K1 invasion of human brain microvascular endothelial cells', *Cell Microbiol*, 9: 169-78.

Khedr, Z.M.A and Farid, S. . 2000. 'Response of Naturally Virus Infected - Tomato Plants to Yeast Extract and Phosphoric Acid Application', *Annals of Agric. Sc., Moshtohor*, 38: 927 - 39.

King, M. M., B. B. Kayastha, M. J. Franklin, and M. A. Patrauchan. 2020. 'Calcium Regulation of Bacterial Virulence', *Adv Exp Med Biol*, 1131: 827-55.

Klein, R., A. K. Kretzschmar, and G. Unden. 2020. 'Control of the bifunctional O(2) -sensor kinase NreB of *Staphylococcus carnosus* by the nitrate sensor NreA: Switching from kinase to phosphatase state', *Mol Microbiol*, 113: 369-80.

Kliegman, J. I., S. L. Griner, J. D. Helmann, R. G. Brennan, and A. Glasfeld. 2006. 'Structural basis for the metal-selective activation of the manganese transport regulator of *Bacillus subtilis*', *Biochemistry*, 45: 3493-505.

Koch, E. J., T. Miyashiro, M. J. McFall-Ngai, and E. G. Ruby. 2014. 'Features governing symbiont persistence in the squid-vibrio association', *Mol Ecol*, 23: 1624-34.

Koehler, S., R. Gaedeke, C. Thompson, C. Bongrand, K. L. Visick, E. Ruby, and M. McFall-Ngai. 2018. 'The model squid-vibrio symbiosis provides a window into the impact of strain- and species-level differences during the initial stages of symbiont engagement', *Environ Microbiol*.

Koh, S., J. Hwang, K. Guchhait, E. G. Lee, S. Y. Kim, S. Kim, S. Lee, J. M. Chung, H. S. Jung, S. J. Lee, C. M. Ryu, S. G. Lee, T. K. Oh, O. Kwon, and M. H. Kim. 2016. 'Molecular Insights into Toluene Sensing in the TodS/TodT Signal Transduction System', *J Biol Chem*, 291: 8575-90.

Koropatnick, T. A., J. R. Kimbell, and M. J. McFall-Ngai. 2007. 'Responses of host hemocytes during the initiation of the squid-*Vibrio* symbiosis', *Biol Bull*, 212: 29-39.

Koropatnick, T., M. S. Goodson, E. A. Heath-Heckman, and M. McFall-Ngai. 2014. 'Identifying the cellular mechanisms of symbiont-induced epithelial morphogenesis in the squid-Vibrio association', *Biol Bull*, 226: 56-68.

Kostakioti, M., M. Hadjifrangiskou, and S. J. Hultgren. 2013. 'Bacterial biofilms: development, dispersal, and therapeutic strategies in the dawn of the postantibiotic era', *Cold Spring Harb Perspect Med*, 3: a010306.

Kremer, N., E. E. Philipp, M. C. Carpentier, C. A. Brennan, L. Kraemer, M. A. Altura, R. Augustin, R. Hasler, E. A. Heath-Heckman, S. M. Peyer, J. Schwartzman, B. A. Rader, E. G. Ruby, P. Rosenstiel, and M. J. McFall-Ngai. 2013. 'Initial symbiont contact orchestrates host-organ-wide transcriptional changes that prime tissue colonization', *Cell Host Microbe*, 14: 183-94.

Kuboniwa, M., J. R. Houser, E. L. Hendrickson, Q. Wang, S. A. Alghamdi, A. Sakanaka, D. P. Miller, J. A. Hutcherson, T. Wang, D. A. C. Beck, M. Whiteley, A. Amano, H. Wang, E. M. Marcotte, M. Hackett, and R. J. Lamont. 2017. 'Metabolic crosstalk regulates *Porphyromonas gingivalis* colonization and virulence during oral polymicrobial infection', *Nat Microbiol*, 2: 1493-99.

Lacal, J., A. Busch, M. E. Guazzaroni, T. Krell, and J. L. Ramos. 2006. 'The TodS-TodT two-component regulatory system recognizes a wide range of effectors and works with DNA-bending proteins', *Proc Natl Acad Sci U S A*, 103: 8191-6.

Lamarcq, L. H., and M. J. McFall-Ngai. 1998. 'Induction of a gradual, reversible morphogenesis of its host's epithelial brush border by *Vibrio fischeri*', *Infect Immun*, 66: 777-85.

Le Roux, F., J. Binesse, D. Saulnier, and D. Mazel. 2007. 'Construction of a *Vibrio splendidus* mutant lacking the metalloprotease gene vsm by use of a novel counterselectable suicide vector', *Appl Environ Microbiol*, 73: 777-84.

Lee, K. H., and E. G. Ruby. 1992. 'Detection of the Light Organ Symbiont, *Vibrio fischeri*, in Hawaiian Seawater by Using *lux* Gene Probes', *Appl Environ Microbiol*, 58: 942-7.

Lee, K., and E. G. Ruby. 1995. 'Symbiotic Role of the Viable but Nonculturable State of *Vibrio fischeri* in Hawaiian Coastal Seawater', *Appl Environ Microbiol*, 61: 278-83.

Lee, V. T., J. M. Matewish, J. L. Kessler, M. Hyodo, Y. Hayakawa, and S. Lory. 2007. 'A cyclic-di-GMP receptor required for bacterial exopolysaccharide production', *Mol Microbiol*, 65: 1474-84.

Lesley, J. A., and C. D. Waldburger. 2001. 'Comparison of the *Pseudomonas aeruginosa* and *Escherichia coli* PhoQ sensor domains: evidence for distinct mechanisms of signal detection', *J Biol Chem*, 276: 30827-33.

Lin, C. S., Y. H. Tsai, C. J. Chang, S. F. Tseng, T. R. Wu, C. C. Lu, T. S. Wu, J. J. Lu, J. T. Horng, J. Martel, D. M. Ojcius, H. C. Lai, and J. D. Young. 2016. 'An iron detection system determines bacterial swarming initiation and biofilm formation', *Sci Rep*, 6: 36747.

Liu, C., D. Sun, J. Zhu, and W. Liu. 2018. 'Two-Component Signal Transduction Systems: A Major Strategy for Connecting Input Stimuli to Biofilm Formation', *Front Microbiol*, 9: 3279.

Lockey, C., R. J. Edwards, D. I. Roper, and A. M. Dixon. 2020. 'The Extracellular Domain of Two-component System Sensor Kinase VanS from *Streptomyces coelicolor* Binds Vancomycin at a Newly Identified Binding Site', *Sci Rep*, 10: 5727.

Lopez, D., H. Vlamakis, and R. Kolter. 2009. 'Generation of multiple cell types in *Bacillus subtilis*', *FEMS Microbiol Rev*, 33: 152-63.

Ludvik, D. A., K. M. Bultman, and M. J. Mandel. 2021. 'Hybrid Histidine Kinase BinK Represses *Vibrio fischeri* Biofilm Signaling at Multiple Developmental Stages', *J Bacteriol*, 203: e0015521.

Lupp, C., and E. G. Ruby. 2004. '*Vibrio fischeri* LuxS and AinS: comparative study of two signal synthases', *J Bacteriol*, 186: 3873-81.

Magana, M., C. Sereti, A. Ioannidis, C. A. Mitchell, A. R. Ball, E. Magiorkinis, S. Chatzipanagiotou, M. R. Hamblin, M. Hadjifrangiskou, and G. P. Tegos. 2018. 'Options and Limitations in Clinical Investigation of Bacterial Biofilms', *Clin Microbiol Rev*, 31.

Mandel, M. J., and A. K. Dunn. 2016. 'Impact and Influence of the Natural Vibrio-Squid Symbiosis in Understanding Bacterial-Animal Interactions', *Front Microbiol*, 7: 1982.

Mandel, M. J., A. L. Schaefer, C. A. Brennan, E. A. Heath-Heckman, C. R. Deloney-Marino, M. J. McFall-Ngai, and E. G. Ruby. 2012. 'Squid-derived chitin oligosaccharides are a chemotactic signal during colonization by *Vibrio fischeri*', *Appl Environ Microbiol*, 78: 4620-6.

Mandel, M. J., M. S. Wollenberg, E. V. Stabb, K. L. Visick, and E. G. Ruby. 2009. 'A single regulatory gene is sufficient to alter bacterial host range', *Nature*, 458: 215-8.

Mann, E. E., K. C. Rice, B. R. Boles, J. L. Endres, D. Ranjit, L. Chandramohan, L. H. Tsang, M. S. Smeltzer, A. R. Horswill, and K. W. Bayles. 2009. 'Modulation of eDNA release and degradation affects *Staphylococcus aureus* biofilm maturation', *PLoS One*, 4: e5822.

Marsden, A. E., K. Grudzinski, J. M. Ondrey, C. R. DeLoney-Marino, and K. L. Visick. 2017. 'Impact of Salt and Nutrient Content on Biofilm Formation by *Vibrio fischeri*', *PLoS One*, 12: e0169521.

Matilla, M. A., F. Velando, D. Martin-Mora, E. Monteagudo-Cascales, and T. Krell. 2022. 'A catalogue of signal molecules that interact with sensor kinases, chemoreceptors and transcriptional regulators', *FEMS Microbiol Rev*, 46.

Matz, C., D. McDougald, A. M. Moreno, P. Y. Yung, F. H. Yildiz, and S. Kjelleberg. 2005. 'Biofilm formation and phenotypic variation enhance predation-driven persistence of *Vibrio cholerae*', *Proc Natl Acad Sci U S A*, 102: 16819-24.

Maynard, C., I. Cummins, J. Green, and D. Weinkove. 2018. 'A bacterial route for folic acid supplementation', *BMC Biol*, 16: 67.

McAnulty, S. J., and S. V. Nyholm. 2016. 'The Role of Hemocytes in the Hawaiian Bobtail Squid, *Euprymna scolopes*: A Model Organism for Studying Beneficial Host-Microbe Interactions', *Front Microbiol*, 7: 2013.

McFall-Ngai, M., and T. C. G. Bosch. 2021. 'Animal development in the microbial world: The power of experimental model systems', *Curr Top Dev Biol*, 141: 371-97.

McFall-Ngai, M. J. 2014. 'The importance of microbes in animal development: lessons from the squid-vibrio symbiosis', *Annu Rev Microbiol*, 68: 177-94.

McFall-Ngai, M. J., and E. G. Ruby. 1991. 'Symbiont recognition and subsequent morphogenesis as early events in an animal-bacterial mutualism', *Science*, 254: 1491-4.

McFall-Ngai, M., and M. K. Montgomery. 1990. 'The Anatomy and Morphology of the Adult Bacterial Light Organ of *Euprymna scolopes* Berry (Cephalopoda:Sepiolidae)', *Biol Bull*, 179: 332-39.

Miller, JH. 1972. 'Experiments in molecular genetics. ', *Cold Spring Harbor Laboratory Press, Cold Spring Harbor, NY*.

Millikan, D. S., and E. G. Ruby. 2002. 'Alterations in *Vibrio fischeri* motility correlate with a delay in symbiosis initiation and are associated with additional symbiotic colonization defects', *Appl Environ Microbiol*, 68: 2519-28.

Millikan, D. S., and E. G. Ruby. 2004. '*Vibrio fischeri* flagellin A is essential for normal motility and for symbiotic competence during initial squid light organ colonization', *J Bacteriol*, 186: 4315-25.

Mix, L. T., M. Hara, R. Rathod, M. Kumauchi, W. D. Hoff, and D. S. Larsen. 2016. 'Noncanonical Photocycle Initiation Dynamics of the Photoactive Yellow Protein (PYP) Domain of the PYP-Phytochrome-Related (Ppr) Photoreceptor', *J Phys Chem Lett*, 7: 5212-18.

Miyashiro, T., and E. G. Ruby. 2012. 'Shedding light on bioluminescence regulation in *Vibrio fischeri*', *Mol Microbiol*, 84: 795-806.

Monk, I. R., N. Shaikh, S. L. Begg, M. Gajdiss, L. K. R. Sharkey, J. Y. H. Lee, S. J. Pidot, T. Seemann, M. Kuiper, B. Winnen, R. Hvorup, B. M. Collins, G. Bierbaum, S. R. Udagedara, J. R. Morey, N. Pulyani, B. P. Howden, M. J. Maher, C. A. McDevitt, G. F. King, and T. P. Stinear. 2019. 'Zinc-binding to the cytoplasmic PAS domain regulates the essential WalK histidine kinase of *Staphylococcus aureus*', *Nat Commun*, 10: 3067.

Montgomery, M. K., and M. J. McFall-Ngai. 1992. 'The muscle-derived lens of a squid bioluminescent organ is biochemically convergent with the ocular lens. Evidence for recruitment of aldehyde dehydrogenase as a predominant structural protein', *J Biol Chem*, 267: 20999-1003.

Montgomery, M. K., and M. J. McFall-Ngai. 1998. 'Late postembryonic development of the symbiotic light organ of *Euprymna scolopes* (Cephalopoda: Sepiolidae)', *Biol Bull*, 195: 326-36.

Morgan, J. L., J. T. McNamara, and J. Zimmer. 2014. 'Mechanism of activation of bacterial cellulose synthase by cyclic di-GMP', *Nat Struct Mol Biol*, 21: 489-96.

Morris, A. R., C. L. Darnell, and K. L. Visick. 2011. 'Inactivation of a novel response regulator is necessary for biofilm formation and host colonization by *Vibrio fischeri*', *Mol Microbiol*, 82: 114-30.

Morris, A. R., and K. L. Visick. 2013a. 'Inhibition of SypG-induced biofilms and host colonization by the negative regulator SypE in *Vibrio fischeri*', *PLoS One*, 8: e60076.

Morris, A. R., and K. L. Visick. 2013b. 'The response regulator SypE controls biofilm formation and colonization through phosphorylation of the syp-encoded regulator SypA in *Vibrio fischeri*', *Mol Microbiol*, 87: 509-25.

Motta, J. P., J. L. Wallace, A. G. Buret, C. Deraison, and N. Vergnolle. 2021. 'Gastrointestinal biofilms in health and disease', *Nat Rev Gastroenterol Hepatol*, 18: 314-34.

Mullner, M., O. Hammel, B. Mienert, S. Schlag, E. Bill, and G. Unden. 2008. 'A PAS domain with an oxygen labile [4Fe-4S](2+) cluster in the oxygen sensor kinase NreB of *Staphylococcus carnosus*', *Biochemistry*, 47: 13921-32.

Nawroth, J. C., H. Guo, E. Koch, E. A. C. Heath-Heckman, J. C. Hermanson, E. G. Ruby, J. O. Dabiri, E. Kanso, and M. McFall-Ngai. 2017. 'Motile cilia create fluid-mechanical microhabitats for the active recruitment of the host microbiome', *Proc Natl Acad Sci U S A*, 114: 9510-16.

Norsworthy, A. N., and K. L. Visick. 2015. 'Signaling between two interacting sensor kinases promotes biofilms and colonization by a bacterial symbiont', *Mol Microbiol*, 96: 233-48.

Nyholm, S. V., B. Deplancke, H. R. Gaskins, M. A. Apicella, and M. J. McFall-Ngai. 2002. 'Roles of *Vibrio fischeri* and nonsymbiotic bacteria in the dynamics of mucus secretion during symbiont colonization of the *Euprymna scolopes* light organ', *Appl Environ Microbiol*, 68: 5113-22.

Nyholm, S. V., and M. J. McFall-Ngai. 1998. 'Sampling the light-organ microenvironment of *Euprymna scolopes*: description of a population of host cells in association with the bacterial symbiont *Vibrio fischeri*', *Biol Bull*, 195: 89-97.

Nyholm, S. V., and M. J. McFall-Ngai. 2004. 'The winnowing: establishing the squid-vibrio symbiosis', *Nat Rev Microbiol*, 2: 632-42.

Nyholm, S. V., and M. J. McFall-Ngai. 2021. 'A lasting symbiosis: how the Hawaiian bobtail squid finds and keeps its bioluminescent bacterial partner', *Nat Rev Microbiol*, 19: 666-79.

Nyholm, S. V., E. V. Stabb, E. G. Ruby, and M. J. McFall-Ngai. 2000. 'Establishment of an animal-bacterial association: recruiting symbiotic vibrios from the environment', *Proc Natl Acad Sci U S A*, 97: 10231-5.

Nyholm, S. V., J. J. Stewart, E. G. Ruby, and M. J. McFall-Ngai. 2009. 'Recognition between symbiotic *Vibrio fischeri* and the haemocytes of *Euprymna scolopes*', *Environ Microbiol*, 11: 483-93.

O'Shea, T. M., C. R. Deloney-Marino, S. Shibata, S. Aizawa, A. J. Wolfe, and K. L. Visick. 2005. 'Magnesium promotes flagellation of *Vibrio fischeri*', *J Bacteriol*, 187: 2058-65.

O'Toole, G. A., and R. Kolter. 1998. 'Initiation of biofilm formation in *Pseudomonas fluorescens* WCS365 proceeds via multiple, convergent signalling pathways: a genetic analysis', *Mol Microbiol*, 28: 449-61.

O'Toole, G., H. B. Kaplan, and R. Kolter. 2000. 'Biofilm formation as microbial development', *Annu Rev Microbiol*, 54: 49-79.

Pankey, S. M., R. L. Foxall, I. M. Ster, L. A. Perry, B. M. Schuster, R. A. Donner, M. Coyle, V. S. Cooper, and C. A. Whistler. 2017. 'Host-selected mutations converging on a global regulator drive an adaptive leap towards symbiosis in bacteria', *Elife*, 6.

Paul, R., S. Abel, P. Wassmann, A. Beck, H. Heerklotz, and U. Jenal. 2007. 'Activation of the diguanylate cyclase PleD by phosphorylation-mediated dimerization', *J Biol Chem*, 282: 29170-7.

Persat, A., C. D. Nadell, M. K. Kim, F. Ingremeau, A. Siryaporn, K. Drescher, N. S. Wingreen, B. L. Bassler, Z. Gitai, and H. A. Stone. 2015. 'The mechanical world of bacteria', *Cell*, 161: 988-97.

Peters, J. M., A. Colavin, H. Shi, T. L. Czarny, M. H. Larson, S. Wong, J. S. Hawkins, C. H. S. Lu, B. M. Koo, E. Marta, A. L. Shiver, E. H. Whitehead, J. S. Weissman, E. D. Brown, L. S. Qi, K. C. Huang, and C. A. Gross. 2016. 'A Comprehensive, CRISPR-based Functional Analysis of Essential Genes in Bacteria', *Cell*, 165: 1493-506.

Pollack-Berti, A., M. S. Wollenberg, and E. G. Ruby. 2010. 'Natural transformation of *Vibrio fischeri* requires *tfoX* and *tfoY*', *Environ Microbiol*, 12: 2302-11.

Pratt, L. A., and R. Kolter. 1998. 'Genetic analysis of *Escherichia coli* biofilm formation: roles of flagella, motility, chemotaxis and type I pili', *Mol Microbiol*, 30: 285-93.

Ray, V. A., A. Driks, and K. L. Visick. 2015. 'Identification of a novel matrix protein that promotes biofilm maturation in *Vibrio fischeri*', *J Bacteriol*, 197: 518-28.

Ray, V. A., J. L. Eddy, E. A. Hussa, M. Misale, and K. L. Visick. 2013. 'The syp enhancer sequence plays a key role in transcriptional activation by the sigma54-dependent response regulator SypG and in biofilm formation and host colonization by *Vibrio fischeri*', *J Bacteriol*, 195: 5402-12.

Rivera-Cancel, G., W. H. Ko, D. R. Tomchick, F. Correa, and K. H. Gardner. 2014. 'Full-length structure of a monomeric histidine kinase reveals basis for sensory regulation', *Proc Natl Acad Sci U S A*, 111: 17839-44.

Romling, U., and M. Y. Galperin. 2015. 'Bacterial cellulose biosynthesis: diversity of operons, subunits, products, and functions', *Trends Microbiol*, 23: 545-57.

Romling, U., M. Y. Galperin, and M. Gomelsky. 2013. 'Cyclic di-GMP: the first 25 years of a universal bacterial second messenger', *Microbiol Mol Biol Rev*, 77: 1-52.

Ross, P., H. Weinhouse, Y. Aloni, D. Michaeli, P. Weinberger-Ohana, R. Mayer, S. Braun, E. de Vroom, G. A. van der Marel, J. H. van Boom, and M. Benziman. 1987. 'Regulation of cellulose synthesis in *Acetobacter xylinum* by cyclic diguanylic acid', *Nature*, 325: 279-81.

Rotman, E. R., K. M. Bultman, J. F. Brooks, 2nd, M. C. Gyllborg, H. L. Burgos, M. S. Wollenberg, and M. J. Mandel. 2019. 'Natural Strain Variation Reveals Diverse Biofilm Regulation in Squid-Colonizing *Vibrio fischeri*', *J Bacteriol*, 201.

Ruby, E. G. 1996. 'Lessons from a cooperative, bacterial-animal association: the *Vibrio fischeri-Euprymna scolopes* light organ symbiosis', *Annu Rev Microbiol*, 50: 591-624.

Ruby, E. G., and L. M. Asato. 1993. 'Growth and flagellation of *Vibrio fischeri* during initiation of the sepiolid squid light organ symbiosis', *Arch Microbiol*, 159: 160-7.

Ruby, E. G., and K. H. Lee. 1998. 'The *Vibrio fischeri-Euprymna scolopes* Light Organ Association: Current Ecological Paradigms', *Appl Environ Microbiol*, 64: 805-12.

Rumbaugh, K. P., and K. Sauer. 2020. 'Biofilm dispersion', *Nat Rev Microbiol*, 18: 571-86.

Sarkisova, S., M. A. Patrauchan, D. Berglund, D. E. Nivens, and M. J. Franklin. 2005. 'Calcium-induced virulence factors associated with the extracellular matrix of mucoid *Pseudomonas aeruginosa* biofilms', *J Bacteriol*, 187: 4327-37.

Schleicher, T. R., and S. V. Nyholm. 2011. 'Characterizing the host and symbiont proteomes in the association between the Bobtail squid, *Euprymna scolopes*, and the bacterium, *Vibrio fischeri*', *PLoS One*, 6: e25649.

Schleicher, T. R., N. C. VerBerkmoes, M. Shah, and S. V. Nyholm. 2014. 'Colonization state influences the hemocyte proteome in a beneficial squid-Vibrio symbiosis', *Mol Cell Proteomics*, 13: 2673-86.

Schwartzman, J. A., E. Koch, E. A. Heath-Heckman, L. Zhou, N. Kremer, M. J. McFall-Ngai, and E. G. Ruby. 2015. 'The chemistry of negotiation: rhythmic, glycan-driven acidification in a symbiotic conversation', *Proc Natl Acad Sci U S A*, 112: 566-71.

Services, National Health. 2020. 'Vitamins and Minerals '. https://www.nhs.uk/conditions/vitamins-and-minerals/others/.

Sharan, A., P. Soni, R. C. Nongpiur, S. L. Singla-Pareek, and A. Pareek. 2017. 'Mapping the 'Two-component system' network in rice', *Sci Rep*, 7: 9287.

Shibata, S., E. S. Yip, K. P. Quirke, J. M. Ondrey, and K. L. Visick. 2012. 'Roles of the structural symbiosis polysaccharide (syp) genes in host colonization, biofilm formation, and polysaccharide biosynthesis in *Vibrio fischeri*', *J Bacteriol*, 194: 6736-47.

Shrout, J. D., D. L. Chopp, C. L. Just, M. Hentzer, M. Givskov, and M. R. Parsek. 2006. 'The impact of quorum sensing and swarming motility on *Pseudomonas aeruginosa* biofilm formation is nutritionally conditional', *Mol Microbiol*, 62: 1264-77.

Silva-Jimenez, H., C. Garcia-Fontana, B. H. Cadirci, M. I. Ramos-Gonzalez, J. L. Ramos, and T. Krell. 2012. 'Study of the TmoS/TmoT two-component system: towards the functional characterization of the family of TodS/TodT like systems', *Microb Biotechnol*, 5: 489-500.

Small, A. L., and M. J. McFall-Ngai. 1999. 'Halide peroxidase in tissues that interact with bacteria in the host squid *Euprymna scolopes*', *J Cell Biochem*, 72: 445-57.

Sommerfeldt, N., A. Possling, G. Becker, C. Pesavento, N. Tschowri, and R. Hengge. 2009. 'Gene expression patterns and differential input into curli fimbriae regulation of all GGDEF/EAL domain proteins in *Escherichia coli*', *Microbiology (Reading)*, 155: 1318-31.

Stabb, E. V., K. A. Reich, and E. G. Ruby. 2001. '*Vibrio fischeri* genes *hvnA* and *hvnB* encode secreted NAD(+)-glycohydrolases', *J Bacteriol*, 183: 309-17.

Stabb, E. V., and E. G. Ruby. 2002. 'RP4-based plasmids for conjugation between *Escherichia coli* and members of the Vibrionaceae', *Methods Enzymol*, 358: 413-26.

Stabb, E.V. and Millikan, D. S. . 2009. 'Is the *Vibrio fischeri* - *Euprymna scolopes* Symbiosis a Defensive Mutualism ' in, *Defensive Mutalism in Microbial Symbiosis*

Stabb, E.V., Schaefer, A., Bose, J.L., and Ruby, E.G. . 2008. 'Quorum signaling and symbiosis in the marine luminous bacterium *Vibrio fischi*', *ASM Press*: 233 - 50

Stanley, P. M. 1983. 'Factors affecting the irreversible attachment of *Pseudomonas aeruginosa* to stainless steel', *Can J Microbiol*, 29: 1493-9.

Stenz, L., P. Francois, A. Fischer, A. Huyghe, M. Tangomo, D. Hernandez, J. Cassat, P. Linder, and J. Schrenzel. 2008. 'Impact of oleic acid (cis-9-octadecenoic acid) on bacterial viability and biofilm production in *Staphylococcus aureus*', *FEMS Microbiol Lett*, 287: 149-55.

Sutherland, I. 2001. 'Biofilm exopolysaccharides: a strong and sticky framework', *Microbiology (Reading)*, 147: 3-9.

Sycuro, L. K., E. G. Ruby, and M. McFall-Ngai. 2006. 'Confocal microscopy of the light organ crypts in juvenile *Euprymna scolopes* reveals their morphological complexity and dynamic function in symbiosis', *J Morphol*, 267: 555-68.

Synowiec, A., K. Zyla, M. Gniewosz, and M. Kieliszek. 2021. 'An effect of positional isomerism of benzoic acid derivatives on antibacterial activity against *Escherichia coli*', *Open Life Sci*, 16: 594-601.

Szurmant, H., R. A. White, and J. A. Hoch. 2007. 'Sensor complexes regulating two-component signal transduction', *Curr Opin Struct Biol*, 17: 706-15.

Tagliabue, L., A. Maciag, D. Antoniani, and P. Landini. 2010. 'The *yddV-dos* operon controls biofilm formation through the regulation of genes encoding curli fibers' subunits in aerobically growing *Escherichia coli*', *FEMS Immunol Med Microbiol*, 59: 477-84.

Takahashi, Y., S. I. Nishiyama, K. Sumita, I. Kawagishi, and K. Imada. 2019. 'Calcium Ions Modulate Amino Acid Sensing of the Chemoreceptor Mlp24 of *Vibrio cholerae*', *J Bacteriol*, 201.

Tal, R., H. C. Wong, R. Calhoon, D. Gelfand, A. L. Fear, G. Volman, R. Mayer, P. Ross, D. Amikam, H. Weinhouse, A. Cohen, S. Sapir, P. Ohana, and M. Benziman. 1998. 'Three cdg operons control cellular turnover of cyclic di-GMP in *Acetobacter xylinum*: genetic organization and occurrence of conserved domains in isoenzymes', *J Bacteriol*, 180: 4416-25.

Thompson, C. M., A. E. Marsden, A. H. Tischler, J. Koo, and K. L. Visick. 2018. '*Vibrio fischeri* Biofilm Formation Prevented by a Trio of Regulators', *Appl Environ Microbiol*, 84.

Thompson, C. M., A. H. Tischler, D. A. Tarnowski, M. J. Mandel, and K. L. Visick. 2019. 'Nitric oxide inhibits biofilm formation by *Vibrio fischeri* via the nitric oxide sensor HnoX', *Mol Microbiol*, 111: 187-203.

Tischler, A. D., and A. Camilli. 2004. 'Cyclic diguanylate (c-di-GMP) regulates *Vibrio cholerae* biofilm formation', *Mol Microbiol*, 53: 857-69.

Tischler, A. H., L. Lie, C. M. Thompson, and K. L. Visick. 2018. 'Discovery of Calcium as a Biofilm-Promoting Signal for *Vibrio fischeri* Reveals New Phenotypes and Underlying Regulatory Complexity', *J Bacteriol*, 200.

Tischler, A. H., M. E. Vanek, N. Peterson, and K. L. Visick. 2021. 'Calcium-Responsive Diguanylate Cyclase CasA Drives Cellulose-Dependent Biofilm Formation and Inhibits Motility in *Vibrio fischeri*', *mBio*, 12: e0257321.

Tischler, Alice H., Kelsey M. Hodge-Hanson, and Karen L. Visick. 2019. '*Vibrio fischeri* - Squid Symbiosis.' in, *eLS*.

Tomarev, S. I., R. D. Zinovieva, V. M. Weis, A. B. Chepelinsky, J. Piatigorsky, and M. J. McFall-Ngai. 1993. 'Abundant mRNAs in the squid light organ encode proteins with a high similarity to mammalian peroxidases', *Gene*, 132: 219-26.

Ukaegbu, U. E., and A. C. Rosenzweig. 2009. 'Structure of the redox sensor domain of *Methylococcus capsulatus* (Bath) MmoS', *Biochemistry*, 48: 2207-15.

Valentini, M., and A. Filloux. 2016. 'Biofilms and Cyclic di-GMP (c-di-GMP) Signaling: Lessons from *Pseudomonas aeruginosa* and Other Bacteria', *J Biol Chem*, 291: 12547-55.

Vasilieva, Svetlana V., Maria S. Petrishcheva, Elizaveta I. Gusarova, and Andreyan N. Osipov. 2016. 'Vitamin Para-Aminobenzoic Acid (PABA) Controls Generation of Nitric Oxide (NO) In Vitro and its Biological Functions in the Bacterial Cells', *Advanced Techniques in Biology & Medicine*, 04.

Ventre, I., A. L. Goodman, I. Vallet-Gely, P. Vasseur, C. Soscia, S. Molin, S. Bleves, A. Lazdunski, S. Lory, and A. Filloux. 2006. 'Multiple sensors control reciprocal expression of *Pseudomonas aeruginosa* regulatory RNA and virulence genes', *Proc Natl Acad Sci U S A*, 103: 171-6.

Verma, S. C., and T. Miyashiro. 2013. 'Quorum sensing in the squid-Vibrio symbiosis', *Int J Mol Sci*, 14: 16386-401.

Vescovi, E. G., Y. M. Ayala, E. Di Cera, and E. A. Groisman. 1997. 'Characterization of the bacterial sensor protein PhoQ. Evidence for distinct binding sites for Mg2+ and Ca2+', *J Biol Chem*, 272: 1440-3.

Visick, K. L., J. Foster, J. Doino, M. McFall-Ngai, and E. G. Ruby. 2000. '*Vibrio fischeri lux* genes play an important role in colonization and development of the host light organ', *J Bacteriol*, 182: 4578-86.

Visick, K. L., K. M. Hodge-Hanson, A. H. Tischler, A. K. Bennett, and V. Mastrodomenico. 2018. 'Tools for Rapid Genetic Engineering of *Vibrio fischeri*', *Appl Environ Microbiol*, 84.

Visick, K. L., K. P. Quirke, and S. M. McEwen. 2013. 'Arabinose induces pellicle formation by *Vibrio fischeri*', *Appl Environ Microbiol*, 79: 2069-80.

Visick, K. L., and E. G. Ruby. 1998. 'The periplasmic, group III catalase of *Vibrio fischeri* is required for normal symbiotic competence and is induced both by oxidative stress and by approach to stationary phase', *J Bacteriol*, 180: 2087-92.

Visick, K. L., and E. G. Ruby. 2006. '*Vibrio fischeri* and its host: it takes two to tango', *Curr Opin Microbiol*, 9: 632-8.

Visick, K. L., and L. M. Skoufos. 2001. 'Two-component sensor required for normal symbiotic colonization of *Euprymna scolopes* by *Vibrio fischeri*', *J Bacteriol*, 183: 835-42.

Visick, K. L., E. V. Stabb, and E. G. Ruby. 2021. 'A lasting symbiosis: how *Vibrio fischeri* finds a squid partner and persists within its natural host', *Nat Rev Microbiol*, 19: 654-65.

Vlamakis, H., C. Aguilar, R. Losick, and R. Kolter. 2008. 'Control of cell fate by the formation of an architecturally complex bacterial community', *Genes Dev*, 22: 945-53.

Wang, D., A. Xu, C. Elmerich, and L. Z. Ma. 2017. 'Biofilm formation enables free-living nitrogen-fixing rhizobacteria to fix nitrogen under aerobic conditions', *ISME J*, 11: 1602-13.

Wang, Y., Y. S. Dufour, H. K. Carlson, T. J. Donohue, M. A. Marletta, and E. G. Ruby. 2010. 'H-NOX-mediated nitric oxide sensing modulates symbiotic colonization by Vibrio fischeri', *Proc Natl Acad Sci U S A*, 107: 8375-80.

Wang, Y., and E. G. Ruby. 2011. 'The roles of NO in microbial symbioses', *Cell Microbiol*, 13: 518-26.

Watnick, P. I., and R. Kolter. 1999. 'Steps in the development of a *Vibrio cholerae* El Tor biofilm', *Mol Microbiol*, 34: 586-95.

Wier, A. M., S. V. Nyholm, M. J. Mandel, R. P. Massengo-Tiasse, A. L. Schaefer, I. Koroleva, S. Splinter-Bondurant, B. Brown, L. Manzella, E. Snir, H. Almabrazi, T. E. Scheetz, F. Bonaldo Mde, T. L. Casavant, M. B. Soares, J. E. Cronan, J. L. Reed, E. G. Ruby, and M. J. McFall-Ngai. 2010. 'Transcriptional patterns in both host and bacterium underlie a daily rhythm of anatomical and metabolic change in a beneficial symbiosis', *Proc Natl Acad Sci U S A*, 107: 2259-64.

Wolfe, A. J. 2010. 'Physiologically relevant small phosphodonors link metabolism to signal transduction', *Curr Opin Microbiol*, 13: 204-9.

Wolfe, A. J., D. S. Millikan, J. M. Campbell, and K. L. Visick. 2004. '*Vibrio fischeri* sigma54 controls motility, biofilm formation, luminescence, and colonization', *Appl Environ Microbiol*, 70: 2520-4.

Wollenberg, M. S., and E. G. Ruby. 2009. 'Population structure of *Vibrio fischeri* within the light organs of *Euprymna scolopes* squid from Two Oahu (Hawaii) populations', *Appl Environ Microbiol*, 75: 193-202.

Wosten, M. M., L. F. Kox, S. Chamnongpol, F. C. Soncini, and E. A. Groisman. 2000. 'A signal transduction system that responds to extracellular iron', *Cell*, 103: 113-25.

Yip, E. S., K. Geszvain, C. R. DeLoney-Marino, and K. L. Visick. 2006. 'The symbiosis regulator *rscS* controls the syp gene locus, biofilm formation and symbiotic aggregation by *Vibrio fischeri*', *Mol Microbiol*, 62: 1586-600.

Yip, E. S., B. T. Grublesky, E. A. Hussa, and K. L. Visick. 2005. 'A novel, conserved cluster of genes promotes symbiotic colonization and sigma-dependent biofilm formation by *Vibrio fischeri*', *Mol Microbiol*, 57: 1485-98.

Zamorano-Sanchez, D., J. C. Fong, S. Kilic, I. Erill, and F. H. Yildiz. 2015. 'Identification and characterization of VpsR and VpsT binding sites in *Vibrio cholerae*', *J Bacteriol*, 197: 1221-35.

Zamorano-Sanchez, D., W. Xian, C. K. Lee, M. Salinas, W. Thongsomboon, L. Cegelski, G. C. L. Wong, and F. H. Yildiz. 2019. 'Functional Specialization in *Vibrio cholerae* Diguanylate Cyclases: Distinct Modes of Motility Suppression and c-di-GMP Production', *mBio*, 10.

Zhou, X., N. Zhang, L. Xia, Q. Li, J. Shao, Q. Shen, and R. Zhang. 2018. 'ResDE Two-Component Regulatory System Mediates Oxygen Limitation-Induced Biofilm Formation by *Bacillus amyloliquefaciens* SQR9', *Appl Environ Microbiol*, 84.

Zschiedrich, C. P., V. Keidel, and H. Szurmant. 2016. 'Molecular Mechanisms of Two-Component Signal Transduction', *J Mol Biol*, 428: 3752-75.

VITA

The author, Courtney Noelle Dial, was born in Naperville, IL, on December 2, 1994, to Jennifer Lynn and Robert Wayne Dial. She attended Lewis University in Romeoville, IL, where she earned a Bachelor of Science, *cum laude* with honors as a distinguished scholar of the university, in Biochemistry with a minor in biology in May 2017. She then earned her Master of Science in Infectious Disease and Immunology from Loyola University Chicago under the mentorship of Dr. Bryan Mounce. During her master's work, she studied how Coxsackievirus B3 responds to polyamine depletion. After graduation in 2019, Courtney matriculated into the Loyola University Chicago Stritch School of Medicine IPBS Graduate Program and began her Ph.D. education in the Microbiology and Immunology track under the mentorship of Dr. Karen Visick.

Courtney's dissertation focuses on new biofilm-inducing conditions in squid symbiont *Vibrio fischeri*. After completing her graduate studies, Courtney will pursue a two–year Postdoctoral Clinical Microbiology Fellowship at UNC–Chapel Hill under the mentorship of Dr. Melissa Miller and Dr. Kevin Alby.